Design of twin foldable and tiltable rotors flight vehicle model

A thesis

submitted in fulfilment

of the requirements for the degree

of

Master of Engineering

at

The University of Waikato

by

Ziqian Zhang

THE UNIVERSITY OF
WAIKATO
Te Whare Wānanga o Waikato

University of Waikato

2017

Abstract

With the increasing number of private cars, traffic congestion is getting worse. Compared to the ground, there is a wider space in the sky due to its three-dimensional space. In consideration of this, flight vehicles would be one of the best ways to solve the traffic problem on the ground.

A new concept of the structure for the flight vehicle has been presented in this thesis. It has two rotors with folding mechanisms to provide lift. The two rotors could be folded to reduce the size when it is in the car mode. Also because of the twin rotors design, the structure of the rotor head becomes simpler than usual helicopter main rotor head. Moreover, by using some gearboxes, it makes the flying car just using one motor to power the two rotors. The use of these gearboxes can also simplify the structure of the rotor head. Due to the research of this concept is in the initial stage, thus, the project just made a model, not a real flying car to verify the feasibility of the concept. What is more, a method to control the model has been shown in this thesis by using a normal controller. This thesis focuses on the process of making the flight vehicle model including calculation, mechanical design, implementation and control method.

Acknowledgements

I gratefully acknowledge the help of Dr. Chikit Au, my supervisor. He gave me several professional suggestions and helped me to purchase components I needed during the project.

I would like to express my heartfelt gratitude to my beloved wife Xiaxi Huang. Without her encouragement and support, I cannot finish this project.

I would also thank Brett Nichol who helped me to laser cut materials.

Last my thanks would go to my parents for supporting me study at Waikato University.

Table of Contents

List of figures

Chapter one: Introduction

Because of the increasing population and the fast development in the automotive industry, traffic congestion turns worse and worse. Numerous cars had been made and brought by people so that many cities had been packed with cars. This situation seemed to be more and more serious every year. In 2014, at least 63.52 million cars had been registered around the world (The Economist, 2016). Moreover, the traffic problem is much worse in the big cities because numbers of people want to go to the large city in order to get convenient life style and more opportunities to find well-paid jobs.

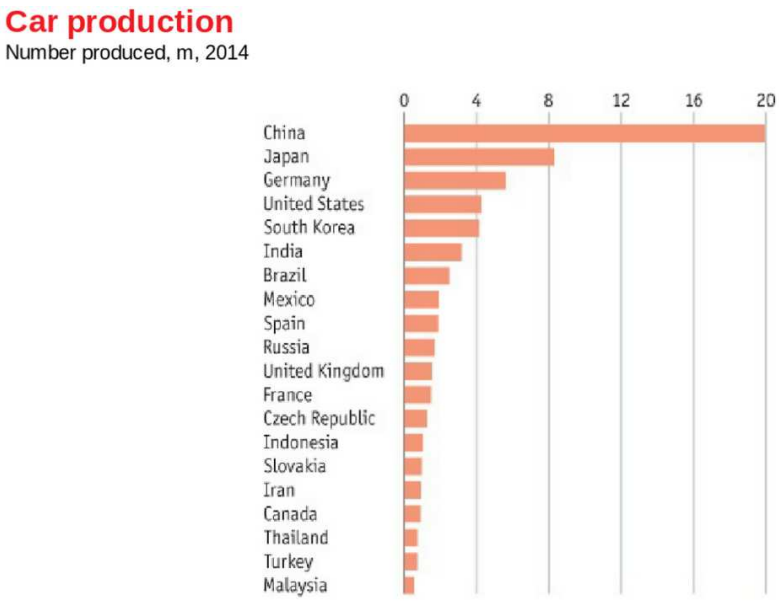

Figure 1.1: The number of cars made in different countries (The Economist, 2016).

Traffic congestion leads to a wide range of problems. "Each year, traffic congestion

costs Americans tens of billions of dollar in wasted time and motor fuel" (Ciment, 2015, p.1762). Traffic jam also caused bad emotion for people which may bring to their companies or take home. Delay emergency assistance is another problem that it will bring. All these problems make people begin to think about the possibility of using the sky. Although fixed-wing aircrafts let us have the ability to travel long distance with more convenient, they need runways to take off and land. That limits the use of fixed-wing aircrafts in cities. Helicopters are another option to solve the traffic problem. However, as the helicopter's rotor is too large and cannot fold, helicopters cannot be as popular as private cars. Therefore, a demand for a vehicle which is not only can be as convenient as a private car but also can fly appeared.

1.1 Motivation

Aircrafts and mass production of cars make our way of life has undergone enormous changes. Cars allow people to travel faster on land, while airplanes greatly reduce the time of the long journey. Since the car and the aircraft had been invented, people never stop to try to combine them together. During this period, many surprising products were invented. Though some of these inventions were even succeefully flight, most of them are based on fixed-wing aircraft design. It means that a runway is required to take off and land. In order to solve this problem, it is crucial to develop a flying car which could vertical take-off and landing (VTOL). Meanwhile, its size needs to be similar as a normal land vehicle. This

thesis provides a new concept by using two foldable and tiltable rotors structure to achieve this purpose. The fold of the rotors can reduce the overall size of the flight vehicle; the tilt of the rotors can control the flight of the flight vehicle. At the mean time, the flight vehicle only uses one engine which placed in the middle of the flight vehicle to power the two rotors. This engine arrangement can reduce the rotors size (compared with those aircraft which place motor directly under rotors), so that the rotor can fold and store into the vehicle. If the twin foldable and tiltable rotors flight vehicle developed successfully, it not only can be used as a convenient traffic vehicle but also can be used in many other fields like military, agriculture, photography, Sightseeing and etc.

1.2 Objectives

In general, the main objective of this project is to put forward a concept of a flight vehicle with twin foldable and tiltable rotors which powered by only one engine. Then, according to the concept, design and implement a model to investigate the feasibility of the concept. There are three main design objectives of this concept should be achieved:

1. Design a mechanism which not only can fold and tilt the rotor but also can transmit power to the rotor.

2. Design a transmission system which can transmit motor power to two rotors.

3. Design a control method to control the flight vehicle.

1.3 Scopes

The scopes of this thesis include the following five aspects:

1. Viable conceptual design.

This thesis will review some prominent previous and present flying cars, helicopters and multi-copters, analyze their advantages and disadvantages, integrate their strengths and bring forward a new concept of flying car.

2. Theoretical calculations.

Design and determine the basic parameters of the model based on the proposed concepts. The main research in this part will calculate the lift and power requirement of the model.

3. Design and implement the mechanical structure of the model.

The flight vehicle model structure and its most parts of the model are designed by the Solidworks software. These parts are customized by three-dimensional printer, laser cutter and factory according to the drawings. There are a variety of materials to be used in the model to make it as light as possible, with sufficient strength and cost-saving at the same time.

4. Design the flight control system

Because it is a new structure, the conventional fixed wing, helicopter and four rotor copter control methods cannot be used to control the flight vehicle model. In this thesis, it presents a method for controlling the model flying by using an 8-channel controller. This method can also control the folding and tilting of the rotors. Another 2-channel controller is used to control the land driving part.

5. Model test

Test if the concept and structure of this twin foldable and tiltable rotors flight vehicle is possible. The test of the flight vehicle is simply divided into two steps. First, test and adjust the pitch, roll, yaw and fold control. Secondly, test whether the transmission system works well.

Chapter Two: Literature Review

The concept of this twin-rotor collapsible flight vehicle arises from the study of flying vehicles, helicopters and multi-rotor aircraft. This paragraph will mainly review the literature related to them. The history of the flight vehicle will be reviewed in the first section. Meanwhile, this section will also introduce and analyze the flying cars which had been invented in recent years. In the second section, the development of helicopters and the development of multi-copters will be introduced. Among them, the thesis will mainly focus on normal helicoperts and dual-rotor copters. In the third section, the thesis will review the structure of the helicopter rotor head. It is one of the most important parts for helicopters to flight steady.

2.1 Flying cars

Flight vehicle is not a new concept for people. After the motor car and the airplane had been invented, mankind never stopped putting them together. In the history of human research the flight vehicle, there were many kinds of flying cars.

2.1.1 The development of flying cars

As early as 1906, Traian Vuia designed, built and successfully flight his first flying machine called Traian Vuia 1 by his own hand in Paris. He pioneered a four-wheel

and light-weight frame structure (Historic Wings, 2013). The lift of the machine is provided by the fixed-wing, a propeller mounted at the front of the flying machine with an approximately fifteen-degree positive angle of attack to the ground. The propeller powered by an engine installed at the middle top of the frame. This flying machine formed the prototype of the flying car.

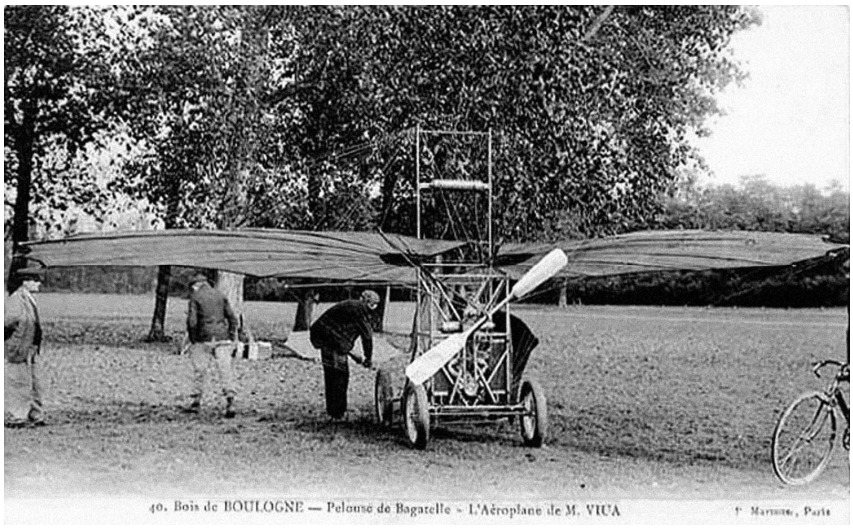

Figure 2.1: The Traian Vuia 1 flying machine (Historic Wings, 2013).

When it goes to 1917, the first flying car called Curtiss Autoplane was designed by Glenn Curtiss. And in the same year, it was debuted at the Pan-American Aeronautical Exposition in New York City. It used aluminum automobile body and equipped with a one hundred horsepower V8 engine (FLYING CARS, 2017). However, his project was shelved and never had a real flight because of World War I. (Matt, 2015, para. 3).

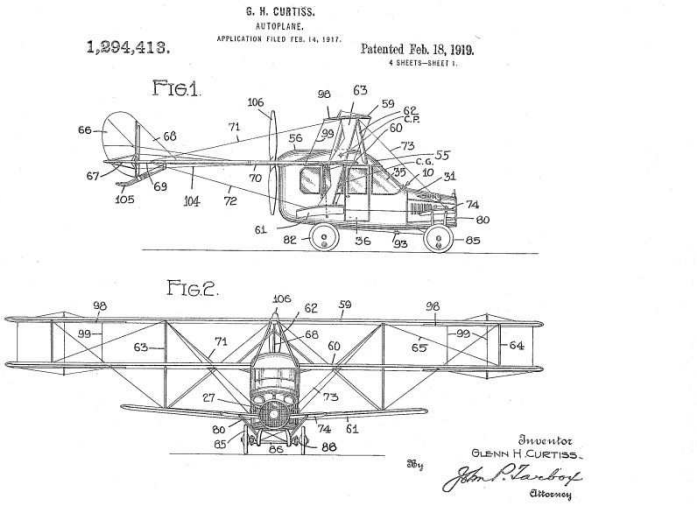

Figure 2.2: The patent of the Curtiss Autoplane flying car (Matt, 2015).

Although the Curtiss Autoplane did not perform a real flight, the realization of the flying car seems to be in sight. Even Henry Ford proclaimed: "A combination of plane and motorcar is coming. You may smile. But it will come" in 1940 (Case, K. 2002). Sure enough, in the next 10 years, there were emerged three typical flight vehicles which must be discussed.

The first one is the ConVaircar Model 118. In 1946, this flying car was successfully taken off from the ground and flew. However, the second model went through an emergency landing due to fuel exhaustion during flight. Although the pilot was not injured, Unfortunately, the flight vehicle was seriously damaged (Huntington, S. 2001).

Figure 2.3: The ConVaircar Model 118 (Matt, 2015).

In the same year, Robert Edison Fulton Jr designed and built the Airphibian which was different from the previous design ideas. The design has not converted a car into an aircraft but divided the car and the fuselage into two parts. Meantime, the two parts can be assembling into an airplane. And in 1950, the Civil Aeronautics Agency (CAA) - now the Federal Aviation Administration (FAA) was authorized the Airphibian (Fulton, 2002). Anonymous (2006) reports that the Airphibian could fly at 180 kilometres per hour when it in the flight model. Meanwhile, it could reach the highest speed of 80 kilometres per hour when it in the car model (p. 62).

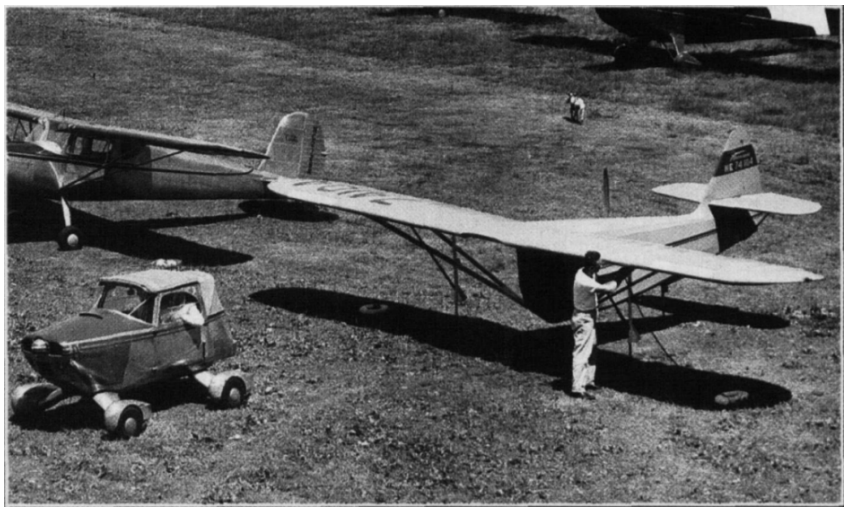

Figure 2.4: The Airphibian (Fulton, 2002).

The last of the three typical flying cars in the period is the Taylor Aerocar. The characteristic of this flying car is that the wings could manually fold back along tail to form towable trailer (FLYING CARS, 2017). And as the Airphibian, its rear airplane part is detachable. The prototype of the Aerocar successfully flew in 1949 (Davisson, 1999). The foldable wings design is an advanced concept, and even today some flying cars still using this idea.

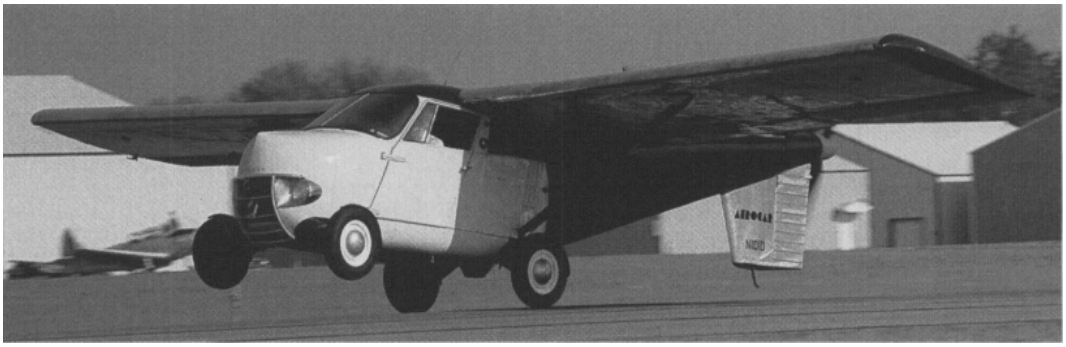

Figure 2.5: The Aerocar (Davisson, 1999).

2.1.2 Flying cars in recent years

After years of development and the demand for convenience from flying cars, several companies began to research new types of flying cars. The following will review and analyze some of the flight projects released in recent years.

2.1.2.1 The Transition

The Transition is a two-seat, roadable aircraft with a folding-wing. The folding-wing mechanism makes the aircraft capable driving on any surface road and parking it in a normal car park (Cable, 2012). It is a star product from Terrafugia Company which starts in 2006 and founded by five award-winning MIT (Massachusetts Institute of Technology) graduates (Terrafugia, 2017). Up to now, the company has received over 100 orders for the Transition (Cable, 2012). However, it needs a 2500-ft runway to take off or land. In other words, it cannot vertical take-off and landing (VTOL). As a result, this reason restricts its use and development.

Figure 2.6: The Transition (Jeffrey, 2013).

2.1.2.2 The TF-X

The Terrafugia Company also realized the problem which mentioned above. To solve it, Terrafugia published a concept of four seats hybrid vertical take-off and landing (VTOL) flying car called TF-X. By using two blades foldable and tiltable rotors, it can be converted into an airplane. The two rotors powered by two 600-hp electrical engines which placed at the tips of the wing. The blades will unfold when it need to vertical take-off. During the flight, the two electrical engines tilt forward and slowly stop. Meanwhile, a petrol engine will power another propeller behind the vehicle which provides thrust and recharges the batteries. After that, the blades of the two rotors fold. When the vehicle needs to land vertically, the electrical engines restart, blades unfold and electrical engines tilt upward to provide lift. According to the plan from the company, the TF-X will be available after 2020 (Warwick, 2013).

Figure 2.7: The concept of the TF-X of taking off (Terrafugia, 2017).

Figure 2.8: The concept of the TF-X of flying (Terrafugia, 2017).

2.1.2.3 The AeroMobil

In 2010, the AeroMobil Company established to make a flying car. After 3 years, a prototype had unveiled with the same name of the company. Moreover, it successfully flew in the next year. Different from the folding mechanism of the Transition, the AeroMobil uses a folding mechanism similar to scissors over the top

of the fuselage. A propeller placed at the end of the aircraft which powered by a 300-hp engine. When the AeroMobil on the ground, an electrical motor powers its front wheels to make it drive (Hemmerdinger, 2017). Up to now, the AeroMobil has been developed to the type 4.0. Simultaneously, it has become more and more perfect (AeroMobil, 2017).

Figure 2.9: The AeroMobil 2.5 (up), 3.0 (middle) and 4.0 (down) (AeroMobil, 2017).

2.1.2.4 The PAL-V (Personal Air and Land Vehicle)

The Transition and the AeroMobil are flying cars that based on fixed-wing, however, not only can this kind of structure let the car take off. A Dutch company unveiled a one-seat flying car PAL-V which combined by a 3 wheel vehicle and a gyroplane. The flying car was powered by an environmentally certified car engine in both flying and driving modes. The engine not only can use petrol but also can use biodiesel or bio-ethanol. Foldable rotor and propeller are used in the PAL-V, also a patented technology called tilting system is used in it ("Flying Car Company" Takes Off, 2007). In 2012, a prototype was passed all tests and successfully took its maiden flight. Due to the gyroplane structure, only a 520feet (165 meters) runway needed (Flying Car Makes Successful Maiden Flight, 2012). It is a quite short take-off distance compare with the runway requirement of the Transition (2500-ft).

Figure 2.10: The two different modes of the PAL-V (PAV-L, 2017).

2.1.2.5 The X-Hawk

The X-Hawk is a VTOL vehicle with two contained rotors and now still researching and developing by the Urban Aeronautics with Bell Helicopter. Several vanes are placed on the top and bottom of the contained rotors. These vanes will control the movement of the X-Hawk (Egozi, 2006). The company claimed that the X-Hawk will save 15% power compare with the analogous twin engine helicopter (Egozi, 2004). Saeed and Grantton (2010) claim that " A scale prototype of the vehicle is reported to have been tested in August 2008 in hover and low-speed forward flight, and flight of the first Mule prototype is projected for mid- 2009" (p. 97).

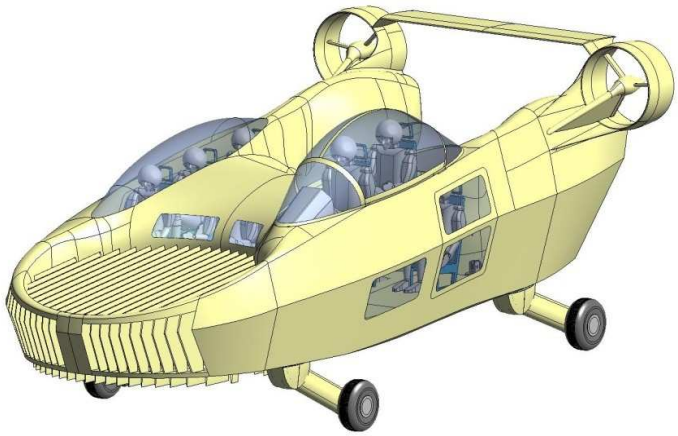

Figure 2.11: The conception of the X-Hawk (Urban Aeronautics, n.d.).

2.1.3 Conclusion.

In this section, it reviewed the history of the flight vehicle and introduced some current flying cars and conceptions at the meantime. It is easy to find that most

flying cars which need a runway to take-off and land now has been achieved. However, those VTOL vehicles are still researching and developing. For this reason, this thesis provides a twin rotors VTOL conception for research which based on helicopter technology and multi-helicopter structure. In the next section, a brief review of the development of the helicopter, multi-copter and their structures of the rotors will be mentioned.

2.2 Helicopters, multi-copters and the representative rotor head structure of typical helicopters.

The helicopter as one of a unique creation of aviation technology in the 20th century greatly expands the scope of application of the aircraft. In recent years, not just helicopters, the research of multi-copters is also popular and made a lot of progress. The first part of this section will briefly review the history of the helicopter and the second part, some typical different types of helicopters will be stated.

2.2.1 The history of helicopters and multi-copters.

Strictly speaking, helicopters are developed from multi- copters. In 1907, Cornu, Paul, a French engineer and inventor, built the first manned helicopter (Cornu, 2008). But it only achieved vertical flight for few seconds because of the unstable control system (13 November 1907, 2016). At that time, the classic single rotor

with tail rotor structure has not yet been invented. So he used two rotors to offset their mutual torque as the bi-copter today.

Figure 2.12: Paul Cornu's helicopter (Helicopters Magazine, 2007).

In the same year, with the physiologist and aviation pioneer Charles Richet's help, the Breguet brothers, Louis and Jacques made their helicopter called Breguet-Richet Gyroplane No.1. It was powered by a 45 horsepower engine, which lifted it about 50 centimeters. It adopted a spider web-like frame and got four rotors (Encyclopedia Britannica Online, 2016, para. 4). The exterior of the helicopter likes the drone that we usually saw. However, it was not stable either.

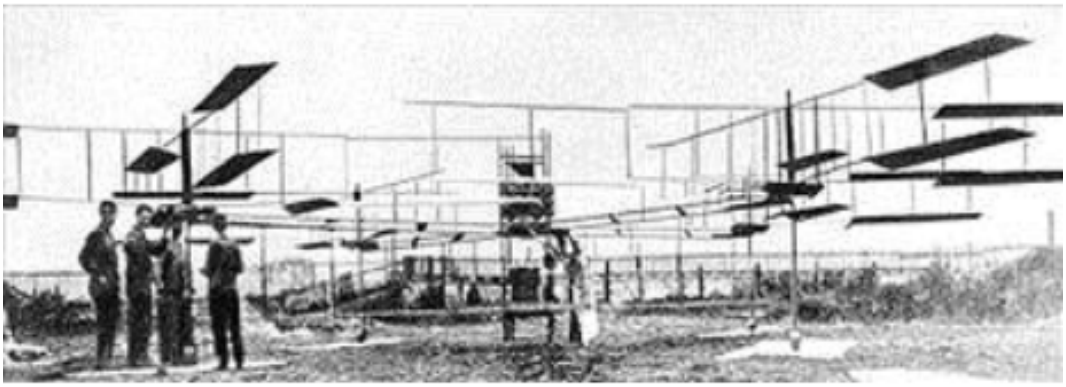

Figure 2.13: The Breguet-Richet Gyroplane No.1 (Gordon Leishman J, 2001).

After 15 years, George De Bothezat arranged a quad-copter with fixed-attack angle blades rotors and named Flying Octopus. However, it was also hard to control and just can lift itself approximately 5 meters due to the limited technology at that time (Radek & Frantisek 2012).

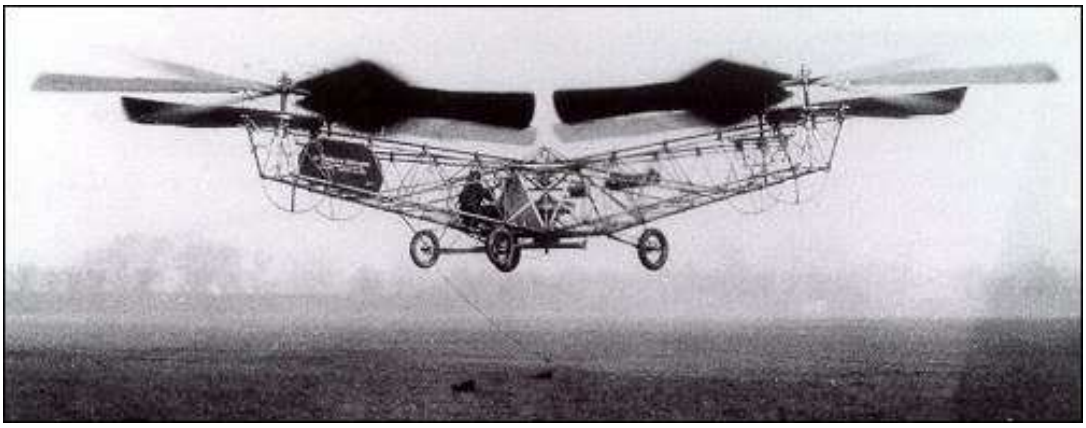

Figure 2.14: The Flying Octopus. (Wikipedia, 2017).

In 1936, Germany built the first successful helicopter, Focke Achgelis 61, which set many records including an altitude flight of 11,243-ft and a cross-country flight of 143 miles in 1938. It had two three-bladed rotors with a 160 horsepower engine

(Encyclopedia Britannica Online, n.d., para. 8). This is the first controllable helicopter (Simonsen, 2012).

Figure 2.15: The Focke Achgelis 61 (Kenneth, G. Munson, 1969).

In 1939, an American Igor Sikorsky built the first particular helicopter: VS-300. It has a single main three-bladed rotor with a tail rotor. This particular and classic arrangement has been used in most helicopters until now (Encyclopedia Britannica Online, n.d., para. 9).

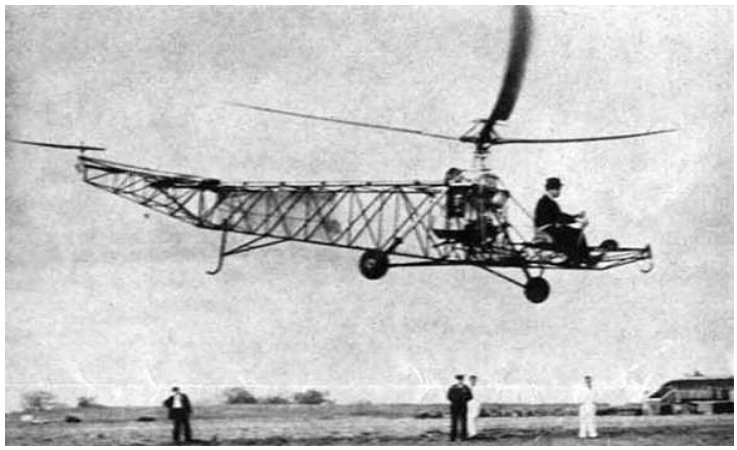

Figure 2.16: The VS-300 (Century of Flight, n.d.).

After the VS-300, the most significant evolution of helicopter was The Transcendental Model 1-G tilt-rotor aircraft in early 1947. It was made by Transcendental Aircraft Corporation of New Castle. Its most important feature was that its rotors can change their angle – it means this aircraft can change from a twin rotor helicopter to a plane (Martin, Demo, & Daniel, 2000). This new design of structure affords a new direction for research to solve the problem that helicopters travel distance is short.

Figure 2.17: The Transcendental Model 1-G (Martin, Demo, & Daniel, 2000).

2.3 Different types of copter.

There are a variety of types of helicopters. This section will review some typical model of them separately, according to the number of their main rotors.

2.3.1 One main rotor helicopters

Most helicopters are using the one rotor structure. In order to counteract the torque of the main rotor, the most common practice is to install a small rotor perpendicular to the main rotor at the tail. The Bell UH-1 Iroquois is one of the famous helicopters which been used on a large scale in counterinsurgency warfare in Vietnam (Bell, 2011).

Figure 2.18: The Bell UH-1 Iroquois helicopter (The Aviation History Online Museum, 2013).

Using tail rotor is not the only way to solve the torque problem. MD500N installed a fan in the tail boom to provide a jet of compressed air squirting out of one side of the tail boom (Doug, 2001). This structure makes the helicopter safer than usual helicopters.

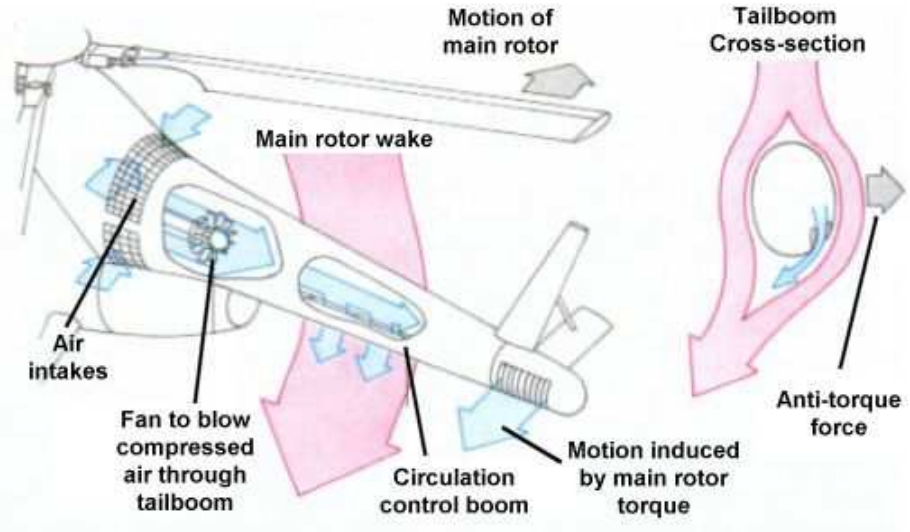

Figure 2.19: The anti-torque concept of MD500N (Doug, 2001).

2.3.2 Two main rotors copters

There are two different layouts of two main rotors copters: the twin rotors non-coaxial and the twin rotors coaxial. By using two opposite rotate rotors, their respective torques will offset each other. The main representative models of the twin rotors non-coaxial are the Mil V-12 (Homer), the Boeing CH-47 (Chinook) and the Boeing V-22 (Osprey). Their characteristics are different. Simultaneously, the Kamov KA-50 (Black Shark) is the main representative model of the twin rotors coaxial.

As the biggest helicopter in the world, Mil V-12 can carry approximately 20 to 25 tons weight. The twin 67 meter-diameter non-coaxial rotors support it have enough lift (Aerotime, 2013). The characteristic of the Mil V-12 is that the two rotors are placed at the tips of the wing each side.

Figure 2.20: The Mil V-12 (Aerotime, 2013).

On the contrary to the Mil V-12, the two rotors of the Boeing CH-47 are placed at the front and rear sides of the fuselage. This arrangement makes it smaller than Mil V-12 meanwhile still powerful to lift the weight. In 1961, Boeing CH-47 did its first flight. And until now, several countries including the United States still use it (The Boeing Company, 2017).

Figure 2.21: The Boeing CH-47 (The Boeing Company, 2017).

Unlike previous models, the Boeing V-22 is a tilt rotor aircraft. Using this technology, V-22 can gain both advantages of helicopters and fixed-wing airplanes (Martin, Demo and Daniel, 2000). Because V-22 is a VTOL aircraft, so there is no need to use the runway. Also, it can travel for long distance which usual helicopters cannot, due to it has the ability to change itself as a normal airplane. All these advantages let it can be used for multiple needs of the military and security forces.

Figure 2.22: The Boeing V-22 Osprey (The Boeing Company, 2017).

Goes to the typical twin rotors coaxial copter, the Kamov KA-50 is the famous one in this kind of structure. As same as twin rotors non-coaxial helicopters, the rotations of the two rotors of the KA-50 are opposite to counteract torque between them. But the coaxial arrangement makes the KA-50 more compact than others twin helicopter.

Figure 2.23: The Kamov KA-50 Black Shark (SKY Berry, 2014).

2.3.3 Eight main rotors copters.

A Chinese company, EHang developed an eight rotors copter: EHang 184. It has the same simple structure as a usual quad-copter model. No complicated hinges structure, gear or transmission, the EHang 184 only use eight electrical motors directly connect with eight propellers. And the EHang 184 is an AAV (Autonomous Aerial Vehicle) that means there is no need to manually control it (EHang, 2017).

Figure 2.24: The EHang 184 (EHang, 2017).

2.3.4 Conclusion.

Compared to the different types of copters from 1907 to present, each of them has its own characteristics. Base on these researches, how to choose, combine their strengths, avoid shortcomings and according to the result, propose a new VTOL flying car concept is one of the aims of this thesis.

2.4 The main rotor head structure of typical helicopters

The main rotor head is an intermediate part used to install the rotor blades and connect the rotor to the helicopter drive system and the steering system. The wildly used main rotor head is the articulated rotor head. Each blade has a flapping hinge, a dragging hinge and a feathering hinge. The combination of these components allows the helicopter to take off and run smoothly. The flapping hinge was designed to keep the balance of the helicopter when it is flying forward. The reason is that when the helicopter is flying forward and its rotor is rotating clockwise, the wind speed of the right blade will higher than the speed of the left one due to the forward speed. It means the right blade will provide more lift than the left one. In this situation, the helicopter will roll to the left side. Flapping hinges can solve this problem; however, the usage of flapping hinges brings another problem: vibration (blades become unstable because the rotate centre will move). So there is needed to use dragging hinges to fix the problem (Watkinson, 2003).

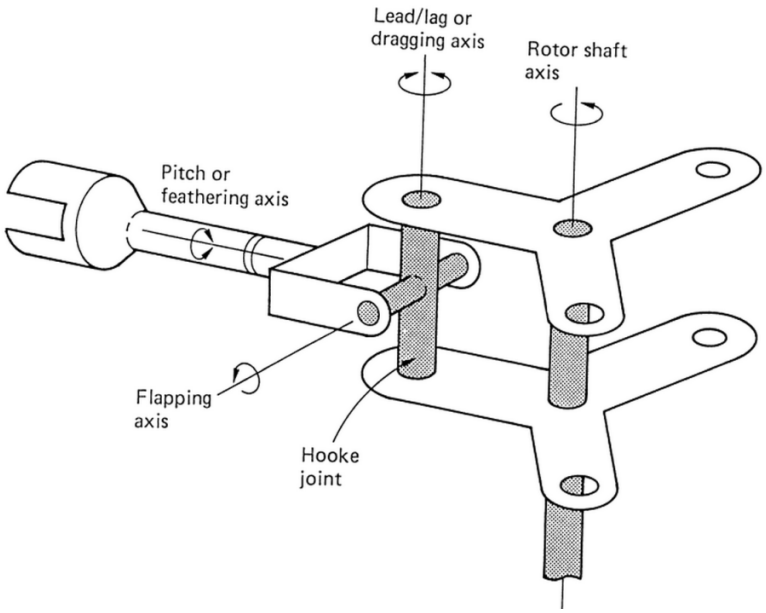

Figure 2.25: Structural simplification diagram of the articulated rotor head (Watkinson, 2003).

Feathering hinges are part of the blade's attack angle control system which controlled by a swashplate. The control structure of the rotor head showed in figure 2.22.

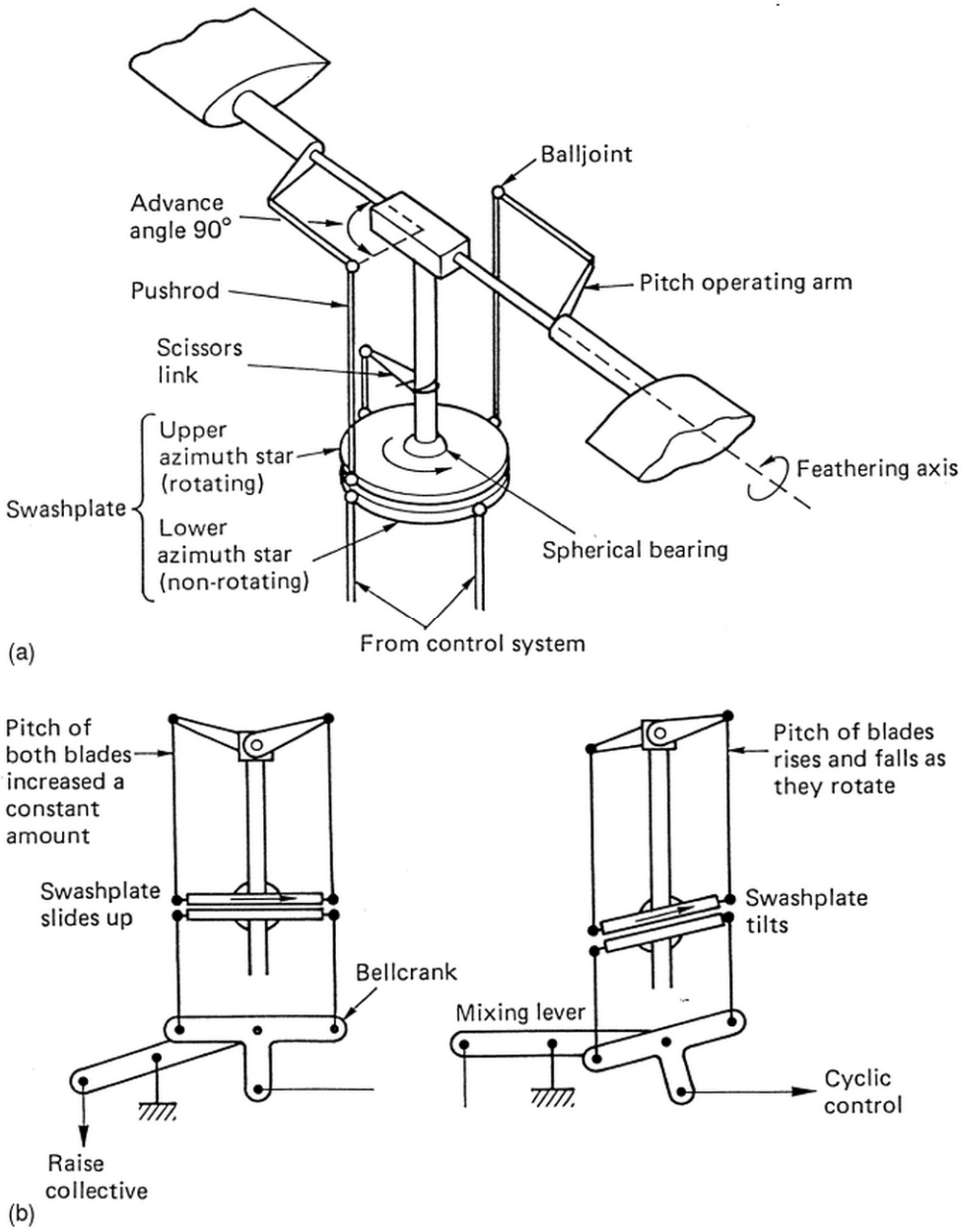

Figure 2.26: One of the control structure of the main rotor head (Watkinson, 2003).

According to figure 2.21 and figure 2.22, it is clear to see that the main rotor head structure is very complicated. Besides, one thing makes it more complicated. The rotor head is one of the most important parts of the helicopter; it needs to be extremely reliable and strong. However, because of the high rotate speed of the

rotor, these structures have to provide a strong centripetal force. That is the reason why the main rotor head is one of the heaviest parts of the helicopter (Watkinson, 2003).

Figure 2.27: The Sikorsky CH-53GS Main Rotor Assembly (Burkhard Domke, 2009).

2.4.1 Conclusion

As a result, the structure of the main rotor head is very complex and heavy. However, flying car has to use the rotor head. Thus, simplifying the rotor head structure is fully significant.

Chapter Three: The concept of the flight vehicle.

The previous chapter reviewed some relevant knowledge of flying cars and helicopters. For existing flying cars, although the size of the vehicle can be reduced by folding the fixed-wing, the need of runway takeoff and landing is an issue. Because of that, it is necessary to design a vertical take-off and landing flying car. The combination of cars and normal helicopters can be a good solution to solve the problem. However, due to the several reasons such as the requirement of tail rotors, the length of the blade beyond the car size restrictions and the heavy and complex normal rotor heads, it is not easy to combine them together. In this chapter, a twin foldable and tiltable rotors structure concept will be presented to solve this problem. And its theoretical calculation will be expressed in next chapter.

The aim of this thesis is to design a flight vehicle which means that the vehicle needs to have a similar car size and shape so that it can travel on normal roads. Considering the normal helicopter has a huge main rotor and a tail rotor so that it is not suitable for designing a flying car. This thesis will design a flying car based on twin rotors structure and truck structure. The twin rotors structure is similar to the Boeing V-22 which shows in figure 3.1 and figure 3.2. And the fuselage structure is similar to the truck which shows in figure 3.3.

Figure 3.1: The Boeing V-22 Osprey in hover flight (Martin, Demo and Daniel, 2000).

Figure 3.2: The Boeing V-22 Osprey in level flight (The Boeing Company, 2017).

Figure 3.3: ISUZU truck (Komarjohari, 2013).

The feature of the flying car is that its two rotors can be folded to the rear of the fuselage as a cargo for a truck to reduce the overall size when it is in driving mode. In order to achieve this feature, there are two problems need to be solved. The first

problem is that the V-22 only has tilt rotor mechanism but not have wing fold mechanism. The two rotors cannot be folded to rear. The second problem is that the engines of the V-22 are placed at the tips of each side of the fixed-wing, under its rotors. Compare with the V-22, the flight vehicle is quite small, so there is no small petrol engine can provide enough power to fit it. What is more, the engine under rotor arrangement will increase the weight and size of the rotor head which makes rotors hard to fold and store.

To solve these problems, the fold and tilt mechanism is arranged. Different from the V-22, the new structure arranged the tilt mechanism on the fuselage of the flying car. Meanwhile, a collapsible mechanism is added to each of the tilt structure, so the rotors can be stored to the rear of the flying car by using tilting and folding mechanisms. This design also determines that the rotors should be placed under the folding mechanism so that the rotors can be stored into the fuselage. The figure 3.4 shows the concept of the flight vehicle.

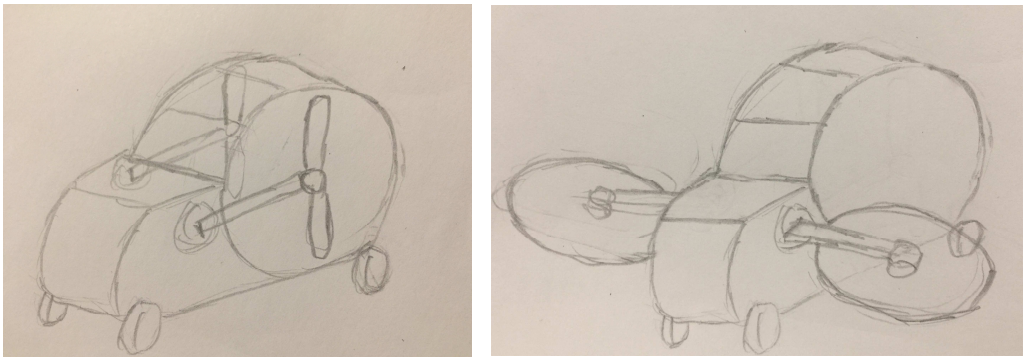

Figure 3.4: The concept of the flight vehicle

Due to the size limitation of the flying car, the two rotors were designed to be driven by only one motor which placed in the middle of the fuselage. The power transmission direction and shaft rotate direction shows in the figure below.

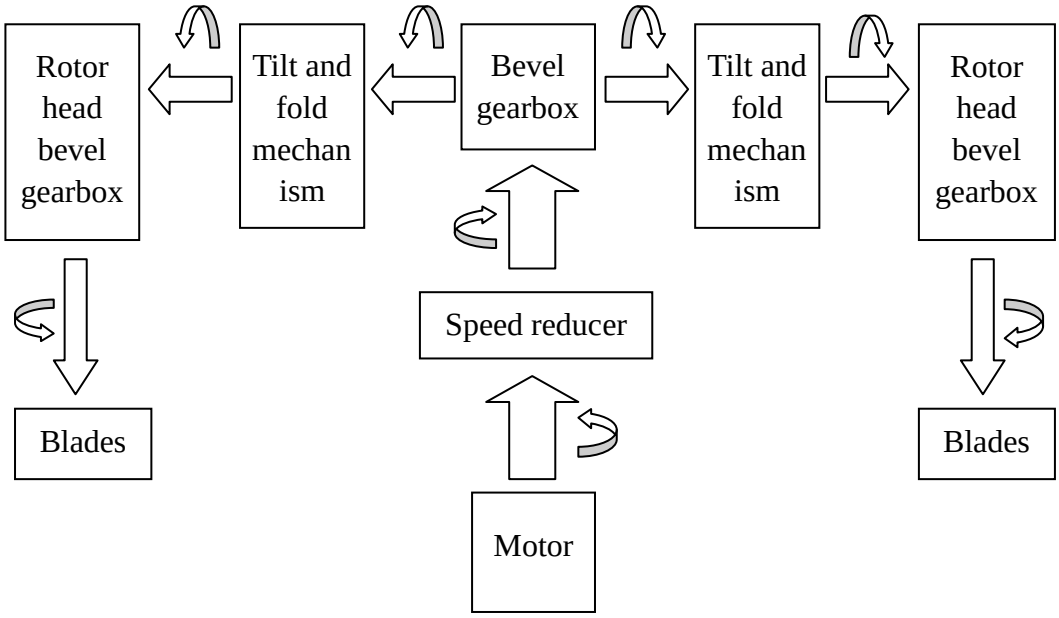

Figure 3.5: The power transmission direction and shaft rotate direction of the flight vehicle.

This arrangement will greatly simplify the rotor head structure. Figure 3.6 and figure 3.7 show the complete SolidWorks 3D model of the flight vehicle model.

Figure 3.6: The 3D model of the flight vehicle in driving mode

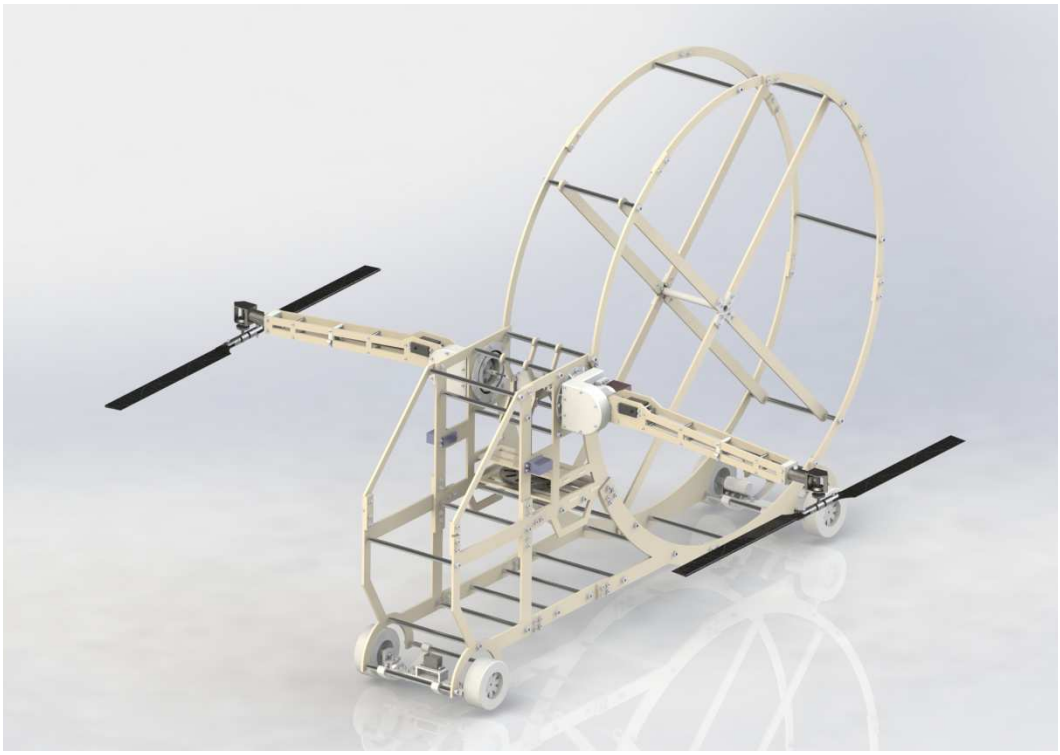

Figure 3.7: The 3D model of the flight vehicle in flying mode

Chapter Four: The theoretical calculation

As this research of the twin foldable and tiltable rotors flying car is not only in the early stages, but also with a limited budget, the project only designed and implemented a model for verifying the feasibility of the concept. This chapter will introduce the theoretical calculation of the lift and power required by the model. Meanwhile, based on the calculation and off-the-shelf components, the blades and motor of the model will be decided.

4.1 The lift calculation of each rotor.

According to the lift equation (NASA, 2015), the lift can be calculated as equation (4.1):

$$L = C_L \frac{\rho V_w^{\,2}}{2} A \qquad (4.1)$$

Where,

L is the lift of the flight vehicle model (N).

C_L is the lift coefficient (The C_L depends on the shape, Reynolds number and attack angle of the blade).

ρ is the density of air ≈ 1.205 kg/m^3 (20 ℃).

V_w is the average velocity of the wing (m/s).

A is the wing area (m^2).

The lift of the airfoil can be calculated. However, different from airfoils, blades are rotating. So the average velocity of the blade is the tip speed of the blade plus centre speed of the blade then divided by two which shows in equasion 4.2.

$$V = \frac{2\pi NR + 2\pi NR_1}{2} \tag{4.2}$$

Where,

V is the average velocity of the blade (m/s).

N is the blade rotate speed per second (rps)

R is the radius of the rotor (m).

R_1 is the radius of the rotor centre which equals to 0.

So, equation 4.2 can be written as:

$$V = \pi NR \tag{4.3}$$

Meanwhile, the wing area of the blade is equal to the blade area:

$$A = \sigma\pi R^2 = nwR \tag{4.4}$$

Where,

σ is the rotor solidity (The ratio of the area of the blades to the area of the blade rotation area).

w is the width of the blade (m).

n is the number of the blades.

According to equation (4.3) and (4.4), the lift equation (4.1) can be written as:

$$L = \frac{1}{2} C_L \rho \sigma N^2 \pi^3 R^4 \quad (4.5)$$

Or

$$L = \frac{1}{2} C_L \rho n w N^2 \pi^2 R^3 \quad (4.6)$$

4.2 The power calculation of each rotor.

The power requirements of the rotor are determined by the drag and speed of the rotor because of the power formula. The induce drag of the blade shows in Figure 4.1. In this figure, 4.1(a) shows the relative air flow (RAF) changes by blade. Figure 4.1(b) shows how the direction of reaction of blade is found when the air is assumed to be inviscid (having no viscosity). The original velocity direction of the RAF changed to the new velocity direction. Due to the inviscid air, the relative airspeed does not change, only the direction. The acceleration to change original velocity to new velocity direction must have been in the direction of the vector V_a so the reaction must be in the opposite direction. It can be seen that this is at right angles to the average airflow direction. And the average airflow direction is the attack angle of the blade. According to the 4.1(b) the induce drag can be calculate according to equation (4.7). Figure 4.1(c) shows that the reaction is increased by increasing the angle of attack since this has the effect of increasing the change of velocity (Watkinson, 2003).

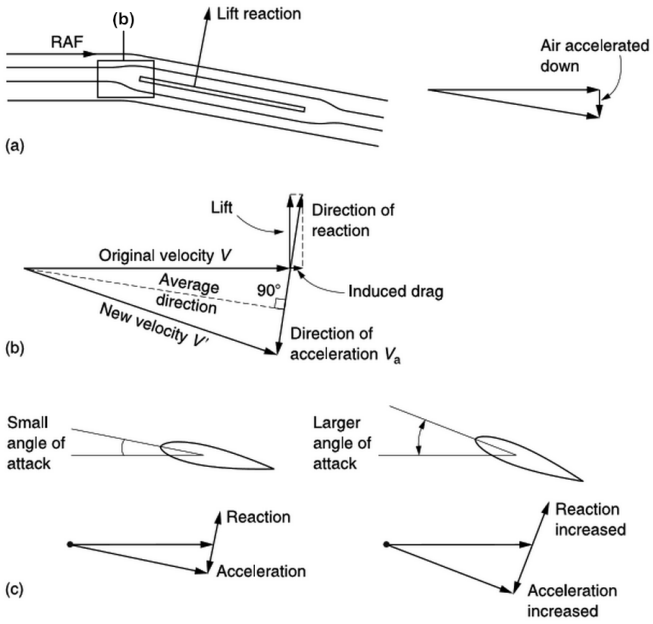

Figure 4.1: The lift and induce drag of the blade (Watkinson, 2003).

$$f_i = (\tan \alpha)L \tag{4.7}$$

Where,

f_i is the induced drag of the blade (N).

α is the attack angle of the blade.

Except the induce drag, there is another drag affecting the blade when it is rotating: the profile drag. The profile drag is determined by C_d (the profile coefficient of the blade) which depends on the shape, Reynolds number and attack angle of the blade.

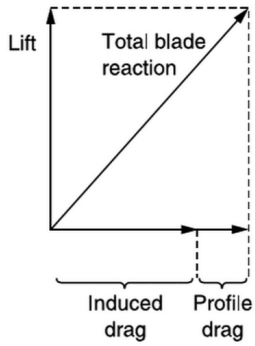

Figure 4.2: The induced drag and profile drag (Watkinson, 2003).

The profile drag equation shows in equation 4.7. The induced drag equation shows in equation 4.8.

$$f_p = \frac{C_d}{C_L} L \tag{4.8}$$

Where,

f_p is the profile drag of the blade (N).

C_d is the profile coefficient of the blade. (The C_d depends on the shape, Reynolds number and attack angle of the blade).

So, according to equation (4.6), (4.7) and (4.8), the total drag of the blade can be written as:

$$F_d = f_p + f_i$$

$$F_d = \frac{1}{2}\left(\frac{C_d}{C_L} + \tan\alpha\right) C_L \rho n w N^2 \pi^2 R^3 \tag{4.9}$$

Where,

F_d is the total drag of the blade.

According to the power equation,

$$P = F_d V \tag{4.10}$$

Where,

P is the power requirement of the rotor (W).

V is the average velocity of the blade (m/s).

And substitute equation (4.3), (4.5), (4.6) and (4.9) into equation (4.10), the equation (4.10) can be written as:

$$P = \frac{1}{2}\left(\frac{C_d}{C_L} + \tan\alpha\right) C_L \rho \sigma N^3 \pi^4 R^5 \tag{4.11}$$

Or

$$P = \frac{1}{2}\left(\frac{C_d}{C_L} + \tan\alpha\right) C_L \rho n w N^3 \pi^3 R^4 \tag{4.12}$$

4.3 The rotor head, blades and motor of the flight vehicle model.

Since the rotor head is the most basic part of the flight vehicle model, the design of the model starts from it. According to the concept, because the flight vehicle have two rotors and using the tilt structure to control roll and pitch, so there is no

need to use main rotor head of the normal helicopter model. The tail rotor head of the helicopter model can meet the requirements.

Figure 4.3: The Align T-REX 700X helicopter model (Align, 2014).

Figure 4.4: The main rotor head of the 700X helicopter model (Align, 2014).

As the figure 4.4 shows, the main rotor head structure is complicated. The use of tail rotor head will simplify the structure of the rotor head and it shows in figure below.

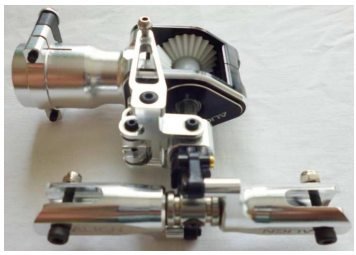

Figure4.5: Tail rotor head (Heli Freak, 2016).

For the blades, there are several shapes and sizes for the main blades of the model helicopter. However, only a few of them can be connected with tail rotor head. Moreover, because the rotate directions of the two rotors of the flying car model are opposite, so the up arc and down arc of the blades needs to be symmetry as figure 4.5 shows.

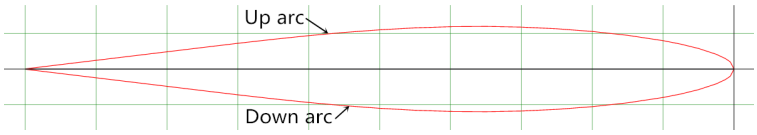

Figure4.6: The arc symmetrical blade shape (Airfoil Tools, 2017).

Taking into account the size of the model and the reasons above, the 380mm blades was chosen as the blades of the model. Its shape shows in figure 4.7. And its overall view shows in figure 4.8.

Figure4.7: The 380mm blade shape.

Figure 4.8: The 380 blades (Ebay, 2017).

According to the actual measurement of the 380mm blade, the length of the blade from tip to the centre of the connect hole is 380mm and the width of the blade is 33.82m. Meanwhile, according to the actual measurement of the tail rotor head, the length from the shaft to the blade connection hole is 35 mm. So the rotor radius of the 380mm blade is 415mm. In other words, the R=0.415m, w=0.03382m.

The Reynolds number is one of the reason affect the C_L of the blade. The equation of Reynolds number shows below:

$$\mathrm{Re} = \frac{\rho w V}{\mu} \tag{4.13}$$

Where,

ρ is the density of air ≈ 1.205 kg/m^3 (20 ℃).

V is the average velocity of the blade (m/s).

w is the width of the blade (m)

R is the radius of the rotor (m).

*μ is the dynamic viscosity of the air ≈ 1.821*10^{-5} kg/ms (20 ℃).*

Substitute equation (4.3) into the equation (4.13), the equation of Reynolds number can be written as:

$$\mathrm{Re} = \frac{\rho w \pi N R}{\mu} \tag{4.14}$$

Because the size of the blades is determined, so equation (4.14) shows that the Re depends on the rotate speed of the blades.

According to the data of the blade, the C_L and attack angle α change of this blade shows as figure 4.9.

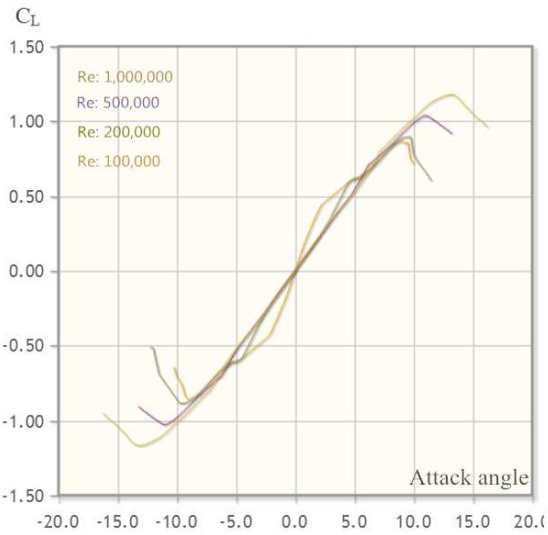

Figure 4.9: The C_L changes with the attack angle of blade (Airfoil Tools, 2017).

The C_d and attack angle α change of this blade shows as figure 4.10.

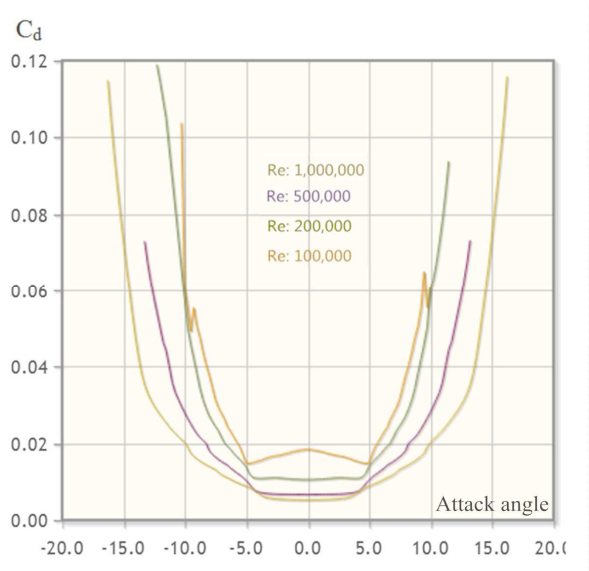

Figure 4.10: The C_d changes with the attack angle of blade (Airfoil Tools, 2017).

Assume:

Blades attack angle α is 9 degree (Because the speed of the rotor is not determined now, so take the value of the lowest C_L turning to calculate).

The model weights 6.5kg (Estimate).

The payload of the model is 1kg.

So based on the figure 4.9, the C_L of the blades is nearly 0.9 as figure 4.11 shows.

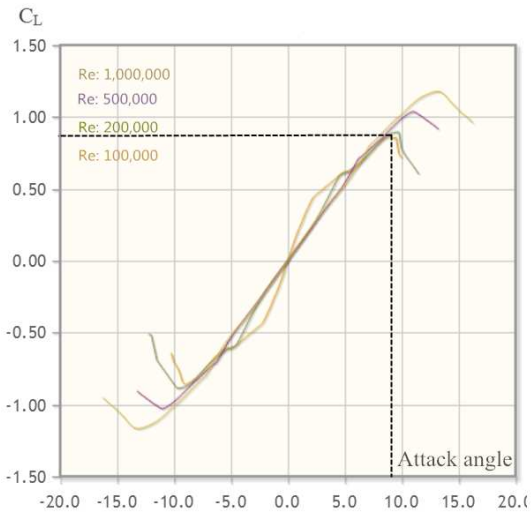

Figure 4.11: The C_L of the blade when attack angle is 9 degree (Airfoil Tools, 2017).

The lift requirement of the flight vehicle model can be calculate according to the gravity equation:

$$G = mg \tag{4.15}$$

Where,

m is the mass of the flight vehicle model should lift (kg).

g is the gravitational acceleration ≈ 9.8 m/s^2.

However, due to there are two rotors, so the equation (4.15) can be expressed as

$$2L = mg$$

So the lift requirement of each rotor of the model is

$$L = \frac{(6.5 + 1) \times 9.8}{2}$$

$$L = 36.75N \tag{4.16}$$

This means the lift of each rotor of the flight vehicle model should be 36.75N.

Choose C_L=0.9, R=0.415m, w=0.03382m, L=36.75N and the number of the blades are two, so substitute them into equation (4.6), the rotate speed can be calculated as below:

$$L = \frac{1}{2} C_L \rho n w N^2 \pi^2 R^3$$

$$36.75 = \frac{1}{2} \times 0.9 \times 1.205 \times 2 \times 0.03382 \times N^2 \times \pi^2 \times 0.415^3$$

Where,

π is the circumference ratio ≈ 3.14

Hence,

$$N \approx 37.69\text{rps} \tag{4.17}$$

The blade rotate speed per minute (rpm) can be written as:

$$N_m = 2261.4\text{rpm} \tag{4.18}$$

Where,

N_m is the blade rotate speed per minute (rpm).

Substitute equation (4.17) into equation (4.14), the Re can be written as:

$$\mathrm{Re} = \frac{\rho w \pi N R}{\mu}$$

$$\mathrm{Re} \approx \frac{1.205 * 0.03382 * 3.14 * 37.69 * 0.415}{1.821 * 10^{-5}}$$

$$\mathrm{Re} \approx 109914.4 \qquad (4.19)$$

Based on the result of Re, the C_d of the blades can be determined as 0.063 as figure 4.12 shows.

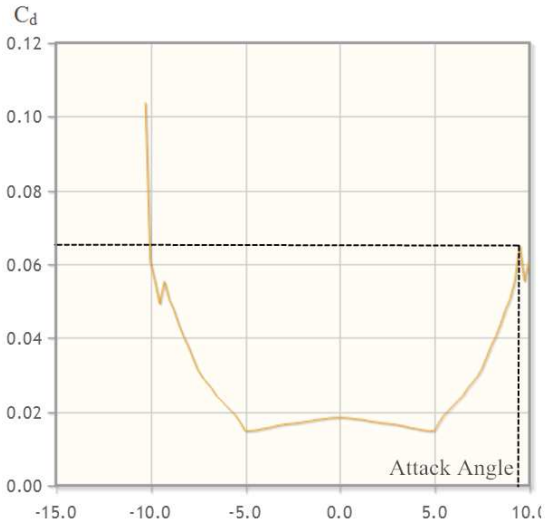

Figure4.12: The C_d of the blade when attack angle is 9 degree and Re is 100000 (Airfoil Tools, 2017).

According to C_L=0.9, C_d=0.063, α=9°, n=2, w=0.03382m, N=37.69rps, R=0.415m and equation (4.12), the power requirement of each rotor can be calculated as follows:

$$P = \frac{1}{2}\left(\frac{C_d}{C_L} + \tan\alpha\right) C_L \rho n w N^3 \pi^3 R^4$$

$$P = \frac{1}{2}\left(\frac{0.063}{0.9} + \tan 9°\right) 0.9 \times 1.205 \times 2 \times 0.03382 \times 37.69^3 \pi^3 0.415^4 \quad (4.20)$$

$$P \approx 412.5W$$

Because the flight vehicle model has two rotors, so:

$$P_r = 2P = 412.5 * 2 = 825W \quad (4.21)$$

Where,

P_r is the power requirement of two rotors.

According to the concept, one spur gear set and four bevel gear sets were estimated to be used between the motor and the rotors. The transmission efficiency of spur gears is higher than 97% and the transmission efficiency of bevel gears is higher than 95% (Jelaska, 2012). The electrical motor minimum nominal efficiency is approximately 78.8% (The engineering ToolBox, 2017). So the minimum power requirement of motor is express as below:

$$P_m = \frac{P_r}{0.95^4 * 0.97 * 0.788}$$

$$P_m \approx 1325W \quad (4.22)$$

Where,

P_m is the power requirement of the motor.

According to the result of equation (4.22), the motor should provide at least 1325W power. But, considering the other power loss during the transmission (such as bearings friction loss and universal joints efficiency), the power of motor should be greater than this value. For the sake of insurance and easy to modify the model, the power of the motor should be at least half larger than this value (at least $1325 \times 1.5 = 1987$W). Meanwhile, it is best that the motor have a matching main reduction gear set due to the high speed of the motor. Through the comparison of the motor online, the ALIGN HML73M01 730MX motor was chosen. The reasons for choosing this motor are:

1. Powerful: It can provide 2550W power by using 6 cells Li-polymer battery (22.2V). The power of this motor meets the requirement of the model and gives some spaces for modification.

2. Reduction gear set: This motor has its own speed reduction gear set (Gear set radio is 11:112). According to the voltage and the KV value (KV: 850) of the motor, the rotate speed of the motor is 18870 rpm. The rotate speed after the speed reducer is 1853.3rpm. Due to the equation (4.18), rotate speed of rotors should be 2261.4rpm. To achieve the 2261.4rpm rotate speed, it is necessary to design another transmission to increase the rotate speed of the rotors. A gear set (radio: 40:32) is designed to raise the rotate speed of the rotors. They will be shown in the next chapter. By using this gear set, the rotor speed will reach approximately 2307rpm.

4.4 Conclusion

This chapter calculated the lift and power requirements of the flight vehicle. At the same time, Blades, motor and speed reducer was determined. Based upon them, the next chapter will introduce the mechanical design and implementation of the whole structure of the model.

Chapter Five: Mechanical design and Implementation

This chapter will first design and assemble the 3D model of the flying car model on computer based on the concepts and data from the previous chapter. During that process, some parts are procured because the design is based on the off-the-shelf parts. Thereafter, according to the 3D model, the remaining parts will be purchased and implemented. Finally, the real model will be implemented.

5.1 Mechanical design

From the initial concept to the final 3D model, several experimental models were designed. This thesis only introduces the final model. The model can be roughly divided into three main parts: the flight part, the fuselage part and the land driving part which show in the figure 5.1. And the three main parts will be introduced separately.

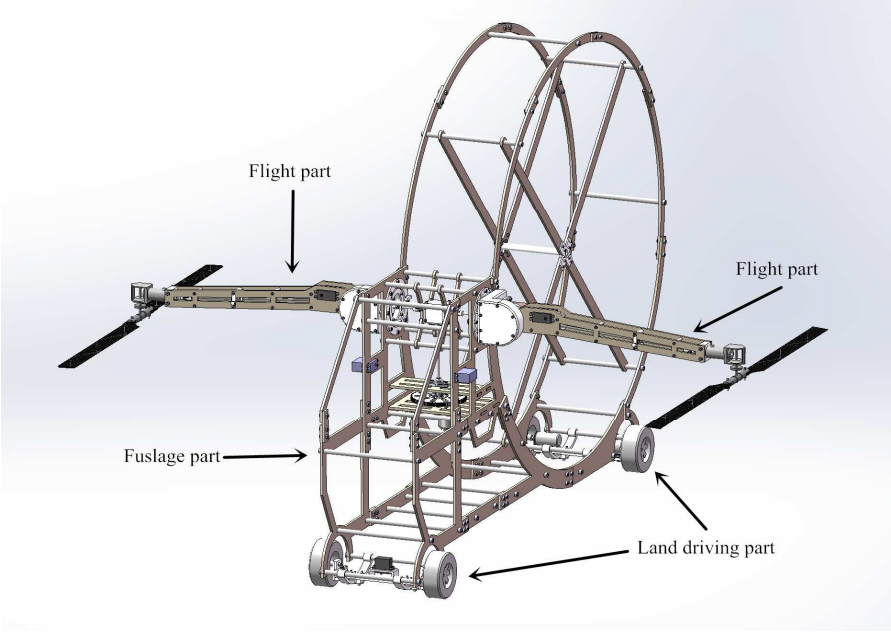

Figure5.1: The composition of the flight vehicle model

5.1.1 The flight part

The flight part is use to connect the blades and the fuselage. Meanwhile it allows the blades to tilt and fold. This part mainly contains the rotor head (which is the tail rotor head of the helicopter model), rotor head connector, auxiliary gearbox, main gearbox, servo rotor (which controls the blade attack angle), shaft, universal joint, shaft support structure, blade attack angle control lever supporter and rotor arm. It shows in figure 5.2 (blade attack angle control lever is not shown in the figure because it designed based on actual measurements).

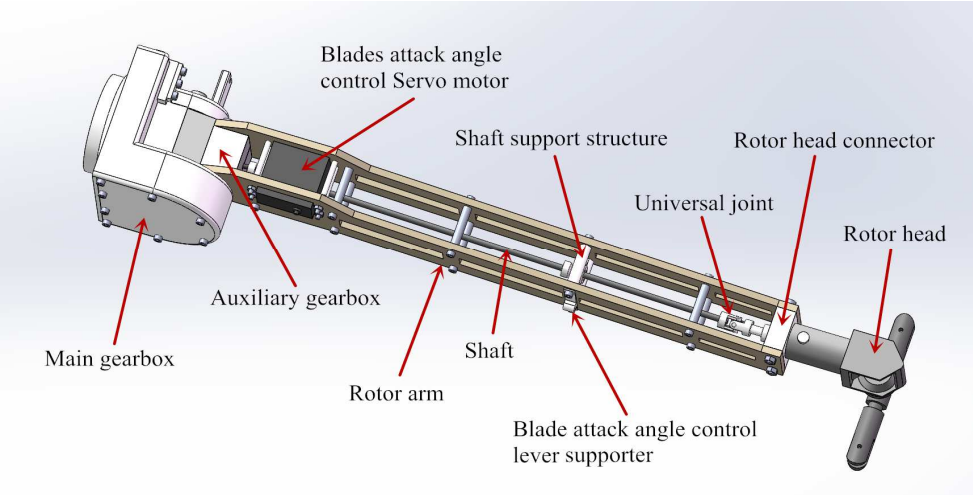

Figure5.2: The flight part

5.1.1.1 The main gearbox and auxiliary gearbox.

The auxiliary gearbox designed to be small so that it can engaged with main gearbox and have space for the bearings. The complete assembly of the auxiliary gearbox shows in figure 5.3 and its assembly process shows in figure 5.4 to figure 5.6.

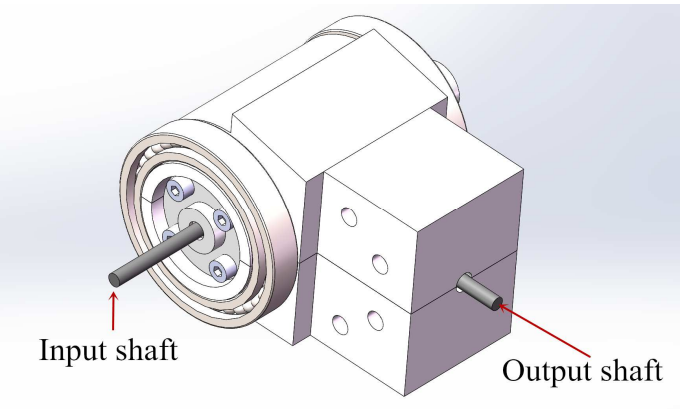

Figure 5.3: The completed assembly of auxiliary gearbox

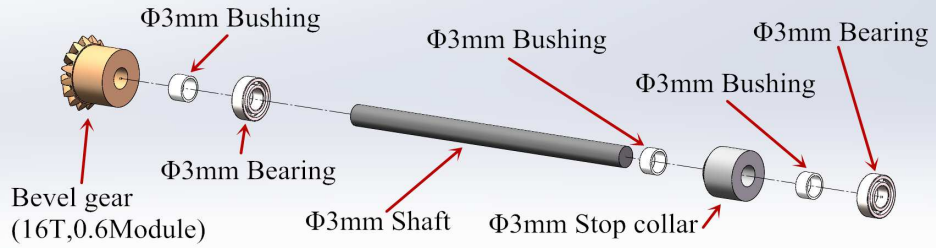

Figure 5.4: The assembly of the input shaft

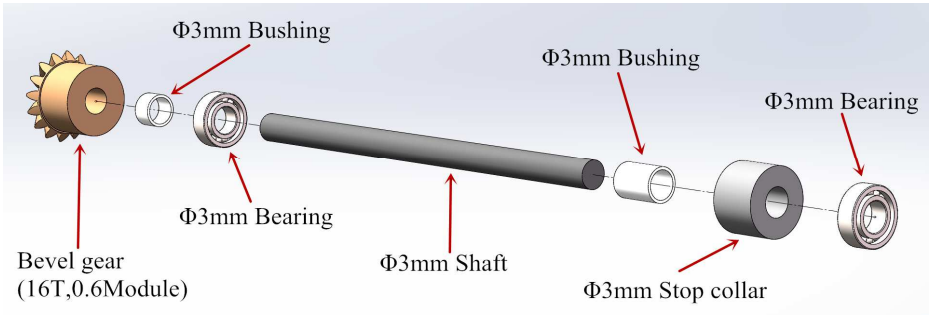

Figure 5.5: The assembly of the output shaft

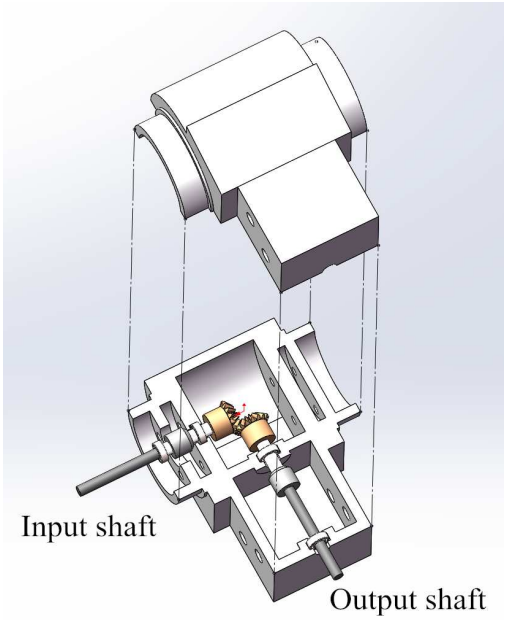

(a)

Figure 5.6: The assembly process of auxiliary gearbox (Continue on next page)

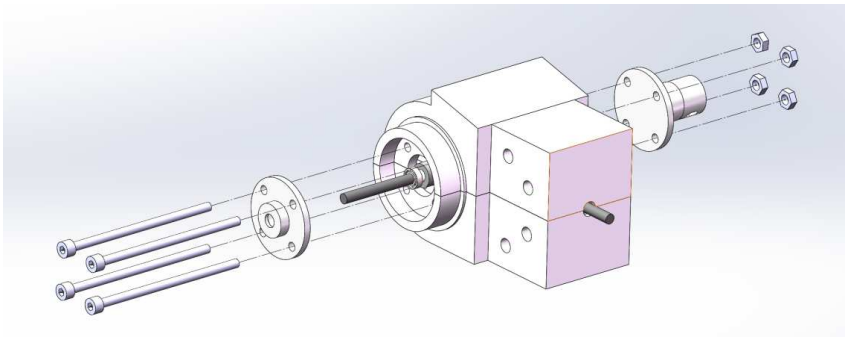

(b)

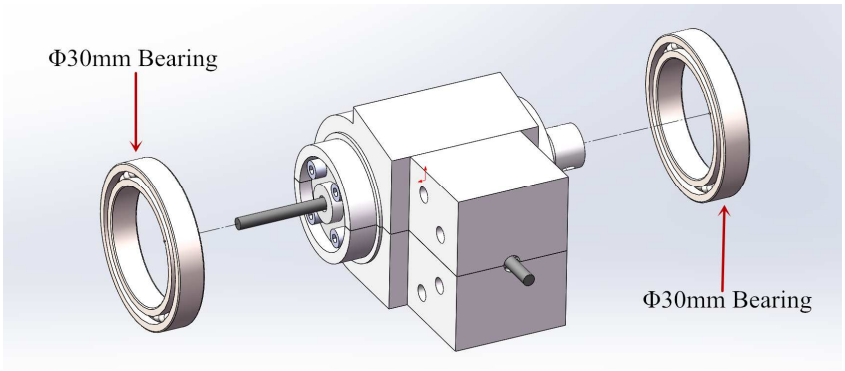

(c)

Figure 5.6: The assembly process of auxiliary gearbox

Figure 5.4 and 5.5 shows the input shaft and output shaft assembly process. Figure 5.6 (a) shows the shafts arrangement in the designed parts and figure 5.6 (b) and (c) show the assembly process of the designed parts with screws and Φ30mm bearings.

The auxiliary gearbox is engaged with the main gearbox. The main gearbox complete assembly with the auxiliary gearbox shows in figure 5.7 (a) and (b). And their assembly process shows in figure 5.8.

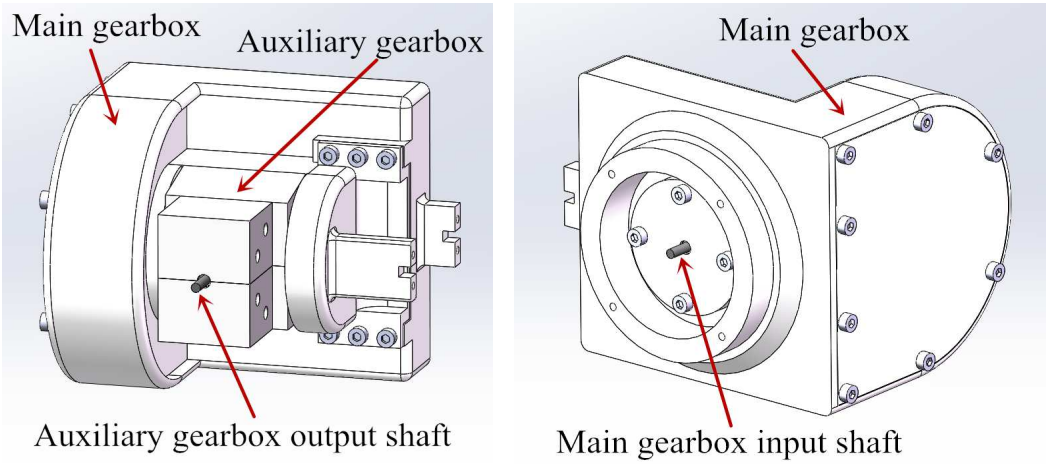

(a) (b)

Figure 5.7: The completed assembly of the main gearbox with the auxiliary gearbox

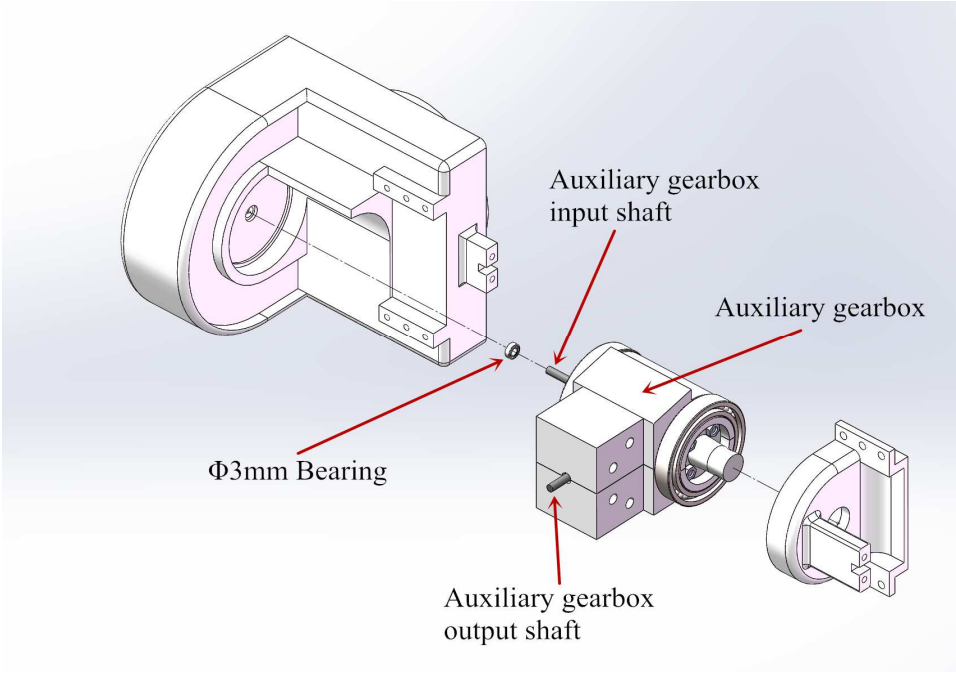

(a)

Figure 5.8: The assembly process of the main gearbox and the auxiliary gearbox

(Continue on next page)

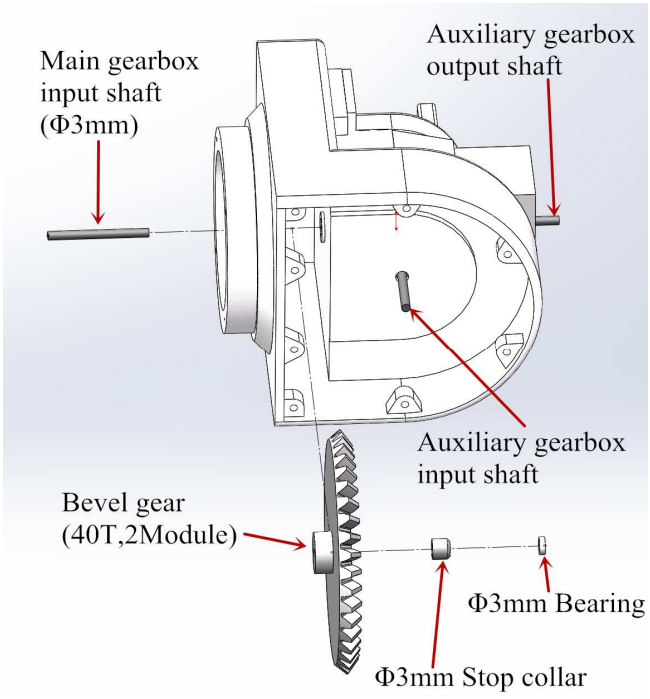

(b)

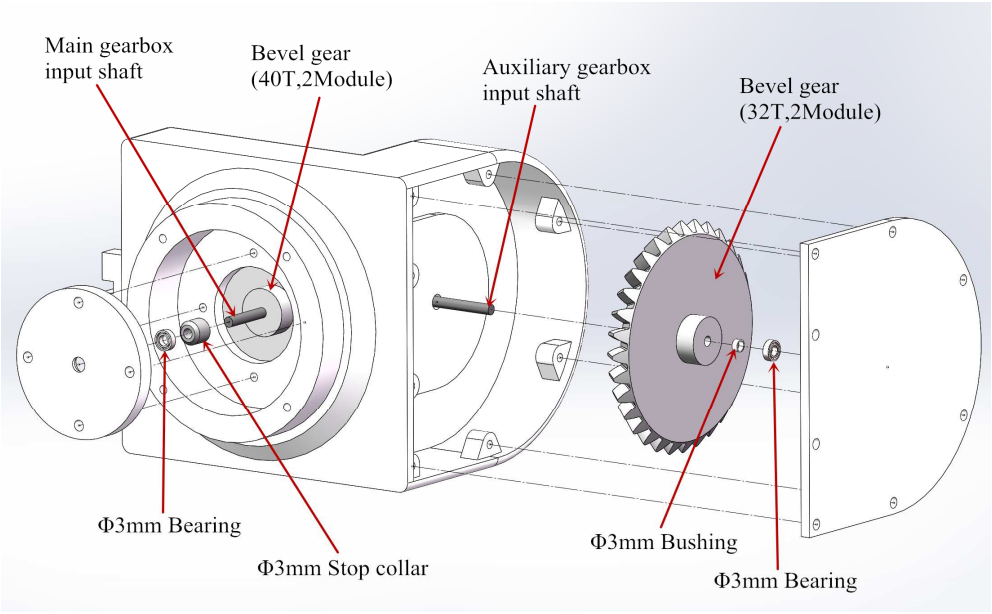

(c)

Figure 5.8: The assembly process of the main gearbox and the auxiliary gearbox

The figure 5.8 (a) shows the engagement of the main gearbox and auxiliary gearbox. Figure 5.8 (b) shows the process of installing bevel gear (40T, 2Module)

into the main gearbox. The bevel gear (40T, 2Module) is plugged in the gearbox. The figure 5.8 (c) shows the other bevel gear (32T, 2Module) is assembled with the main gearbox. The bevel gear is installed on the auxiliary gearbox input shaft. The figure also shows how the main gearbox sealed.

The figure 5.9 shows the cross section of the complete assembly of main gearbox and auxiliary gearbox. Figure 5.10 shows the assembly of the two gearboxes with the fuselage and rotor arm (exterior) and figure 5.11 shows their interior details.

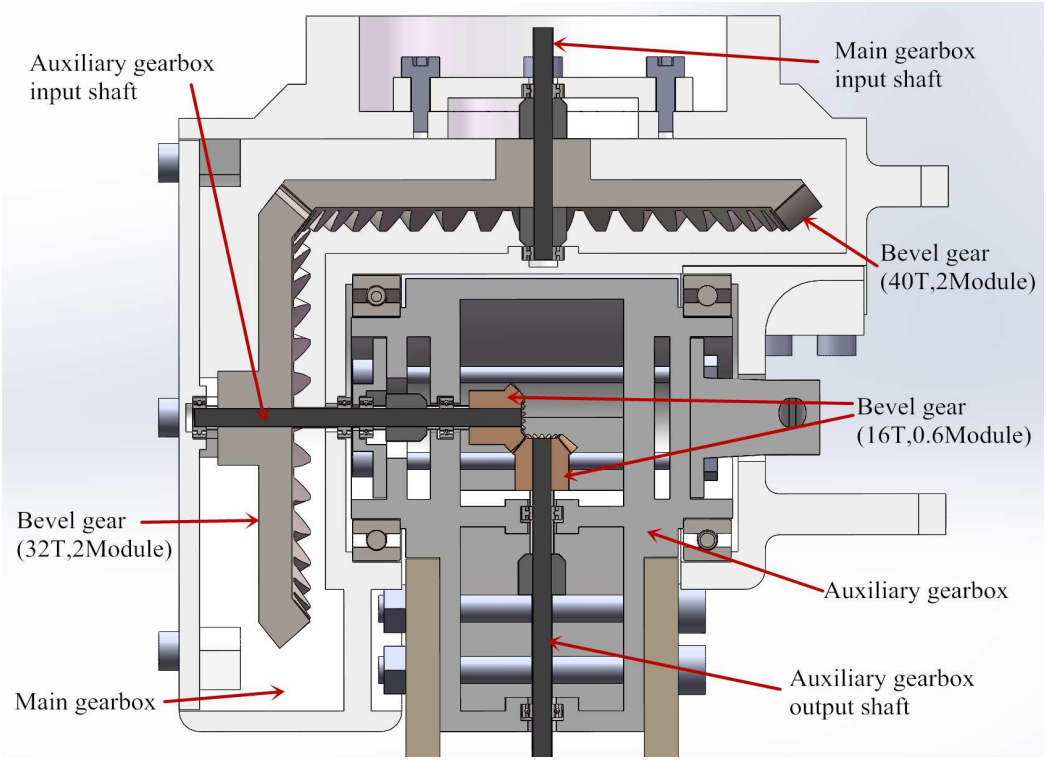

Figure 5.9: Cross section of the complete assembly of main gearbox and auxiliary gearbox

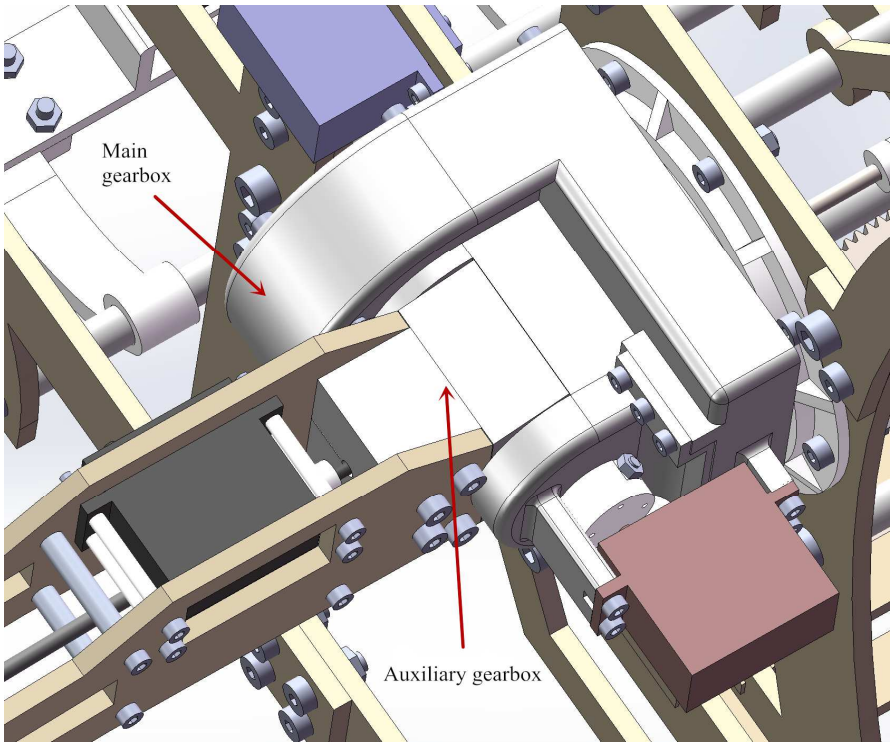

Figure 5.10: The exterior of the gearboxes

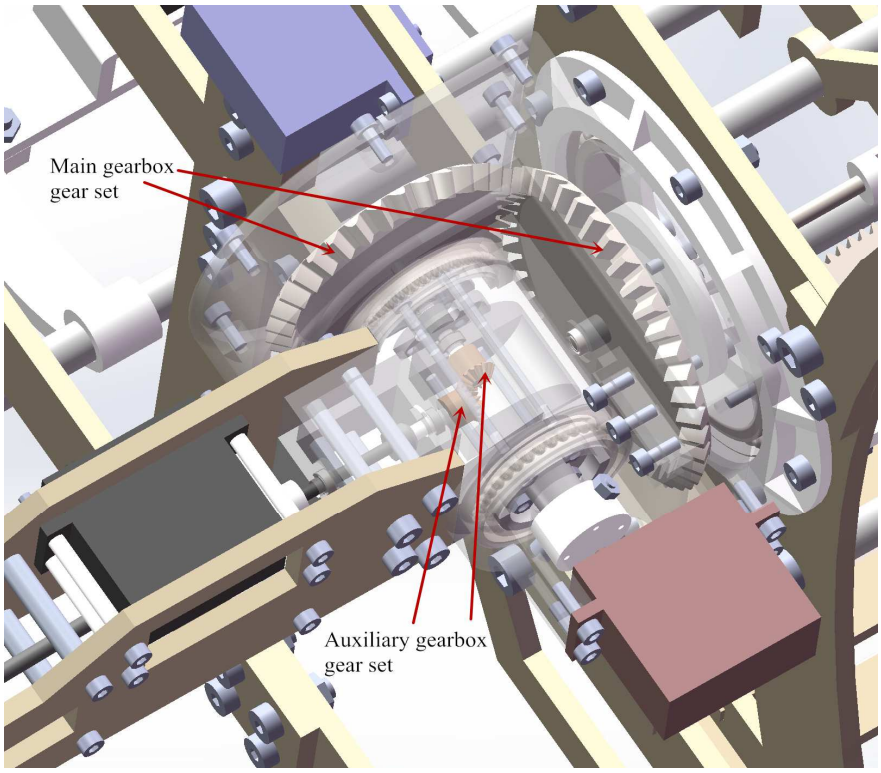

Figure 5.11: The interior of the gearboxes

In the actual installation, the auxiliary gearbox must first be installed with the rotor arm and then engage with the main gearbox. Here they are combined together for the introduction of convenience. The connection of the auxiliary gearbox and rotor arm shows in the 5.1.1.3 section.

5.1.1.2 The design and assembly of the rotor head connector.

The rotor head connector is used to connect the rotor arm to the rotor head (which is the tail rotor head of the helicopter model). The complete assembly of the rotor head connector with the rotor head shows in figure 5.12.

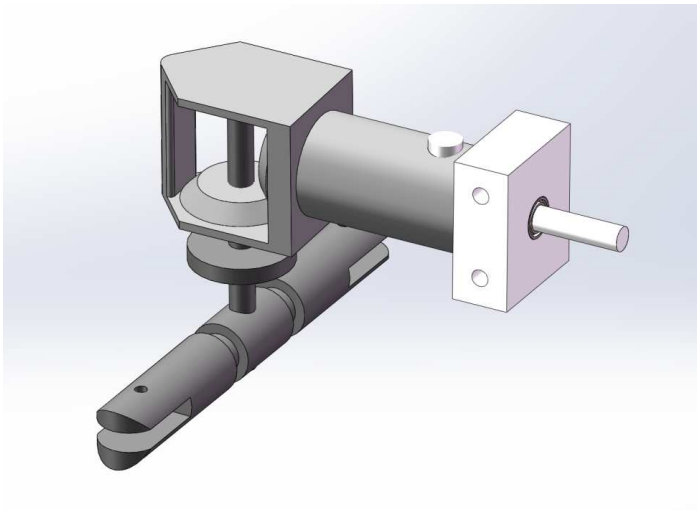

Figure 5.12: The complete assembly of the rotor head connector with the rotor head

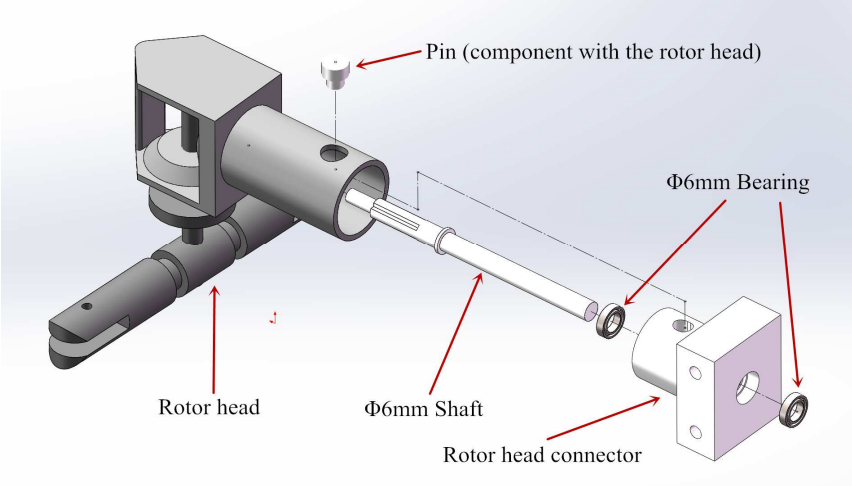

Figure 5.13: The assembly process of the tail rotor connector

Figure 5.13 shows how the rotor head connector connects with the rotor head.

5.1.1.3 The design and assembly of the rotor arm.

The rotor head connector is connected with the auxiliary gearbox by a rotor arm. The complete assembly of the rotor arm with the rotor head and auxiliary gearbox shows in the figure below.

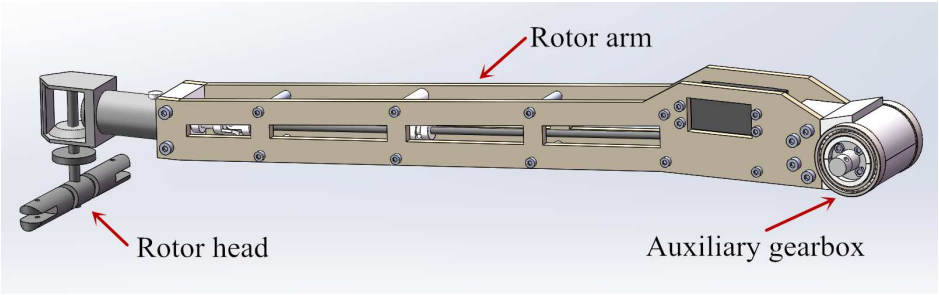

Figure 5.14: The complete assembly of the rotor head, the auxiliary gear box and the rotor arm

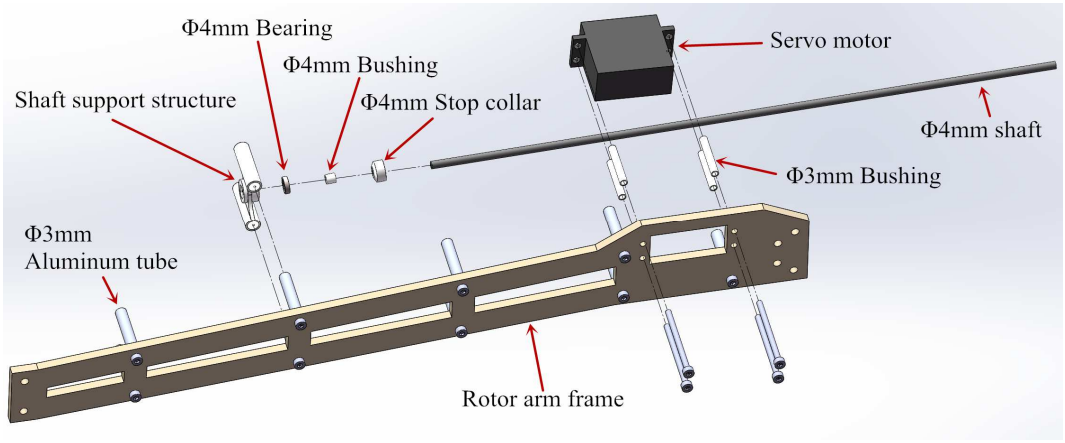

(a)

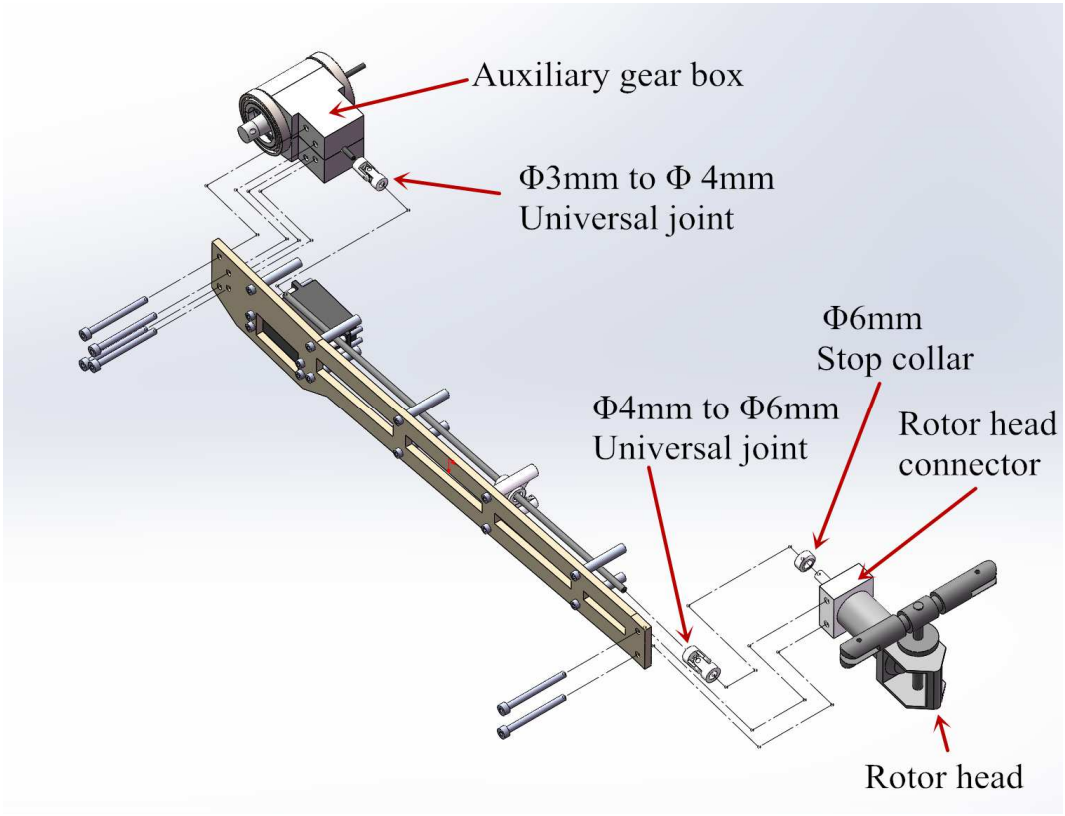

(b)

Figure 5.15: The assembly process of the rotor arm (Continue on next page)

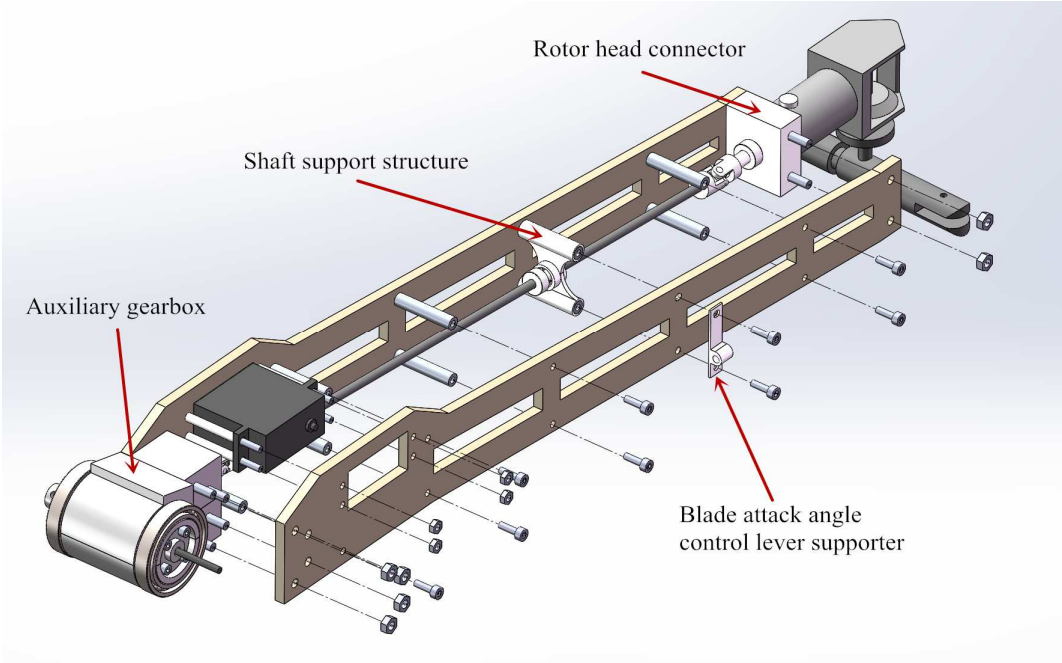

(c)

Figure 5.15: The assembly process of the rotor arm

Figure 5.15 (a) shows the shaft and servo motor are installed on the rotor arm frame. Figure 5.15 (b) shows the installation of the auxiliary gearbox, rotor arm and rotor head connector. Two universal joints are used to connect the Φ4mm shaft with the output shaft of the auxiliary and the rotor head connector shaft. Figure 5.15 (c) shows the blade attack angel control lever supporter is installed on the rotor arm.

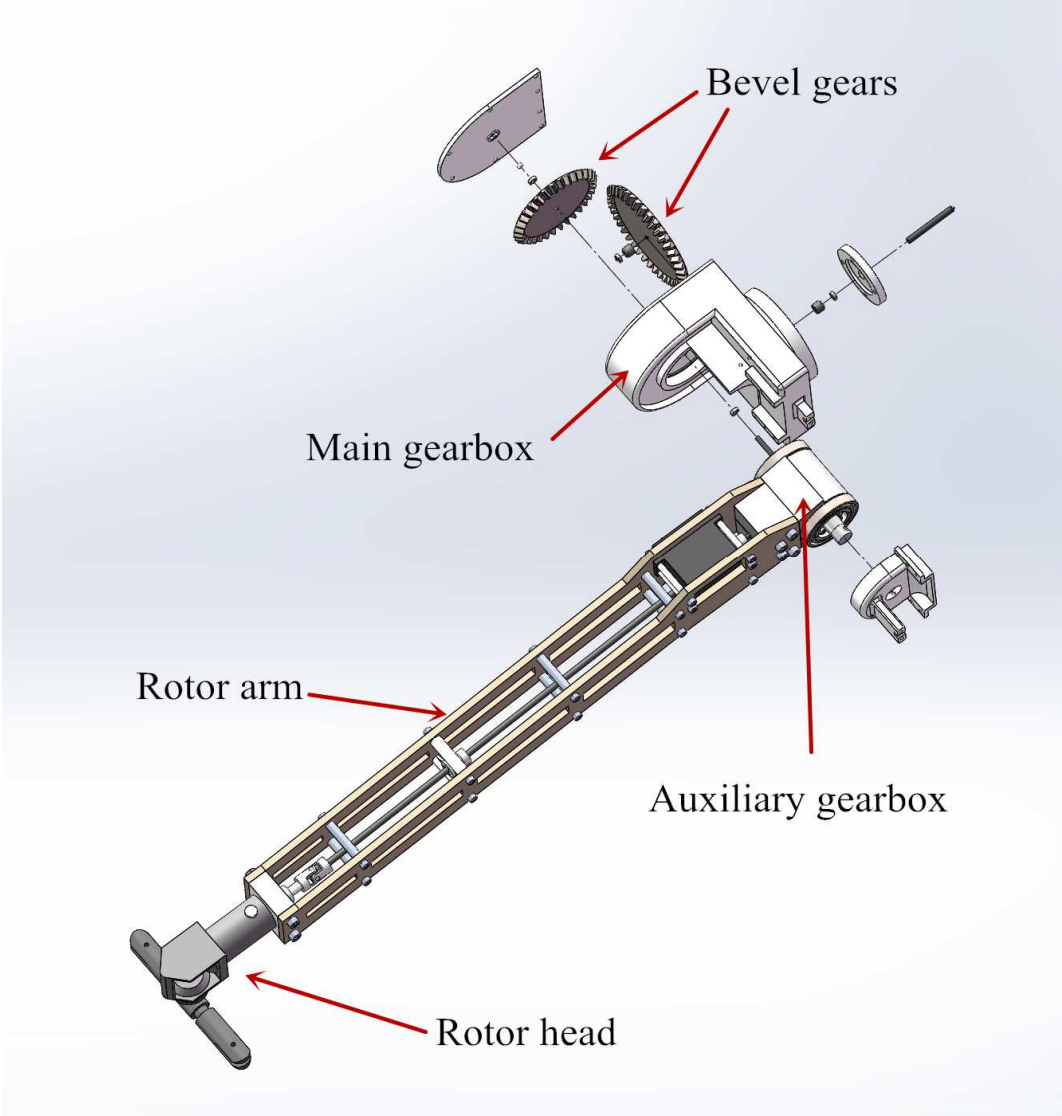

Figure 5.16: The assembly process of the main gearbox and auxiliary gearbox with rotor arm.

Figure 5.16 shows the assembly of the main gearbox and auxiliary gearbox with rotor arm. The connect process can refer to the figure 5.8.

The complete assembly of the main gearbox and auxiliary gearbox with rotor arm shows in the figure 5.17 and 5.18.

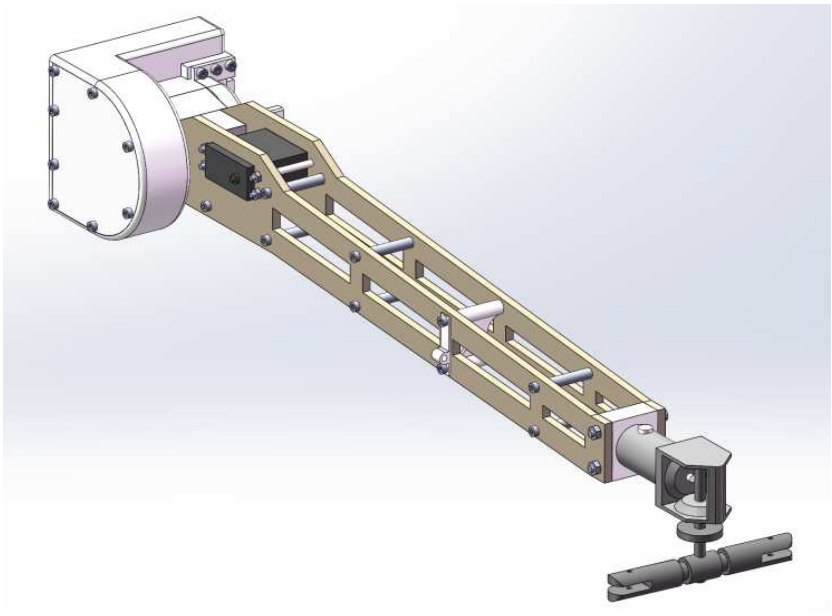

Figure 5.17: Flight part (Open)

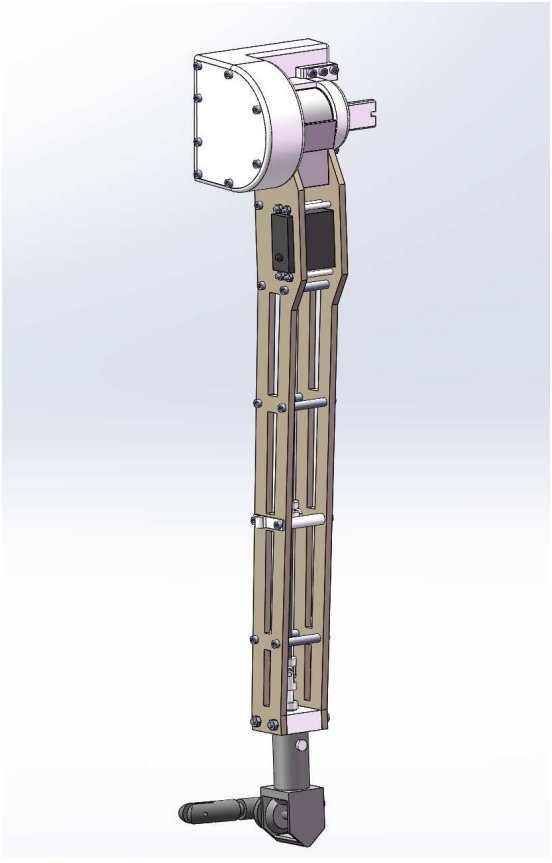

Figure 5.18: Flight part (Fold)

5.1.2 The fuselage part.

The fuselage part consists of the speed reducer, the fuselage frame, the rotor container and the bevel gearbox which show as the figure below. The speed reducer contains the motor, speed reduction gear set (the motor gear and main gear which reduce the motor speed from 18870rpm to 1853.3rpm) and motor bracket (fix the motor and speed reduction gear set). The Bevel gearbox is used to divide and transmit the power from the motor to the two rotor arms. The rotor container is used to store and support the blades in the fuselage.

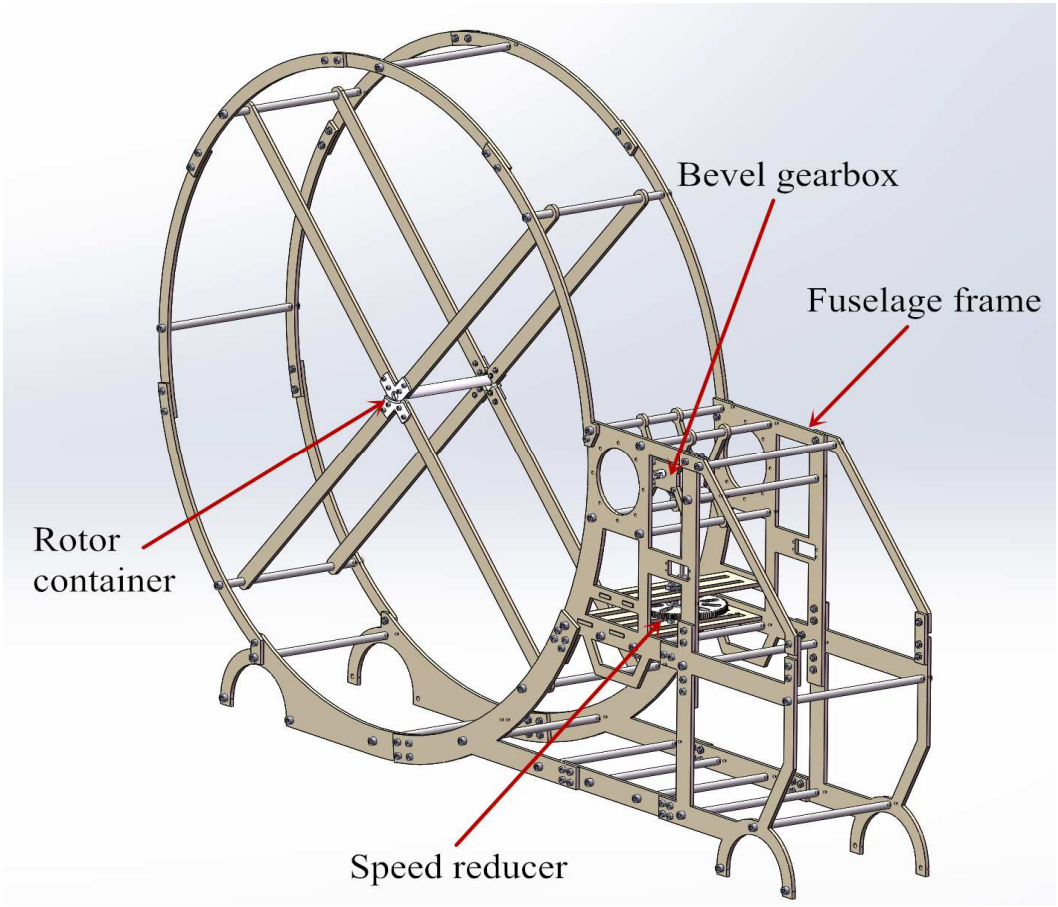

Figure 5.19: The fuselage part of the flight vehicle model.

5.1.2.1 The design and assembly of the speed reducer

The speed reducer is used to place the motor and the main gear of the flight vehicle model and reduce the rotate speed of the motor. For the position of the motor, it should be as low as possible to keep the gravity of center low. However, considering the stability of the main shaft, it is placed in the middle of the model. The radio of the motor gear and the speed reduce gear is 11:112. The complete assembly of the speed reducer shows in figure 5.20.

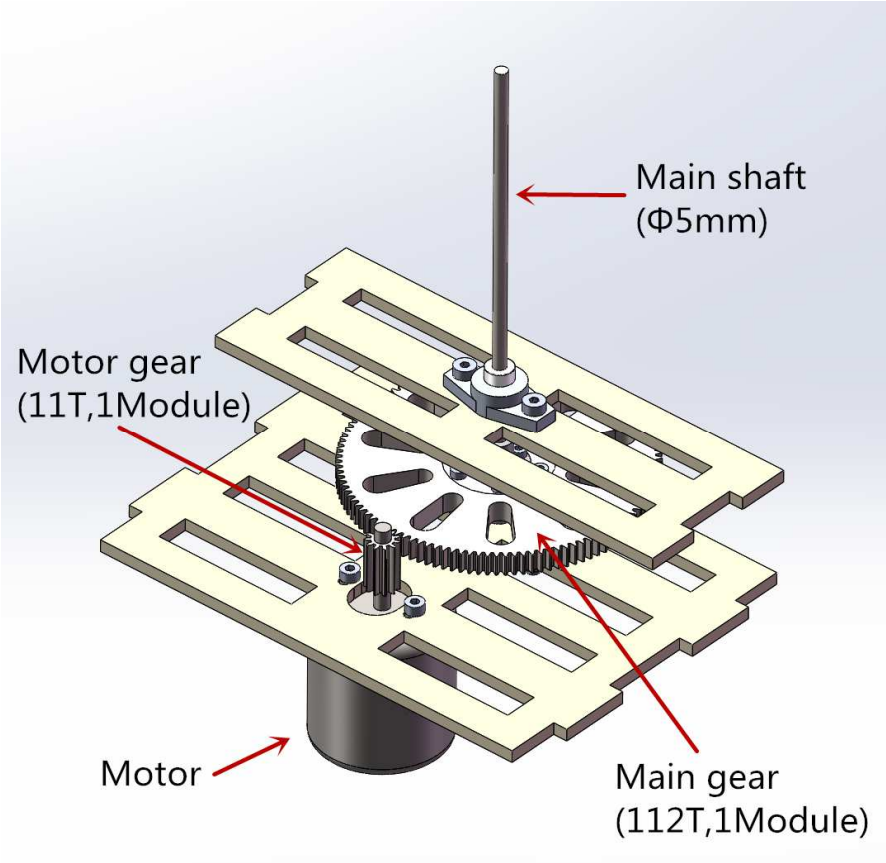

Figure 5.20: The speed reducer

The main gear complete assembly shows in figure 5.21.

Figure 5.21: The main gear

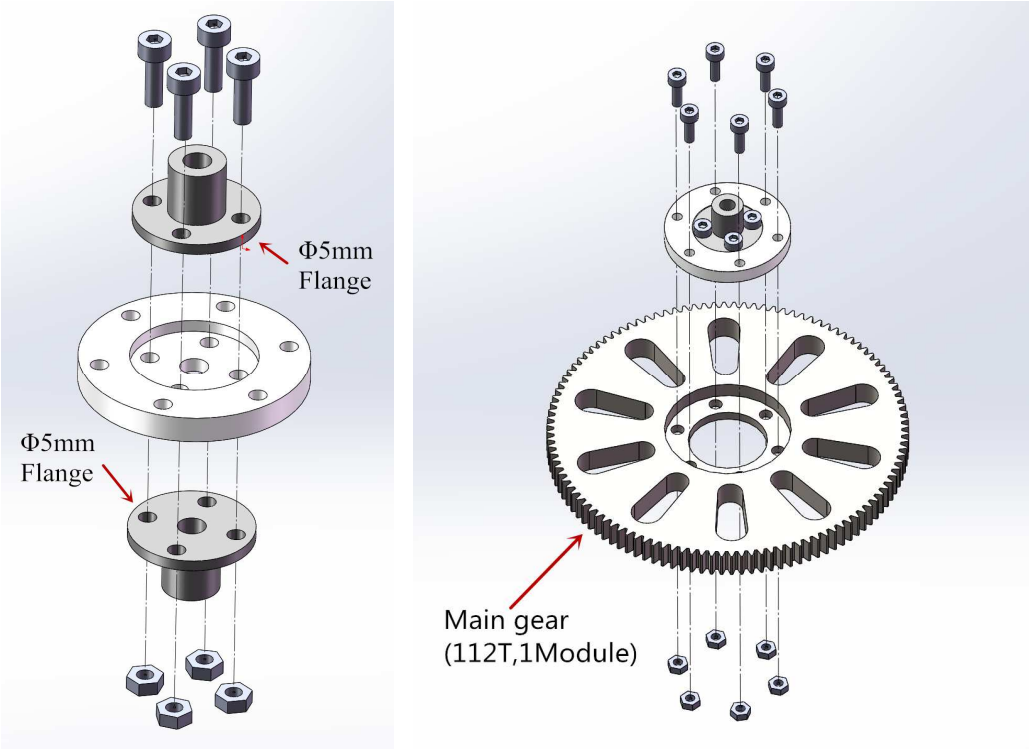

(a) (b)

Figure 5.22: The assembly process of the main gear

Figure 5.22 shows how the main gear connects with two flanges (which is used to

link the main gear to the main shaft).

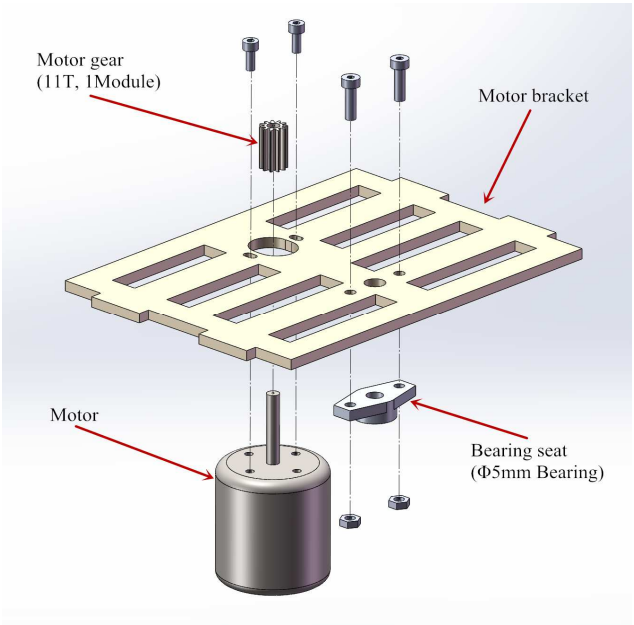

(a)

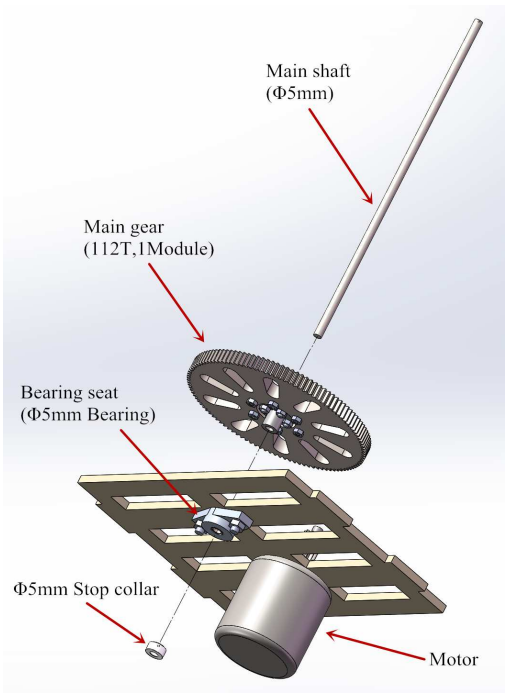

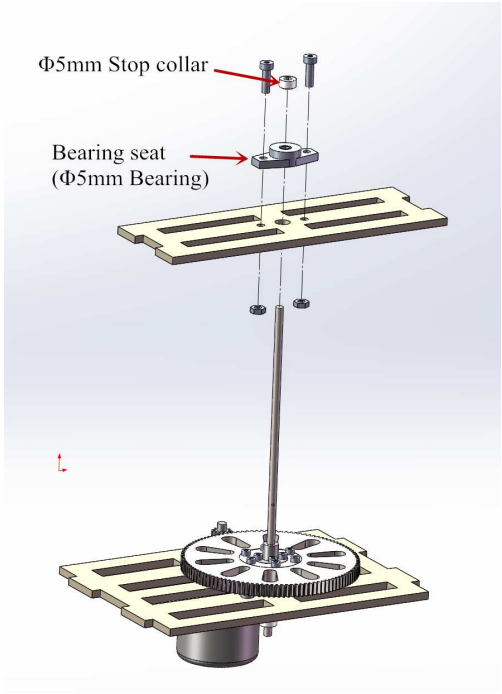

(b) (c)

Figure 5.23: The assembly process of the speed reducer

Figure 5.23 (a) shows the motor and bearing seat is installed on the motor bracket.

Figure 5.23 (b) shows the main gear and main shaft is placed on the motor bracket.

Figure 5.23 (c) shows another frame and bearing seat arranged on the main shaft.

5.1.2.2 The design and assembly of the bevel gearbox.

The bevel gearbox is used to transmit motor power to each rotor. It is placed on the main shaft as figure 5.24 shows.

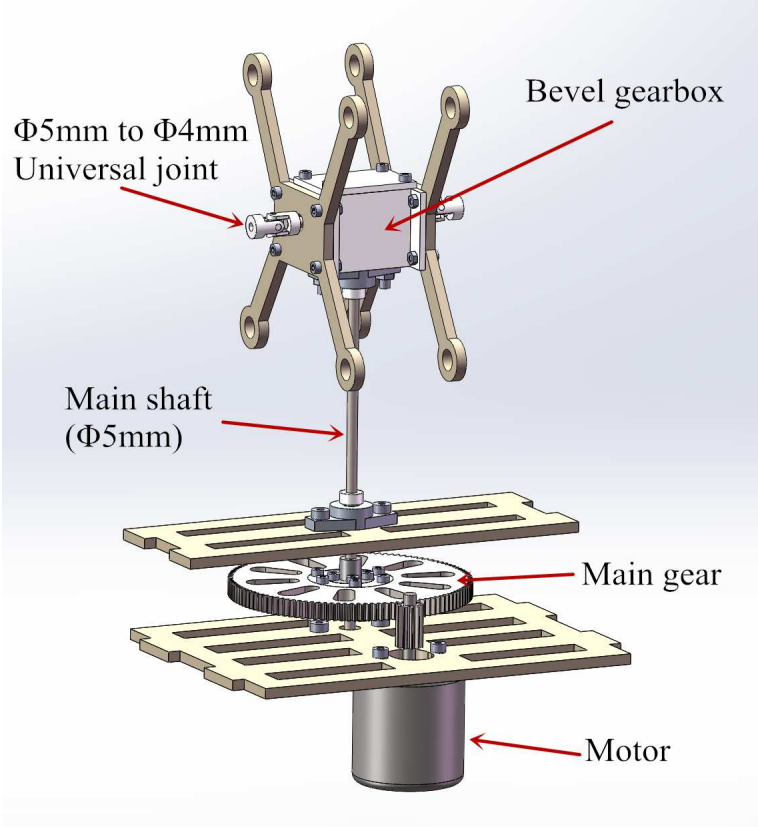

Figure 5.24: The bevel gearbox with the speed reducer

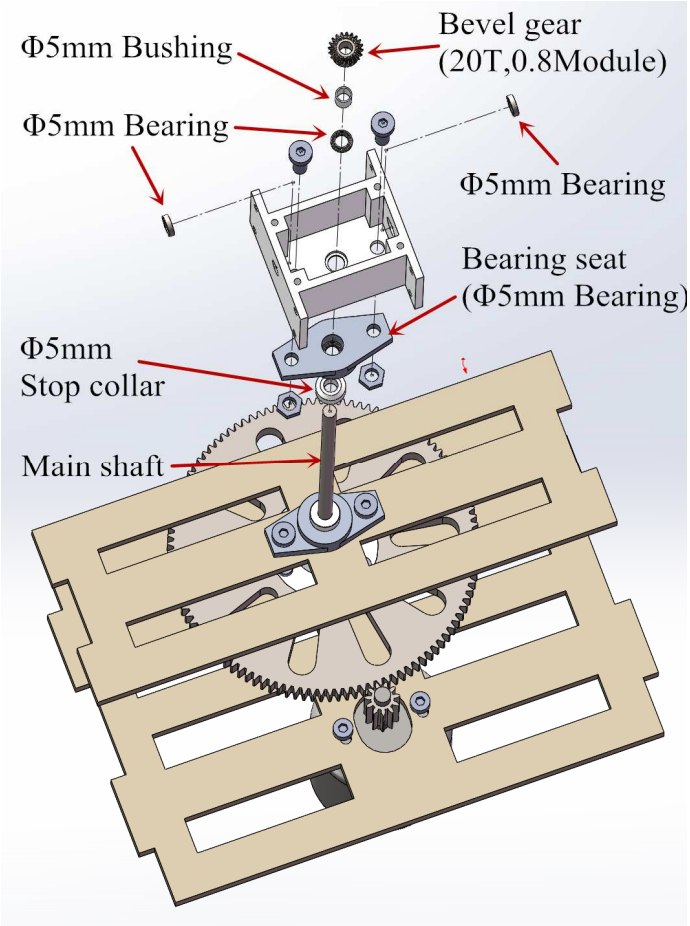

(a)

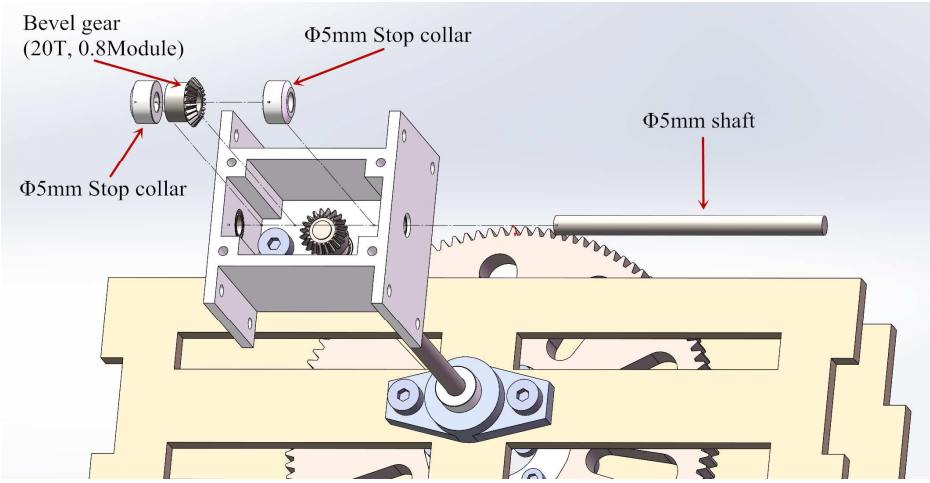

(b)

Figure 5.25: The assembly process of the bevel gearbox with the speed reducer

(Continue on next page)

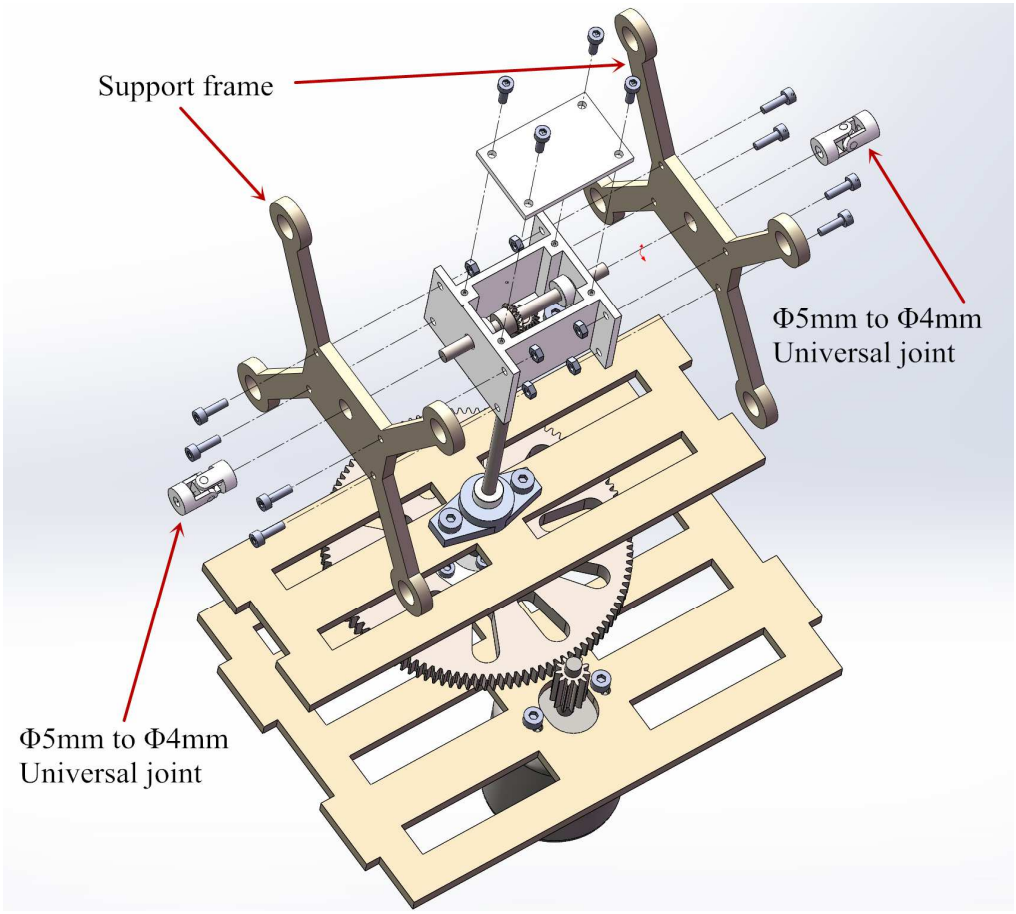

(c)

Figure 5.25: The assembly process of the bevel gearbox with the speed reducer

Figure 5.25 (a) shows how the bevel gearbox is placed on the main shaft. Figure 5.25 (b) shows the bevel gear (20T, 0.8Module) installed into the gearbox. Figure 5.25 (c) shows the support frames (which are used to locate the bevel gearbox on the fuselage) and universal joint is installed on the gearbox.

5.1.2.3 The design and assembly of the fuselage frame.

The main fuselage frame is divided into twelve pieces each side due to laser cutting

machine size. Its complete assembly shows in figure 5.26 and its assembly process shows in figure 5.27.

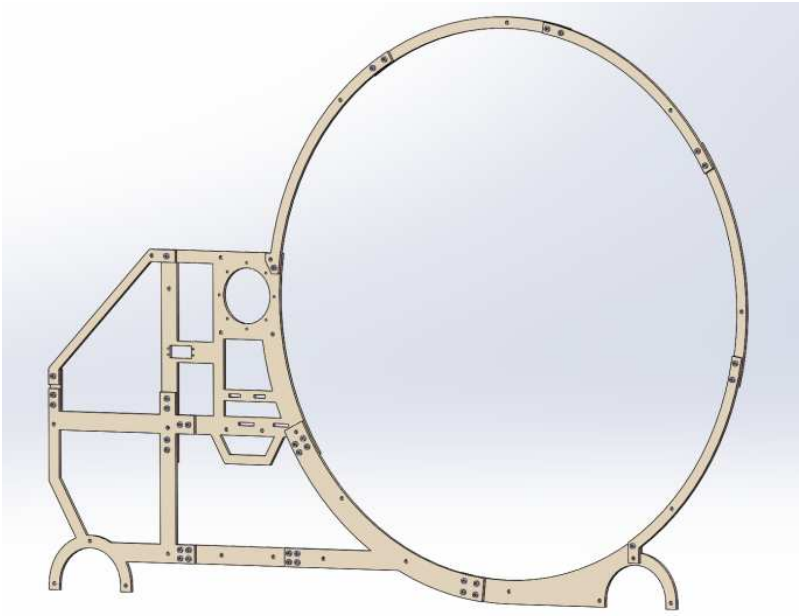

Figure 5.26: The complete assembly of fuselage frame

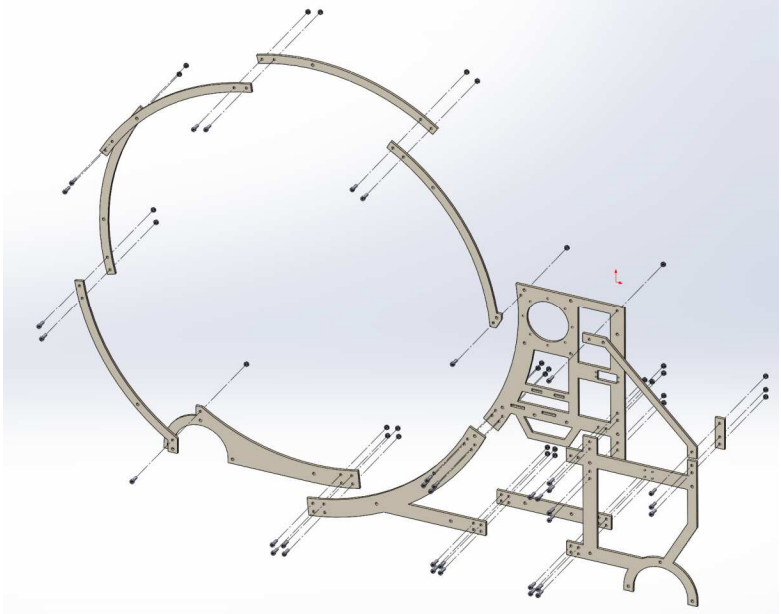

Figure 5.27: The assembly of the Fuselage 1

Meanwhile, the rotor container is also designed to store the rotors. The complete assembly shows in figure 5.28. The assembly process of the rotor container shows in the figures 5.29.

Figure 5.28: The complete assembly of rotor container

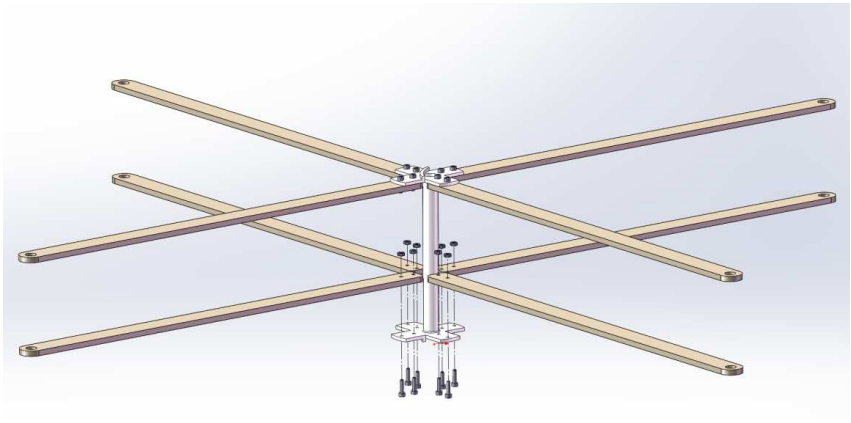

Figure 5.29: The assembly process of the rotor container

5.1.2.4 The assembly of the fuselage part.

The fuselage part is installed by fuselage frame, the speed reducer, bevel gear box

and rotor container. The figure 5.30 shows the complete assembly of the fuselage part. And its install process shows in figure 5.31.

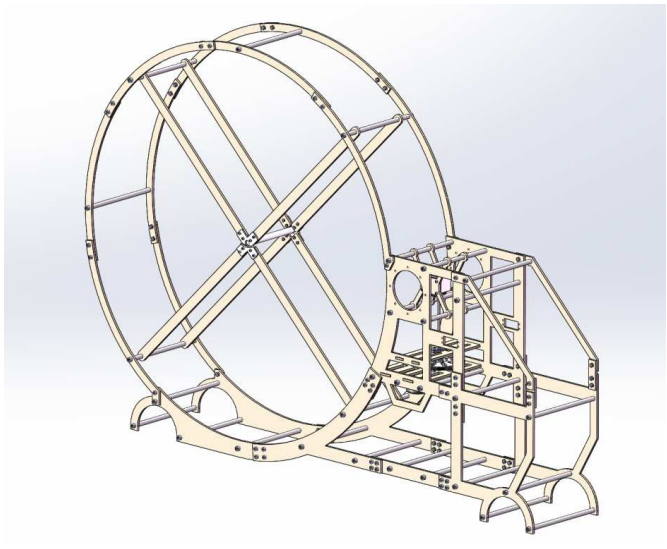

Figure 5.30: The complete assembly of the fuselage part

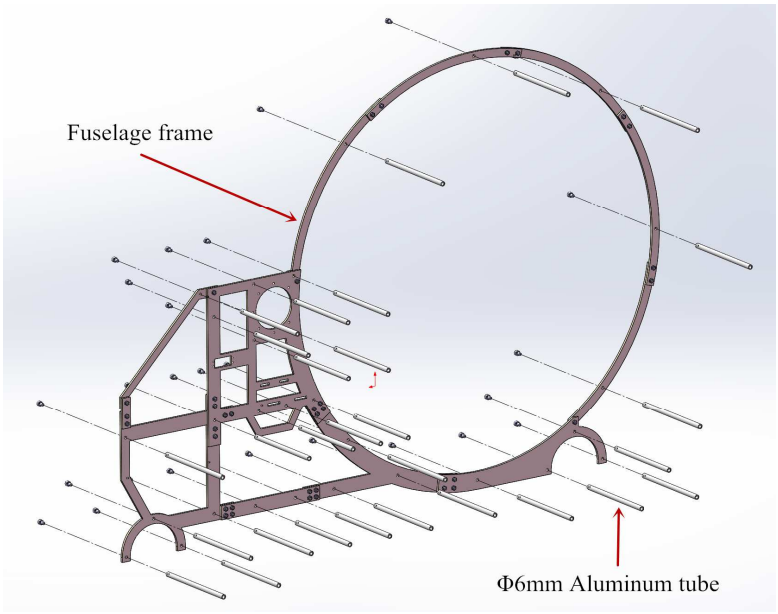

(a)

Figure 5.31: The assembly process of the fuselage part (Continue on next page)

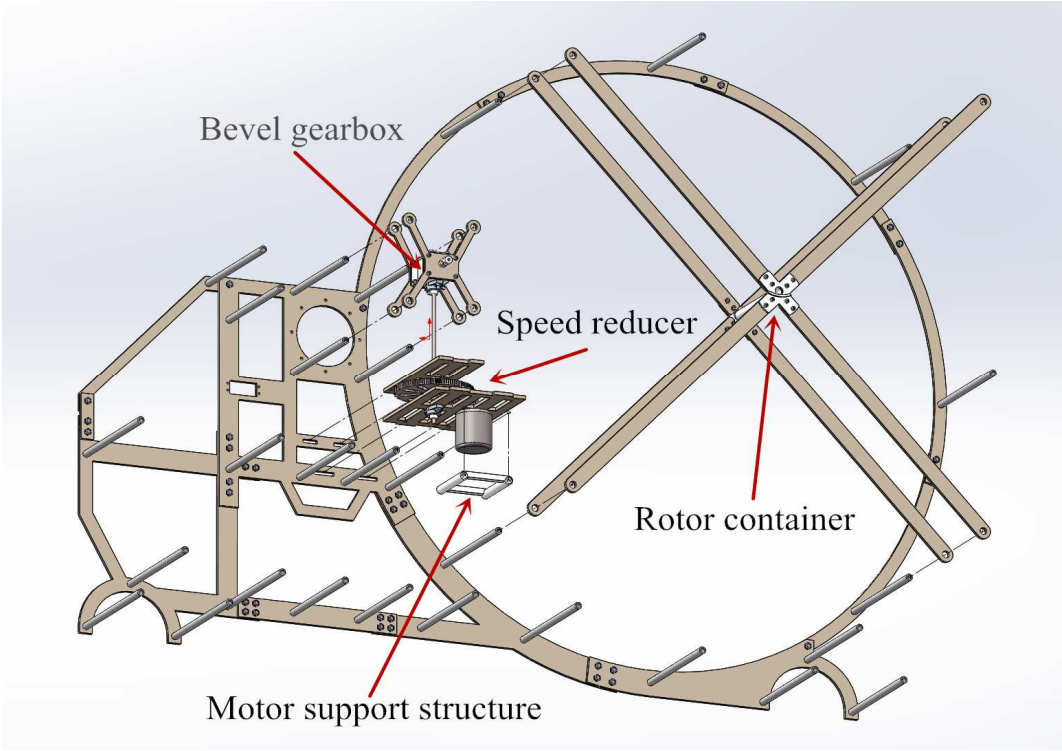

(b)

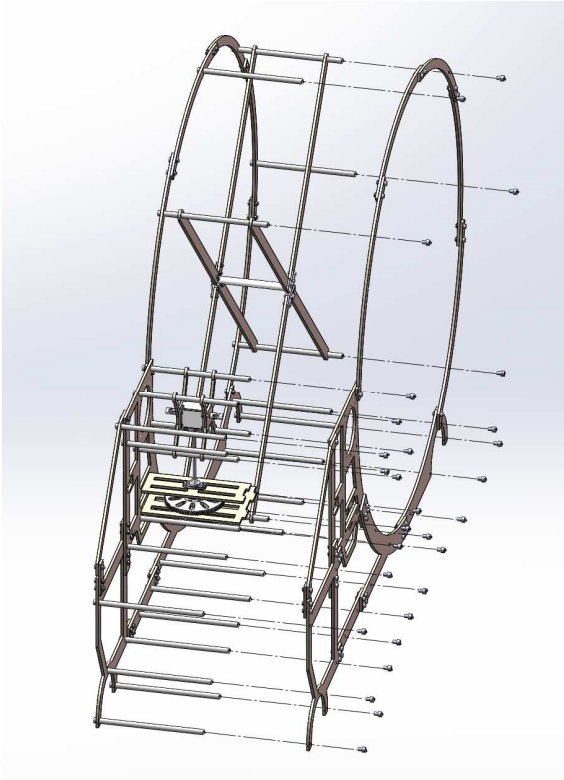

(c)

Figure 5.31: The assembly process of the fuselage part

Figure 5.31 (a) shows the fuselage frame is connect with aluminum tube. Figure 5.31 (b) shows the bevel gearbox, speed reducer, motor support structure and rotor container installed on the fuselage frame. Figure 5.31 (b) shows the two fuselage frame combination.

5.1.3 The design and assembly of the land driving part

The land driving part of this model is designed based on the truck axle structure, because the structures of the truck front axle and rear axle are simple and easy to install. Two small motors were arranged in the rear axle for driving the model. While a servo motor is mounted on the front axle for steering. The complete assembly of the front axle shows in figure 5.32.

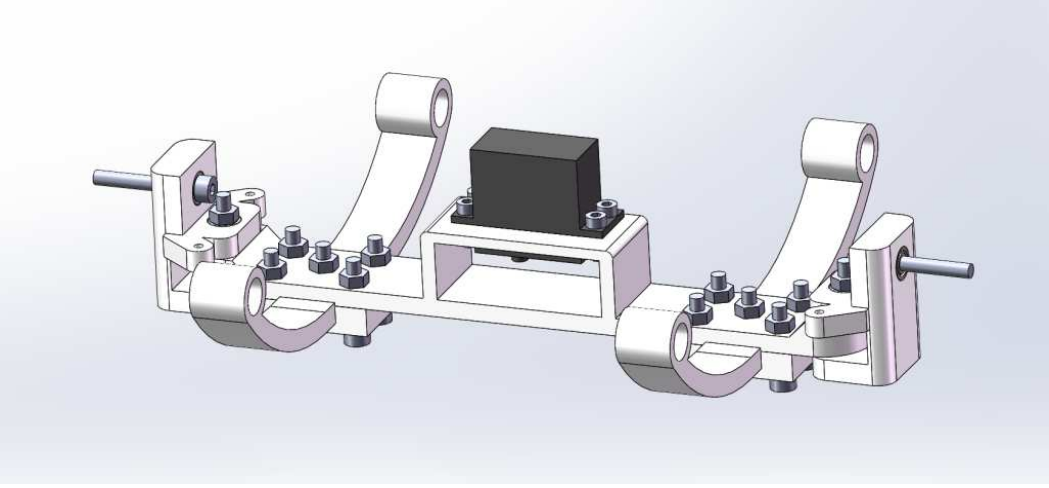

Figure 5.32: The front axle

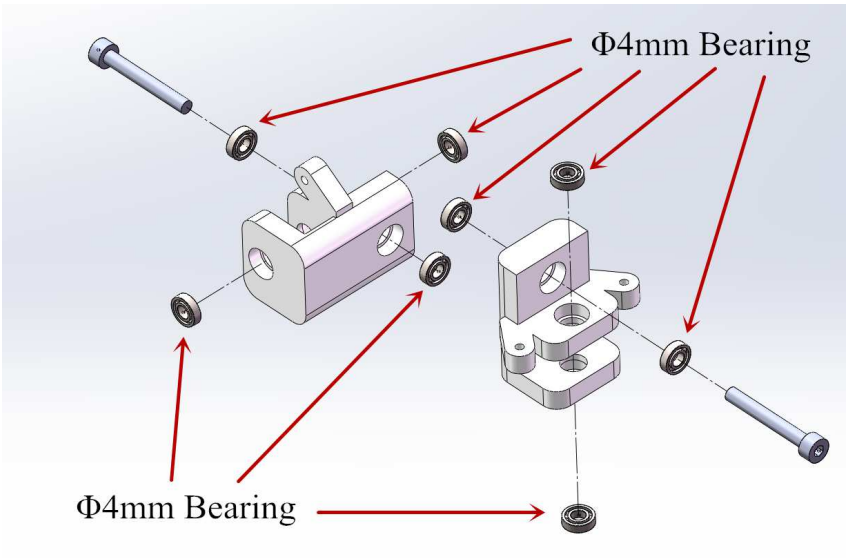

(a)

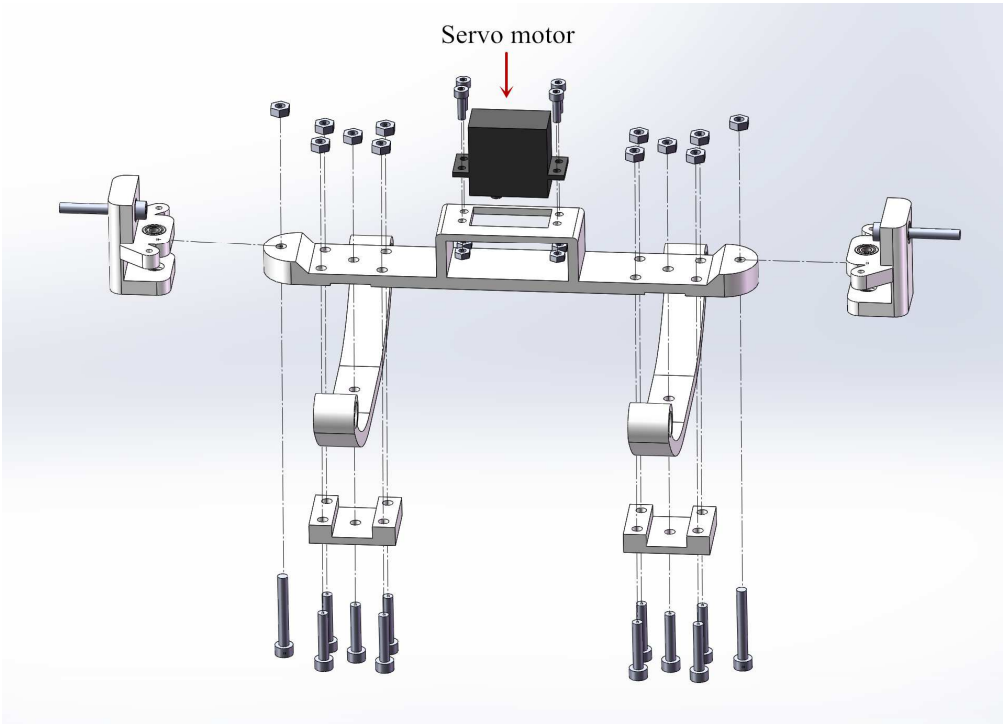

(b)

Figure 5.33: The assembly process of the front axle

Figure 5.33 (a) shows the Φ4mm bearings and screws are installed in the designed parts. Figure 5.33 (b) shows the servo motor and designed parts installation.

Figure 5.34 shows the complete assembly of the rear axle.

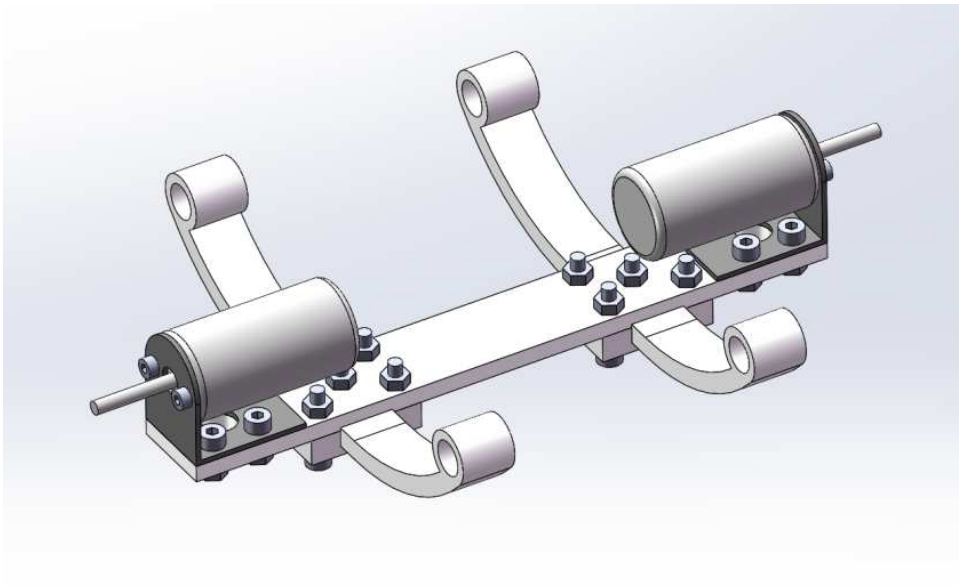

Figure 5.34: The complete assembly of the rear axle

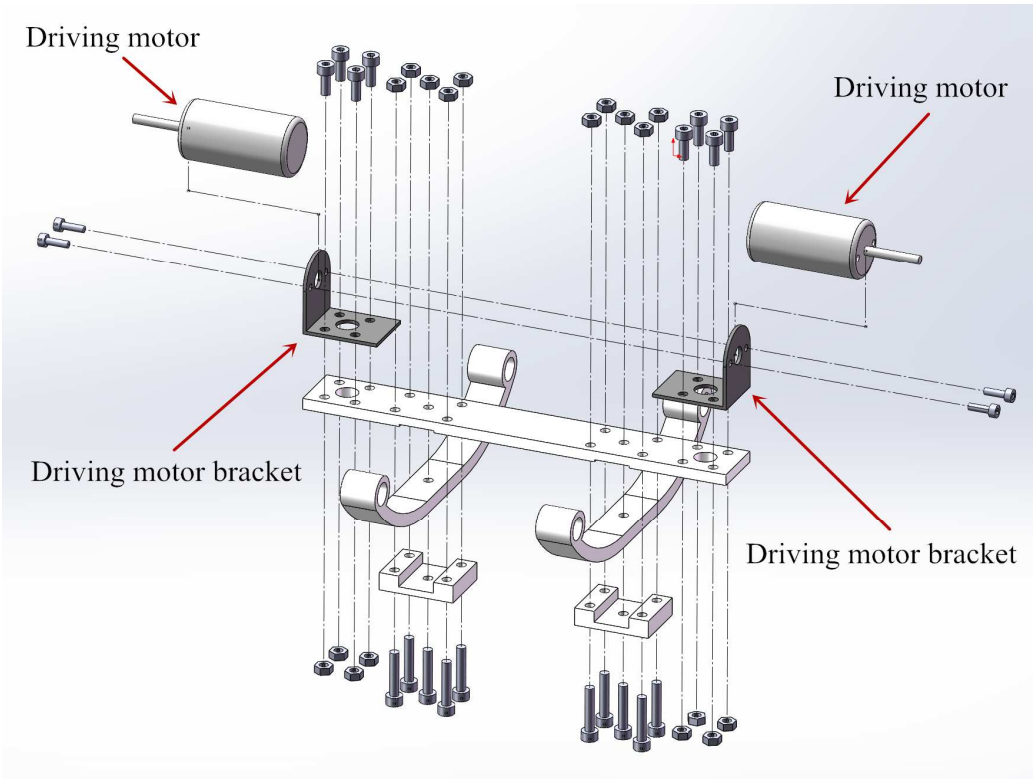

Figure 5.35: The assembly of the front axle

Figure 5.35 shows the driving motors, driving motor brackets are installed on the designed parts.

5.1.4 Final assembly.

The final assembly is the assembly of the flight part, the fuselage part and the land driving part. First, the flight part is installed on the fuselage part. The figure 5.36 and figure 5.37 show the complete assembly of the flight part with the fuselage part.

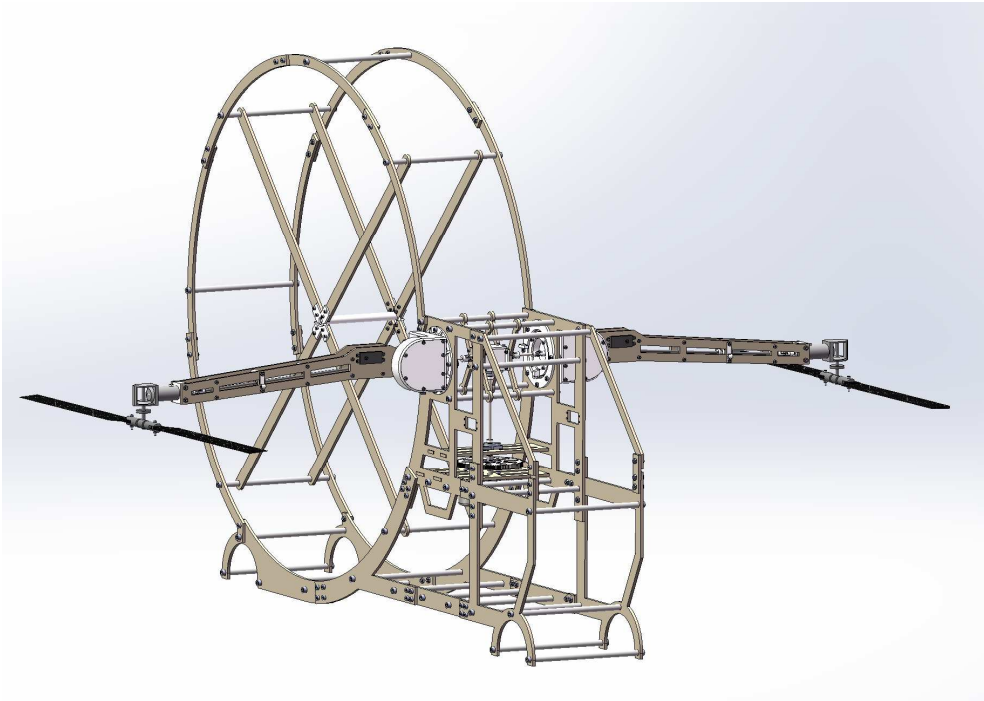

Figure 5.36: The complete assembly of the flight part with the fuselage part (Rotor arms open)

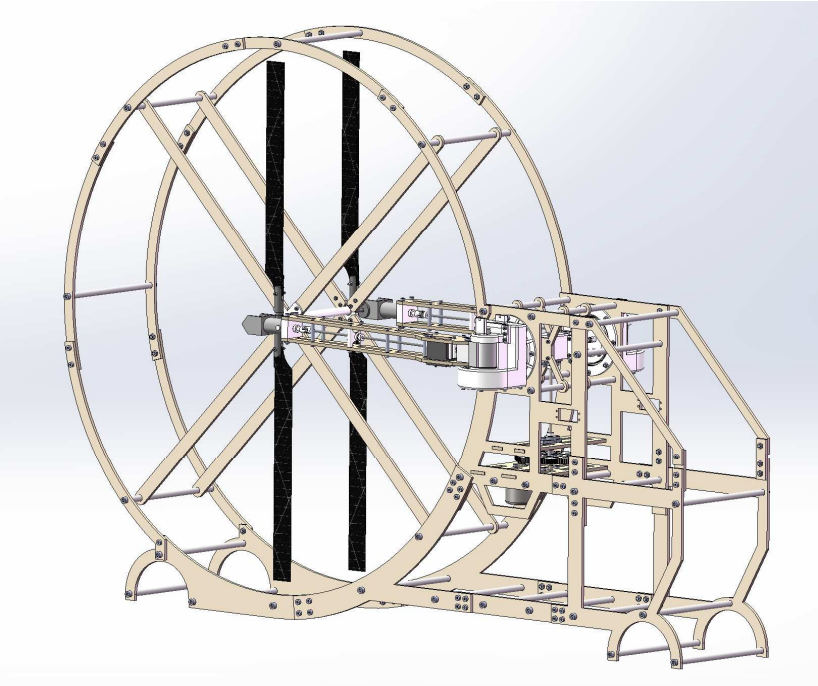

Figure 5.37: The complete assembly of the flight part with the fuselage part (Rotor arms fold)

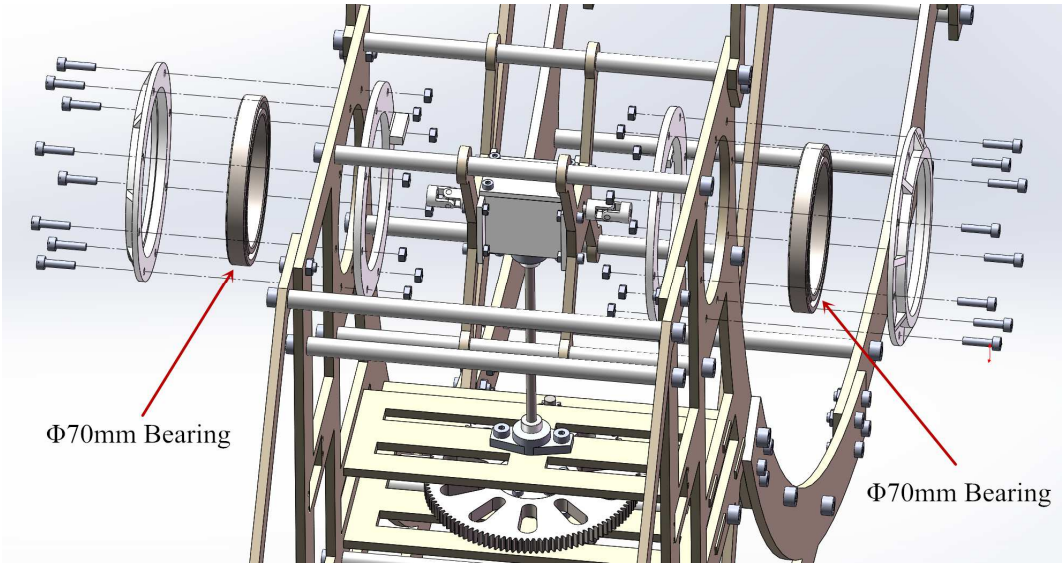

(a)

Figure 5.38: The assembly process of the flight part and fuselage part (Continue on next page)

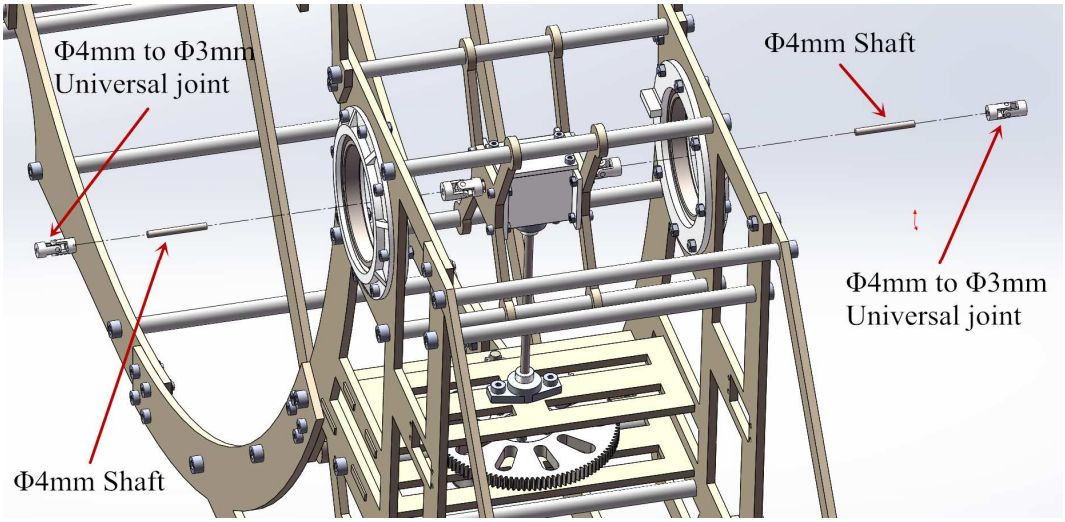

(b)

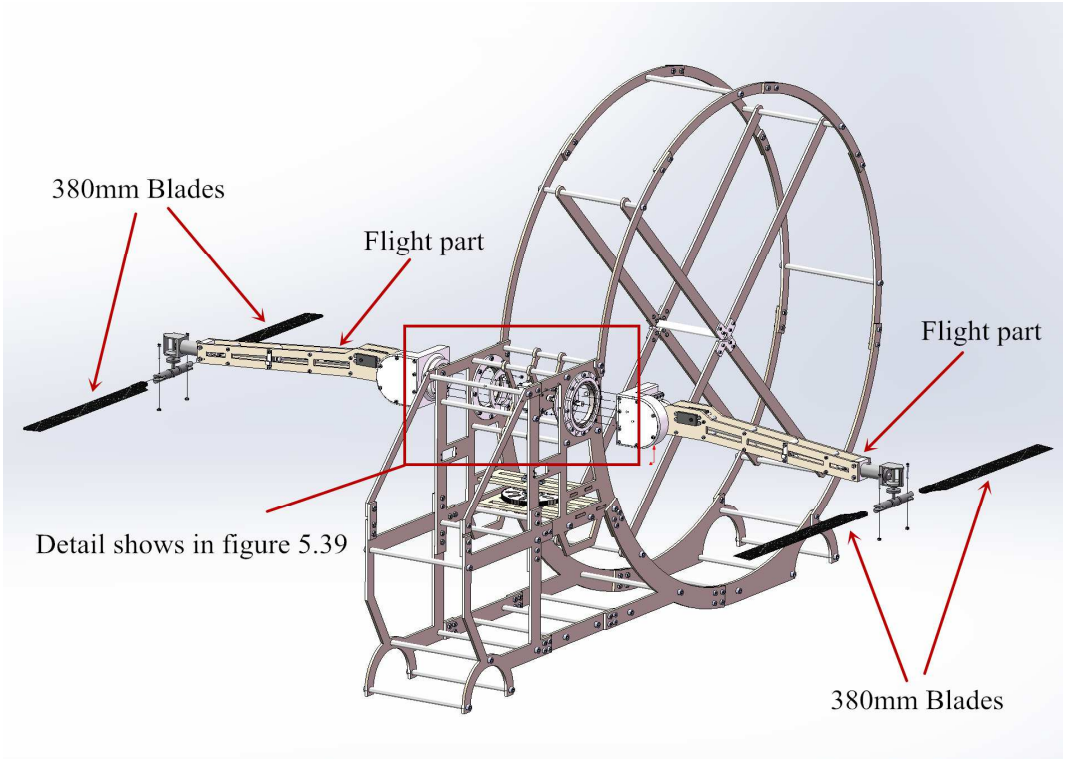

(c)

Figure 5.38: The assembly process of the flight part and fuselage part

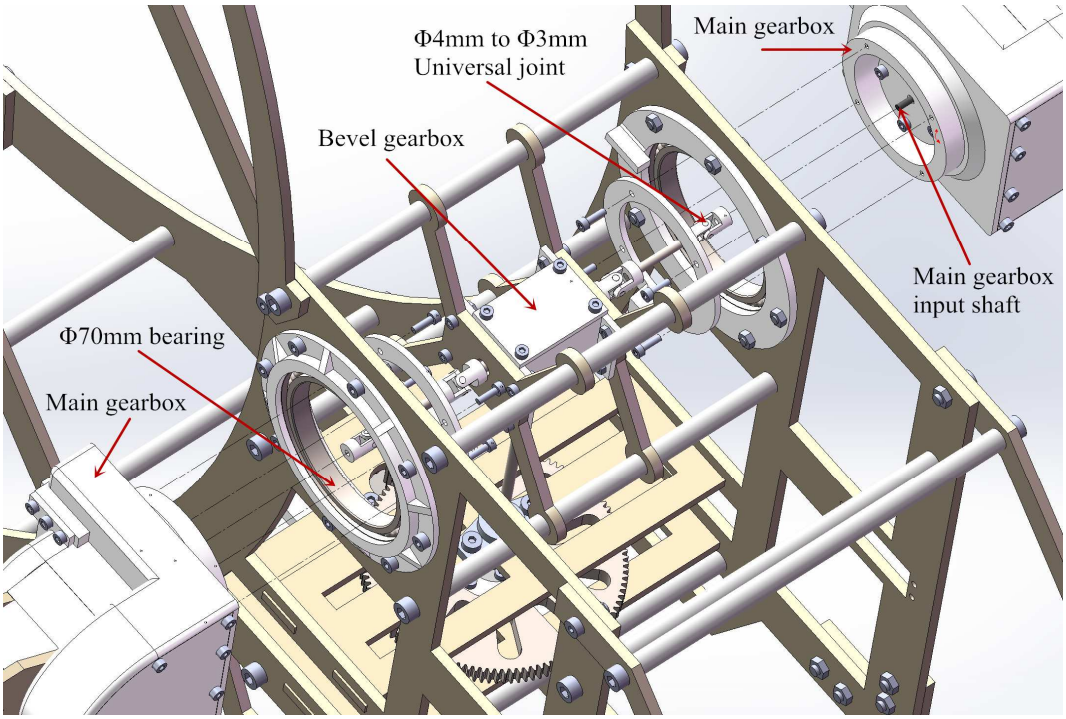

Figure 5.39: The assembly detail of figure 5.38 (c)

Figure 5.38 (a) shows the Φ70mm bearings are installed on the fuselage part. The Φ70mm bearings allow the rotor arms and blades to tilt. Figure 5.38 (b) shows the shafts and universal joints are connected with the bevel gearbox. Figure 5.38 (c) shows the flight parts connect with the fuselage part and the blades are installed on the rotor head. Figure 5.39 shows the detail of the flight parts connect with the fuselage part.

Then the land driving part is connected with the fuselage. The figure 5.40 shows the complete assembly of the flight parts, the fuselage part and the land driving part.

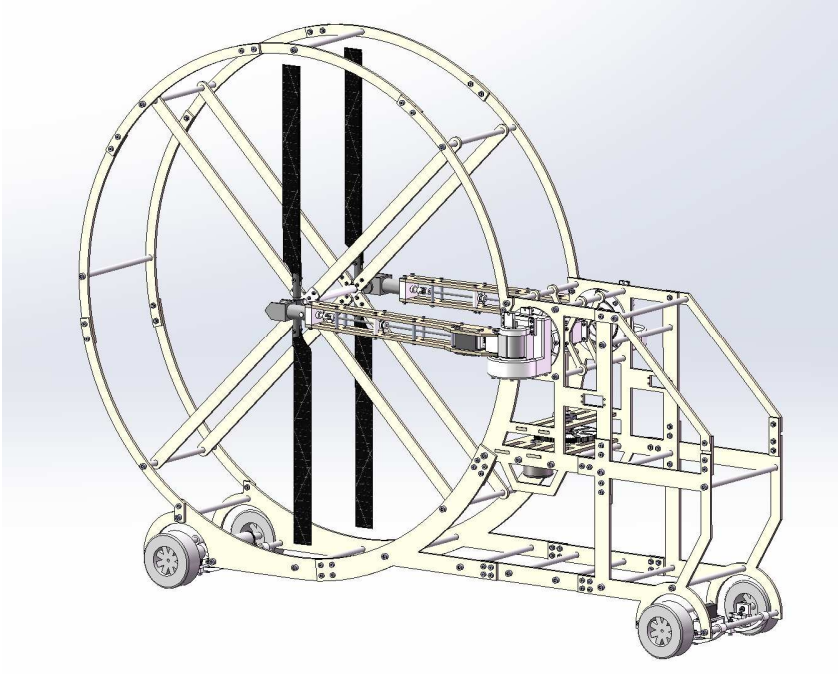

Figure 5.40: The complete assembly of the flight part, the fuselage part and the land driving part

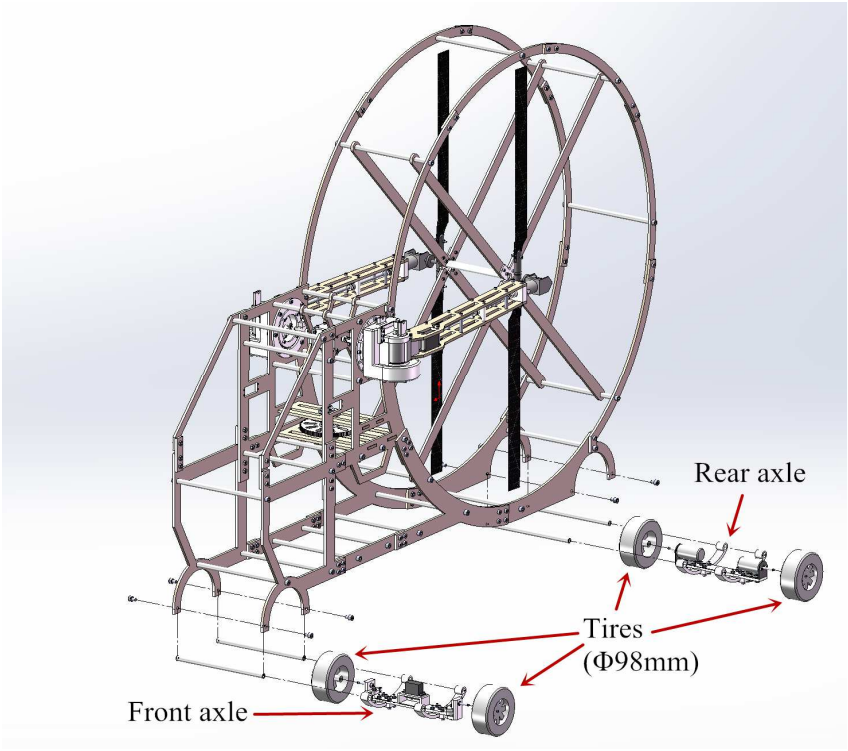

Figure 5.41: The assembly process of the front axle and rear axle

Figure 5.41 shows how the tires, front axle, rear axle installed on the fuselage part.

Two servo motors are placed on the main gearbox to control the rotor arm fold and other two servo motors are placed on the fuselage frame to control the rotor arms tilt. The assembly process shows in figure 5.42

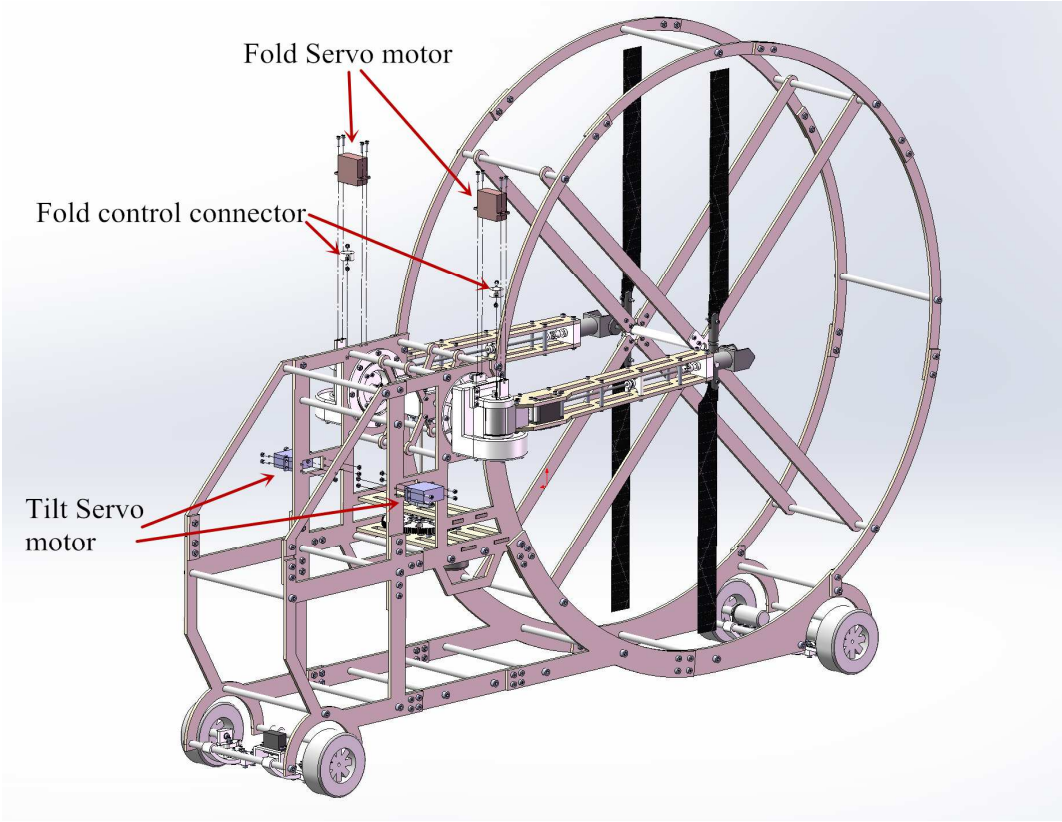

Figure 5.42: The assembly of servo motors

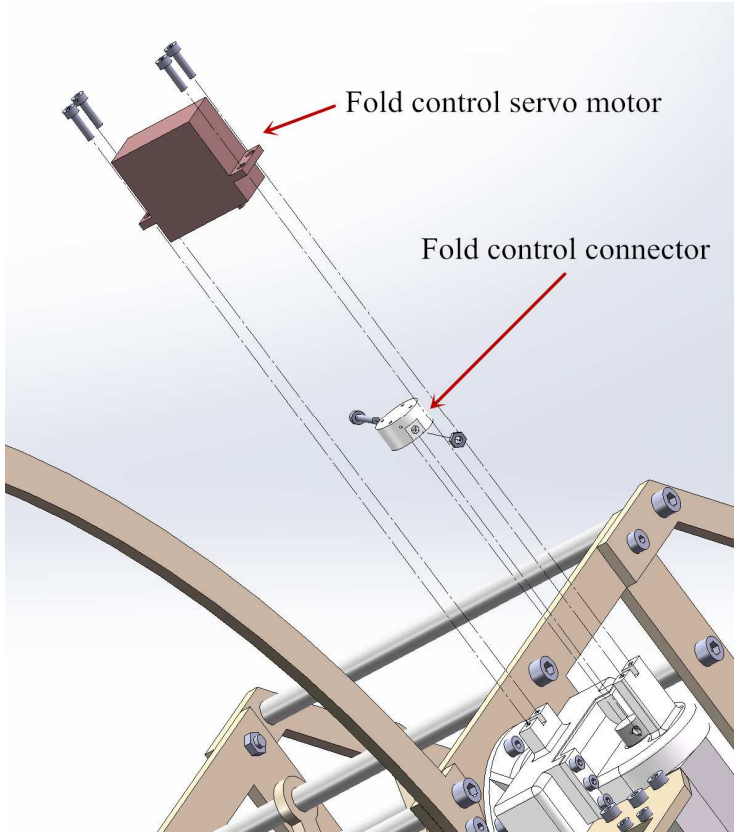

Figure 5.43: The assembly detail of the fold servo motor

Figure 5.43 shows the assemble detail of the fold servo motor. Figure 5.44 and figure 5.45 shows the whole complete 3D model of the flight vehicle model.

Figure 5.44: The whole 3D model of the flight vehicle model (Fold)

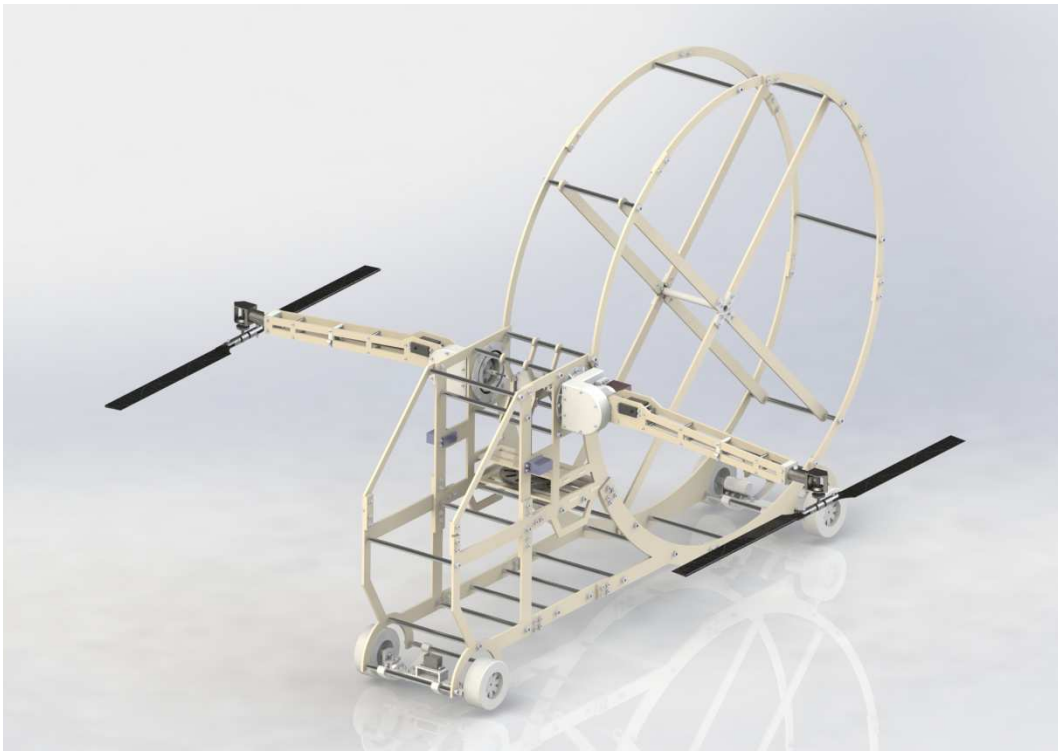

Figure 5.45: The whole 3D model of the flight vehicle model (Open)

5.2 The implementation

The previous section introduced the design of the final 3D model. The following sections will introduce what materials the model used and how the designed parts are made. Moreover, not all parts are showed in the 3D model in the last section. Some parts like control levers and the links of the rotor container to the tail rotor heads are not shown in the 3D model. These parts are designed according to actual condition and will be introduced in next section. After that, some important install process and model detail will be shown. The figure below is the implementation of the flight vehicle model. The size of the model: 1335mm×394mm×1022mm.

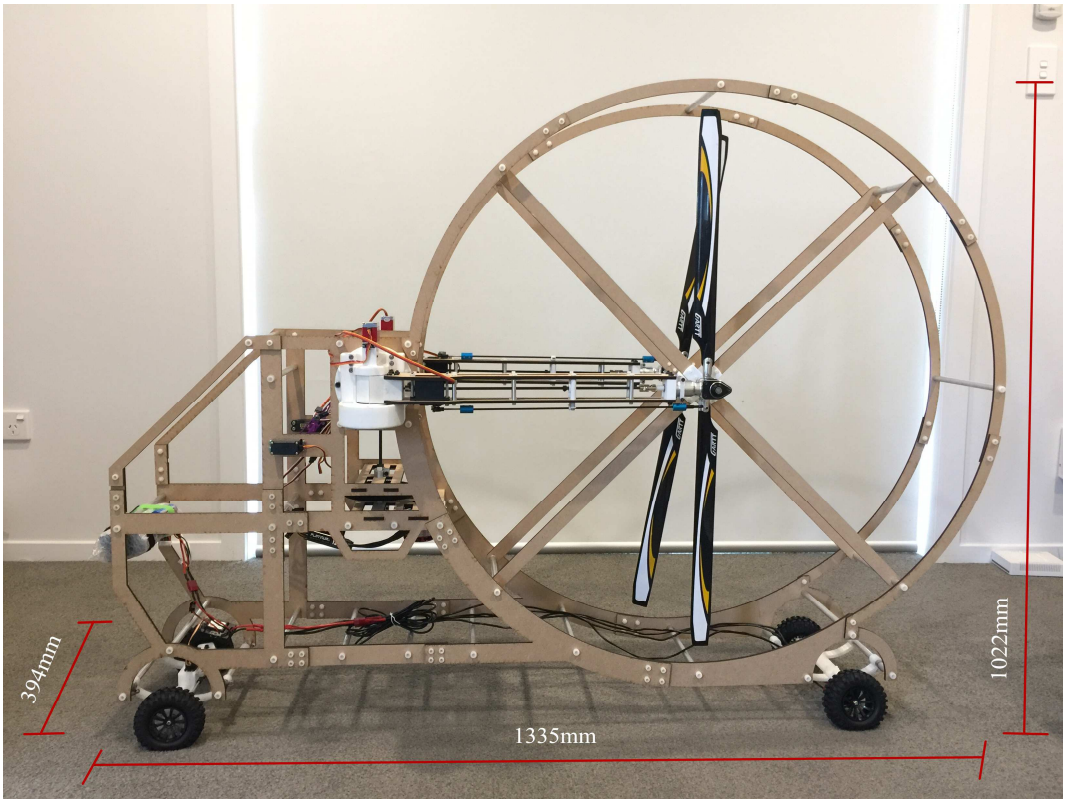

Figure 5.46: The implementation of the flight vehicle model (Fold)

5.2.1 Parts fabrication and purchase

From the 3D model, most parts are procured and customized. The remaining parts are purchased or made according to the actual installation. All purchased parts have are listed in the appendix 1. For the customized parts, some methods are used to make them. Three-dimensional print (3D print) is the method which been used to make complex parts. Among these complex parts, some of them due to the high accuracy requirement are printed by Selective Laser Sintering (SLS) 3D printer and their material is nylon. The other of the complex part are printed by Fused Deposition Modeling (FDM) 3D printer and their material is Acrylonitrile Butadiene Styrene (ABS). All the frame parts are cut from medium density fiberboard (MDF) by laser cutting machine. The main gearbox gear set is made by factory according to the drawing. And the material of the gear set is polyoxymethylene (POM). The drawing shows in the appendix 2. Most shafts are carbon fiber shafts which are used to reduce weight.

5.2.2 Model details

This section will show the details of the flight vehicle model. Figure 5.47 briefly shows the components of the model (The ESC is the Electronic Speed Control). All electronic control components will be described in the next chapter. The other figures show some main parts detail of the model.

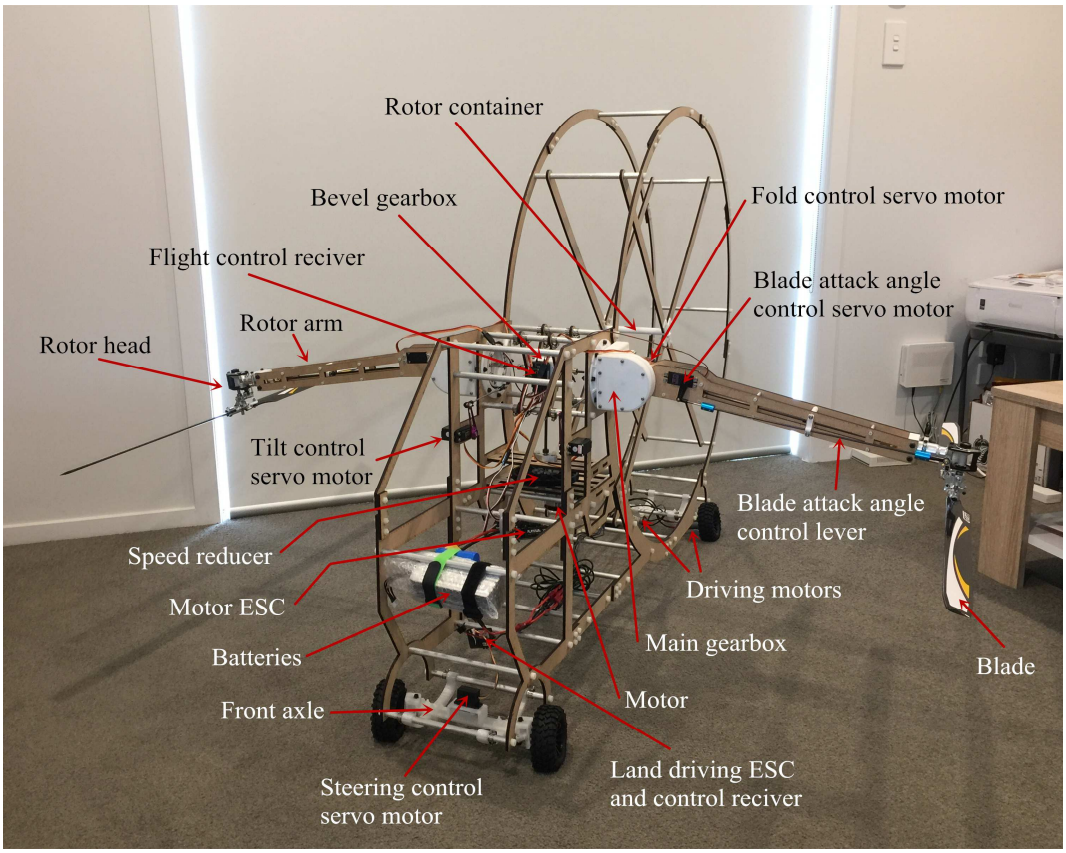

Figure 5.47: The composition of the flight vehicle model (open)

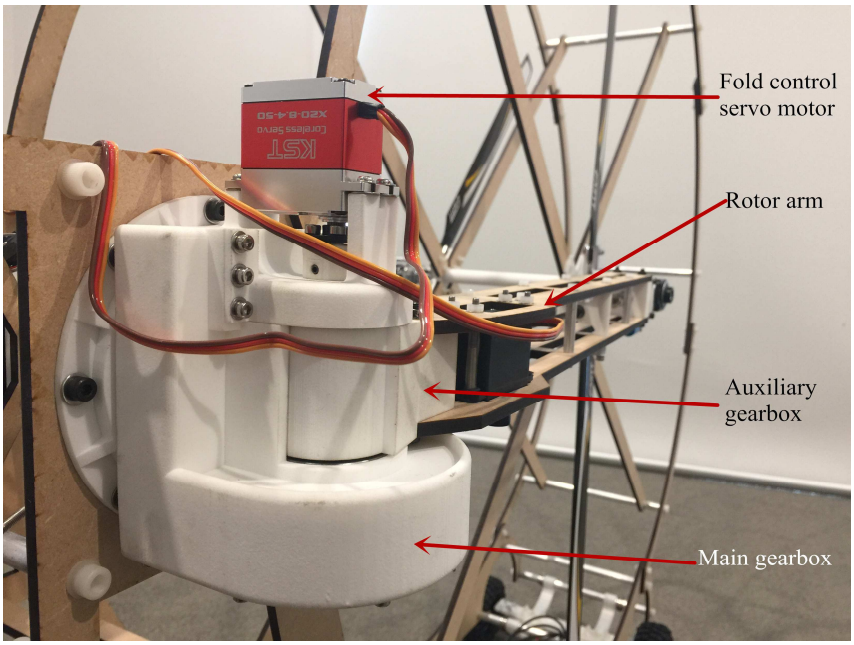

Figure 5.48: The main gearbox and auxiliary gearbox

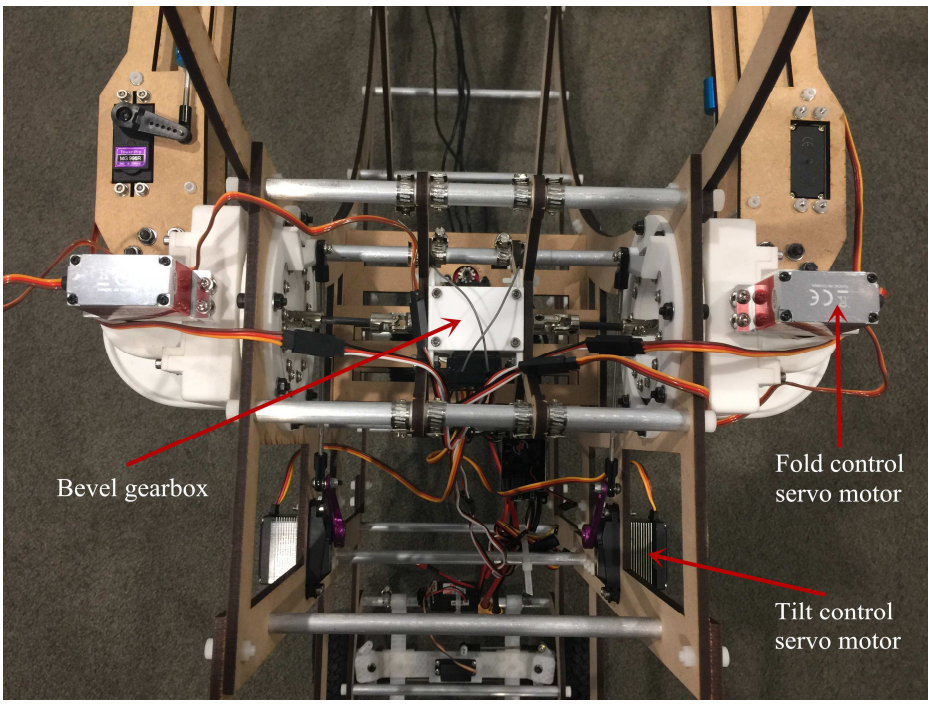

(1)

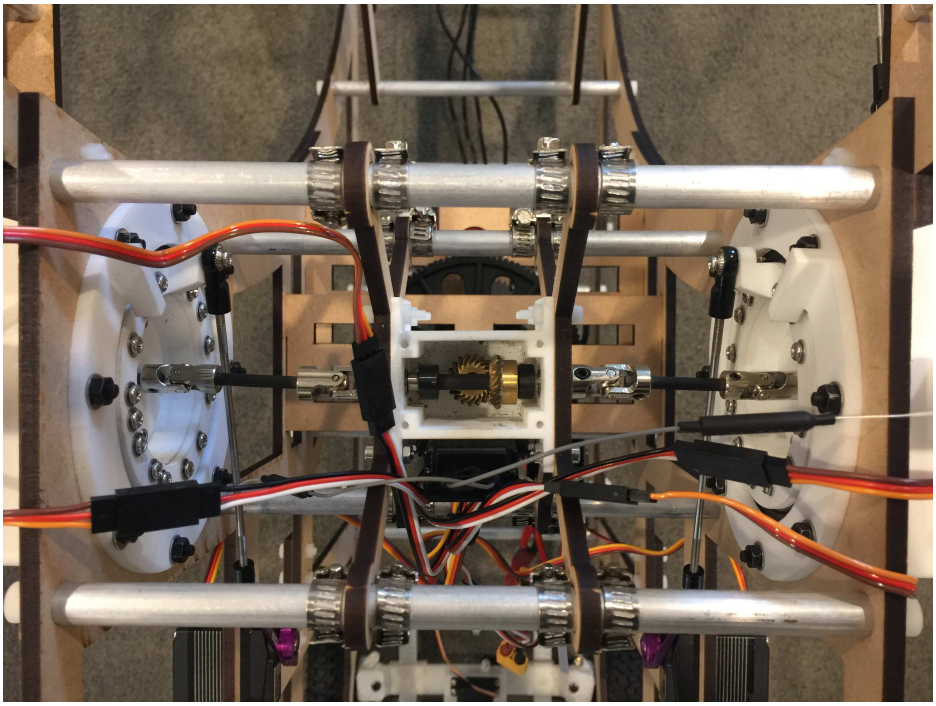

(2)

Figure 5.49: The bevel gearbox exterior (1) and interior (2)

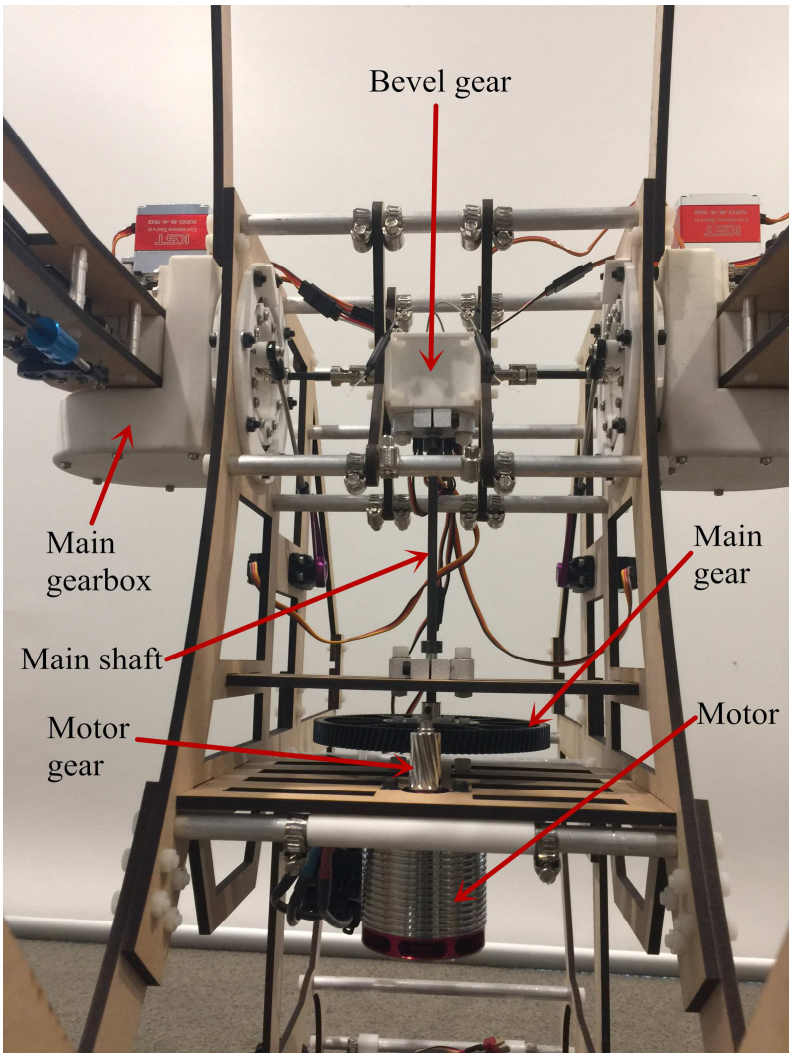

Figure 5.50: The transmission structure of the model

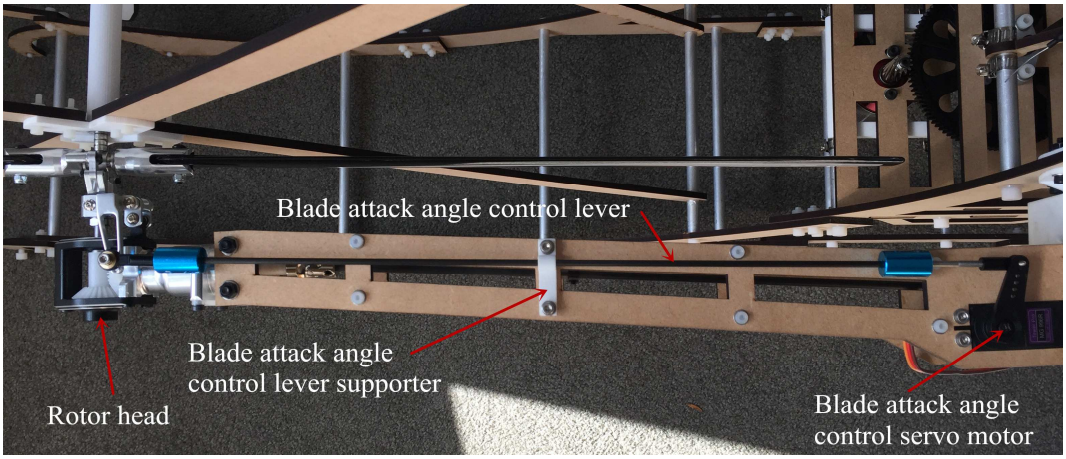

Figure 5.51: The blade attack angle control structure

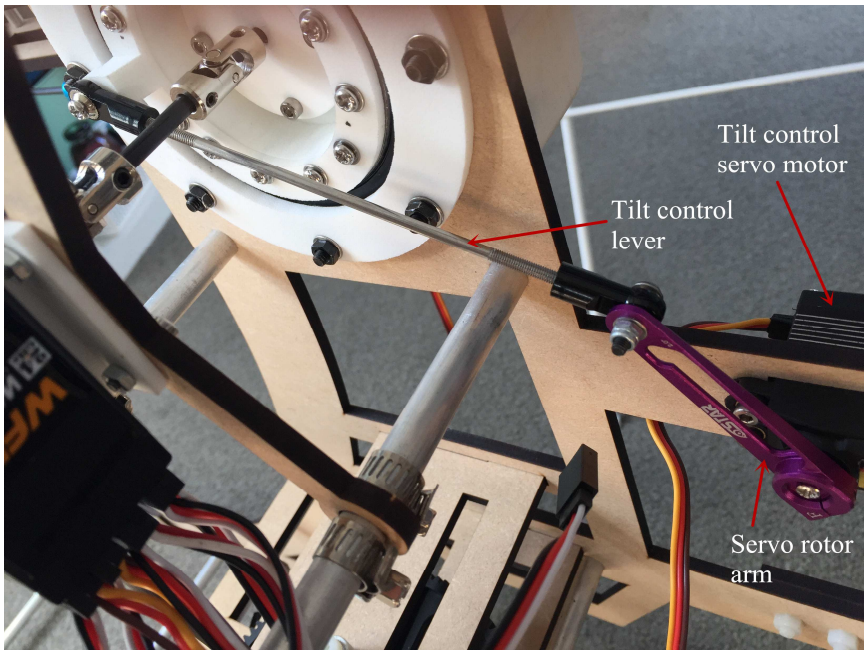

Figure 5.52: The tilt control structure

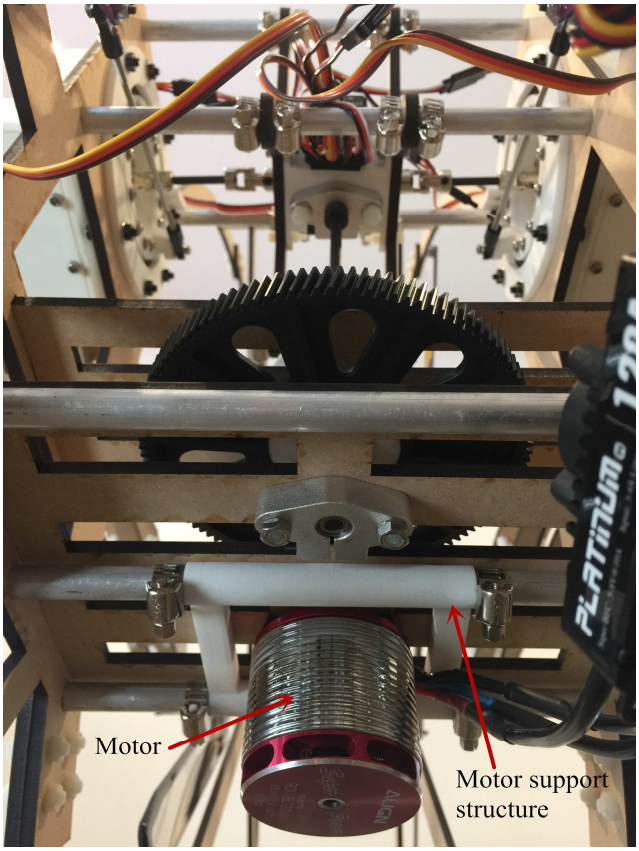

Figure 5.53: The main motor and speed reducer

The design of the blade attack angle control structure and the tilt control structure are based on the actual installation. The following figures will show the other designs which did not show in the 3D model.

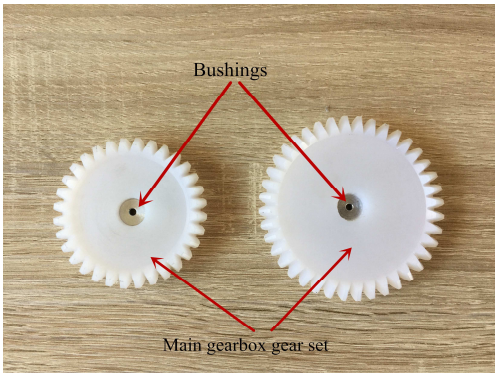

Figure 5.54: The customized gears with bushings

Figure 5.54 shows two bushings are mounted in the main gearbox gear set. The bushing are used because the minimum shaft diameter of the gears can only be 12mm during the customize process in factory. So, bushings are mounted in these gears for connecting gears and Φ3mm shafts

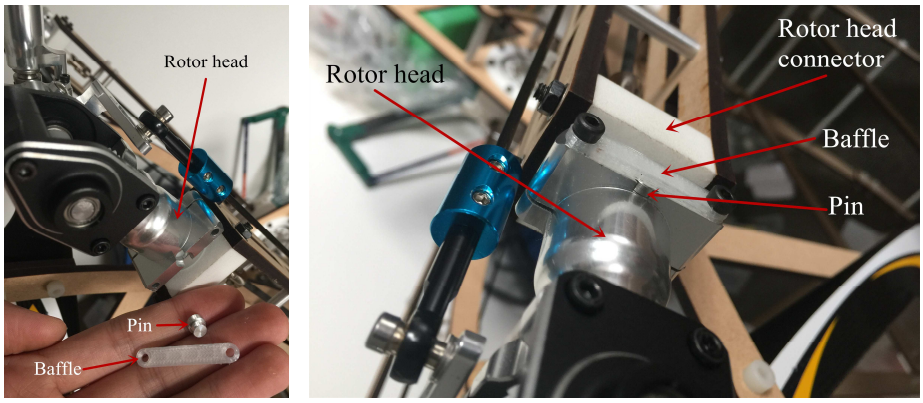

Figure 5.55: The pin and baffle of the rotor head

Figure 5.55 shows a pin and a baffle are installed on the rotor head. Their role is to prevent the rotor head moving from the rotor head connector.

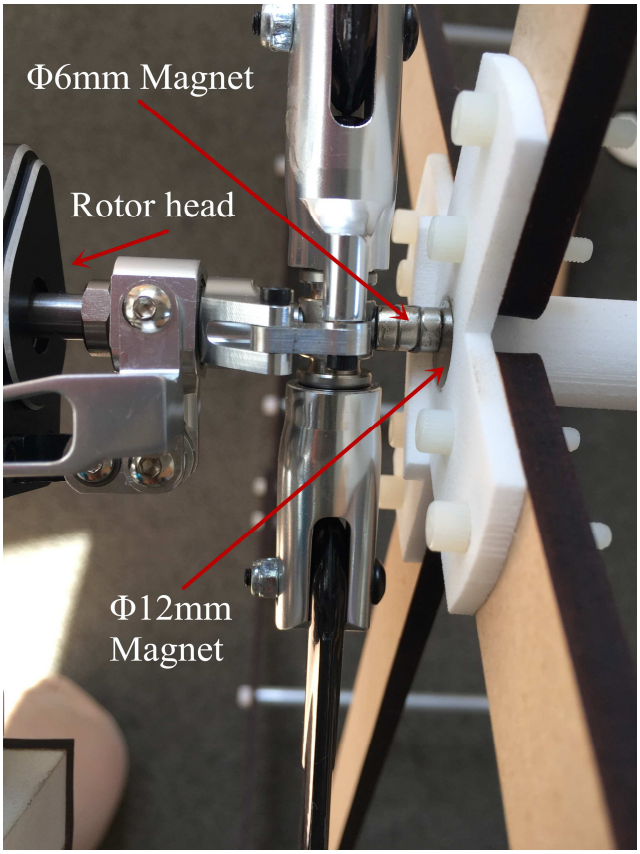

Figure 5.56: The link between the rotor head and the rotor container

Figure 5.56 shows the link of the tail rotor head and the rotor container. The link is worked by magnets. The Φ6mm magnets are glued on the rotor head while the Φ12mm magnet is glued on the container. The reason for using a large magnet is to increase the contact range by taking the installation deviation into account so that the rotor head can be successfully connected with the rotor container.

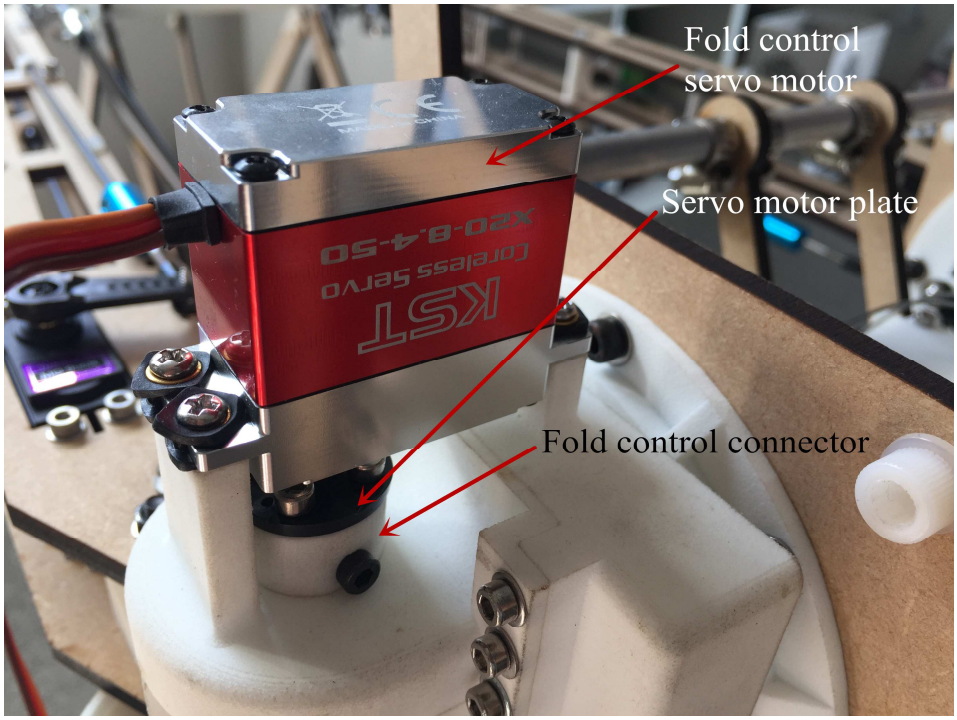

Figure 5.57: The folding control structure

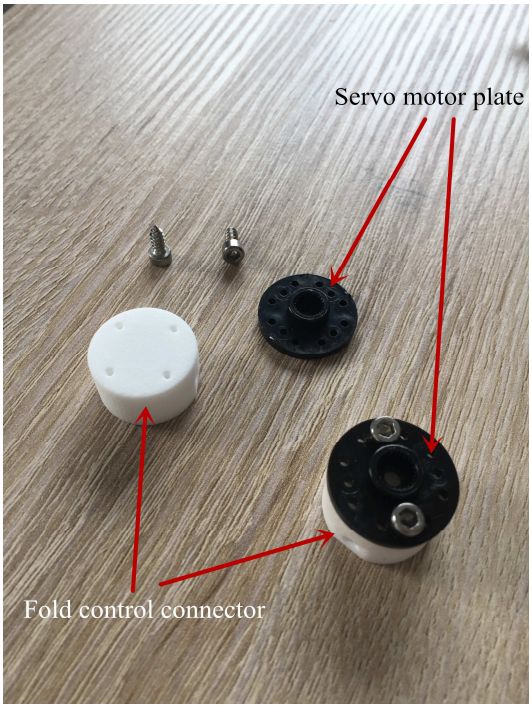

Figure 5.58: The servo motor control plate and fold control connector

Figure 5.57 shows the connection between the fold control servo motor and the

fold control connector. The fold control connector is linked to the auxiliary gearbox so that the servo motor can fold the rotor arm.

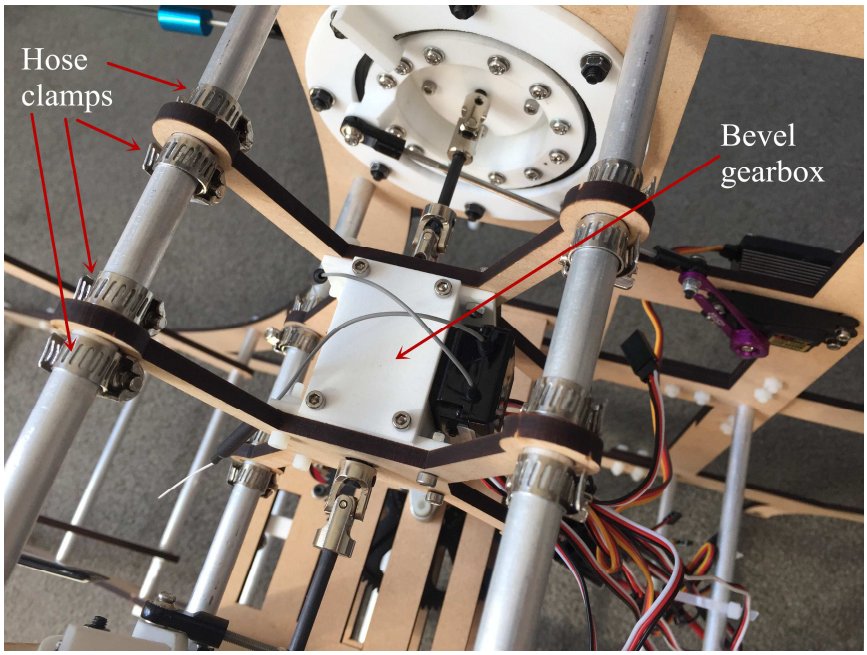

Figure 5.59: The hose clamps are used on the model

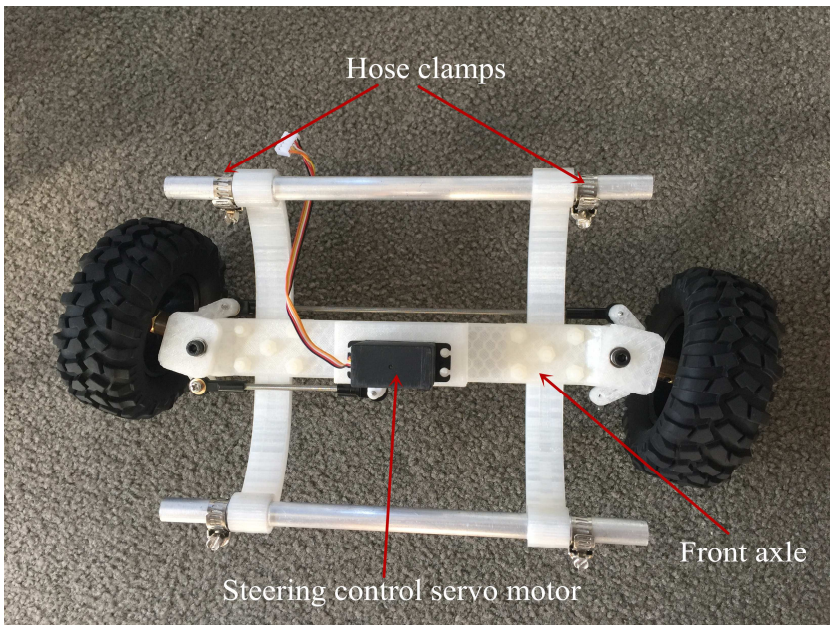

Figure 5.60: The front axle with tire

Figure 5.59 shows the bevel gearbox is located and fixed on the aluminum tubes by hose clamps. The hose clamps are lighter and much cheaper than collars. And they also can locate and fix the gearbox. Furthermore, the front axle and rear axle are also using this method to install and locate on the aluminum tubes which shows in figure 5.60.

Figure 5.61: The original connection of the main gearbox and the fuselage

Figure 5.62: The improved connection of the main gearbox and the fuselage

The figure 5.61 shows the original connection of the main gearbox and the fuselage by using 4 screws (red circle marked). Figure 5.62 shows the improved connection of the main gearbox and the fuselage. The strength of using four screws to connect the main gearbox and fuselage is not strong enough. To improve it, several holes were drilled by using the drill press and many screws were added to increase the connection strength.

5.2.3 Install of the model

Some key installation procedures and final models are also described in the following figures.

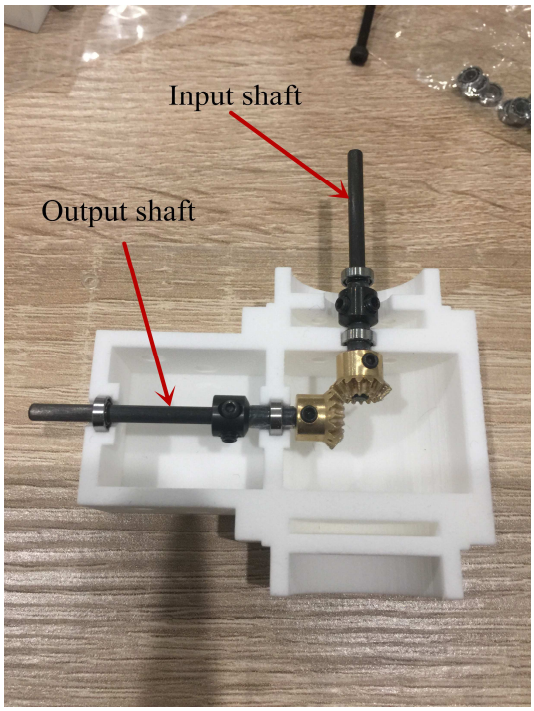

Figure 5.63: The installation of input shaft and output shaft

Figure 5.64: The auxiliary gearbox

Figure 5.65: The auxiliary gearbox installed with the rotor arm

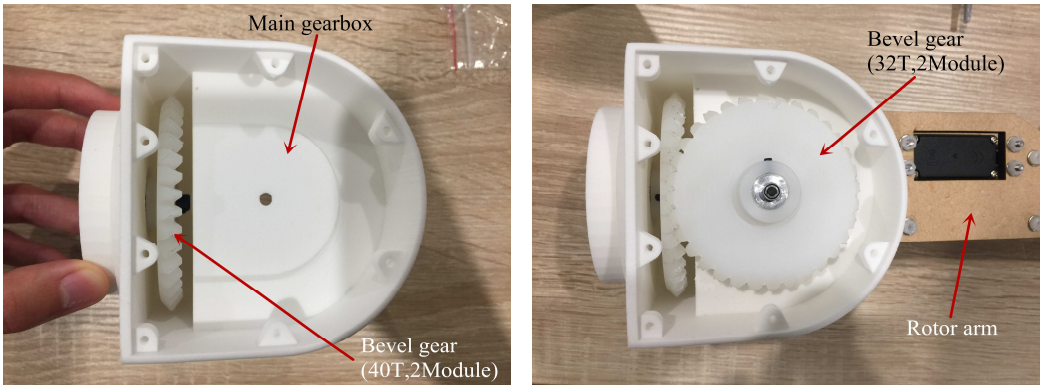

Figure 5.66: Main gearbox set installation in the main gearbox

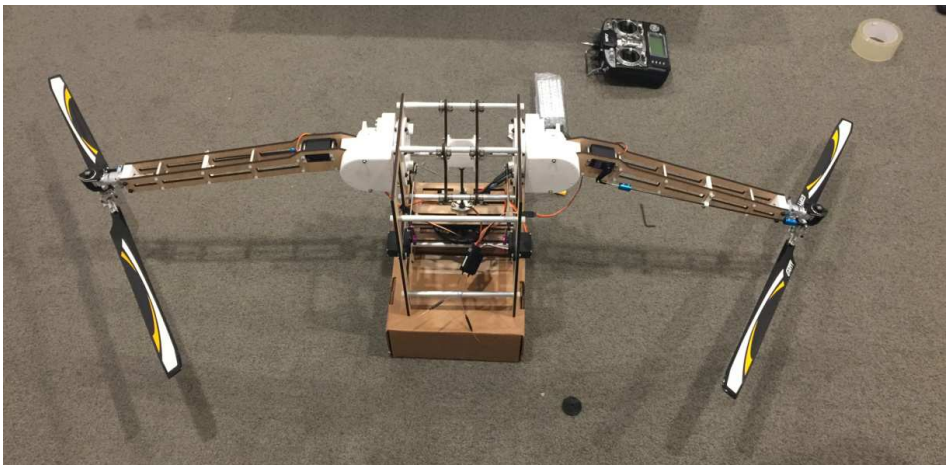

Figure 5.67: The flight part with the upper fuselage

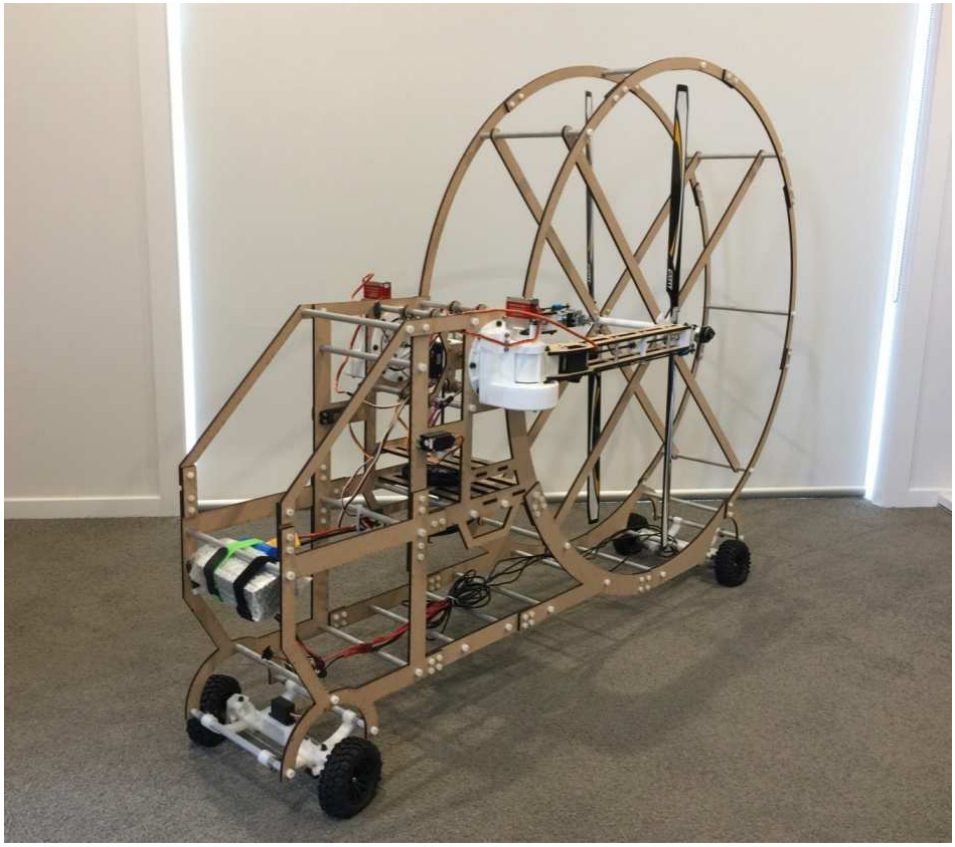

(a)

Figure 5.68: The flight vehicle model (fold) (Continue on next page)

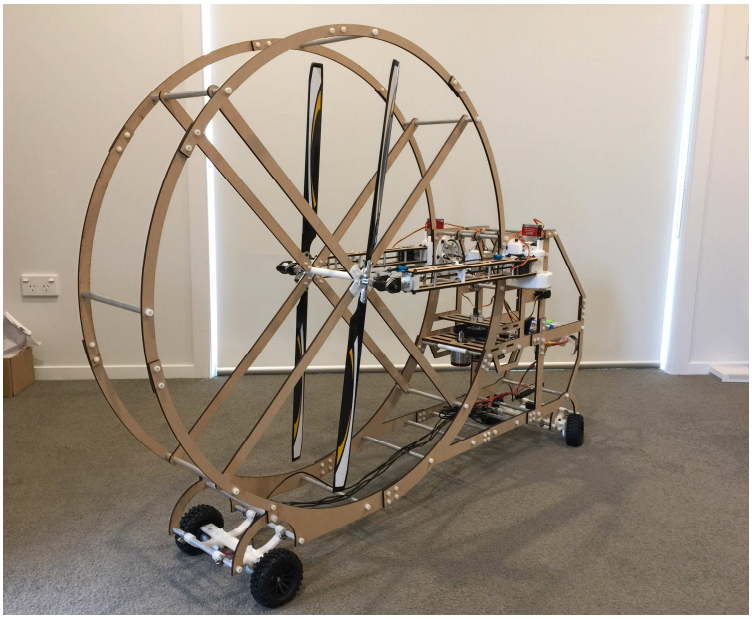

(b)

Figure 5.69: The flight vehicle model (fold)

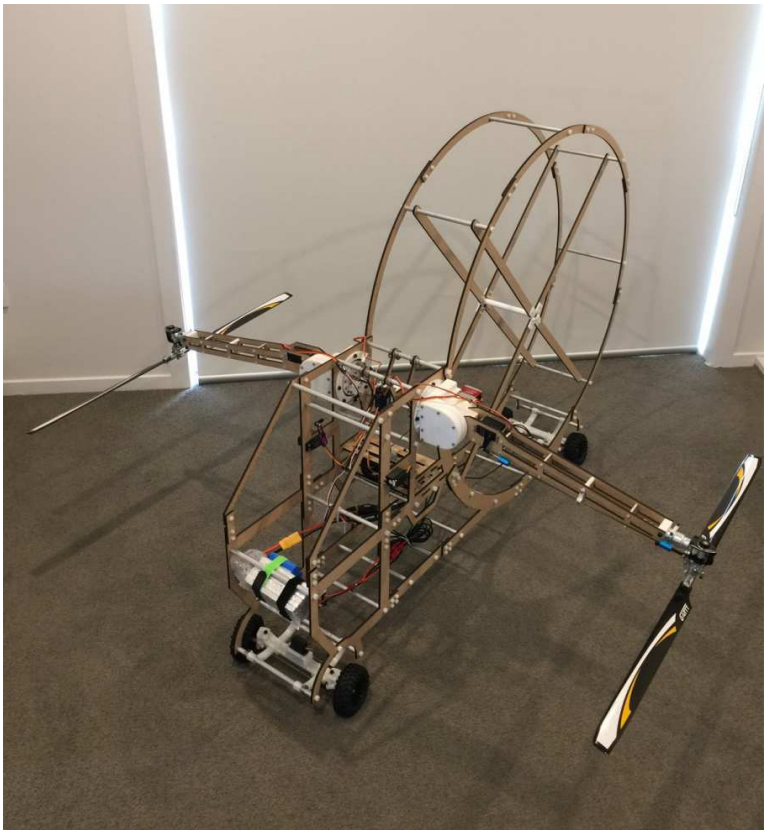

Figure 5.70: The flight vehicle model (open)

Chapter Six: Control system

How to set the control system of the flight vehicle is another main objective of this project. Due to the tilt flight mechanism, the common fixed-wing and helicopter control modes cannot be used on this model. This thesis designed a method to control the model flight by an eight-channel transmitter. The whole control system is divided into two parts: flight part and land driving part, because different motors have different voltage requirements.

6.1 The land driving part control system

The land driving part is simply controlled by a two channel remoter. Two motors are used to drive the model and a five-line servo motor is used to control the steering of the model. The motors and servo motors are powered by a 7.5V battery. At the same time, an Electronic Speed Control (ESC) and receiver integrated receiver is used to transmit signals to control steering and driving motors speed. The two motors are connected in parallel to maintain the same speed. The land driving part shows in figure 6.1.

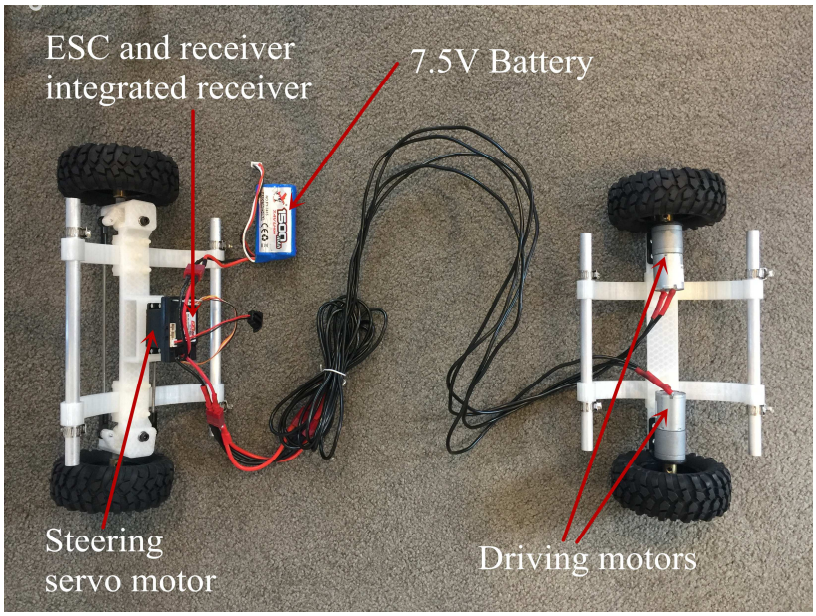

Figure 6.1: The land driving system

Figure 6.2: The two-channel transmitter

6.2 The flight part control system

A mixed-control method was designed to control the flight and rotor fold of the model by using an eight-channel transmitter which shows in the figure 6.3.

Figure 6.3: The eight-channel transmitter

The motor and servo motors of the flight part are powered by a 22.2V battery. A 120A Electronic Speed Control (ESC) is used to control the main motor speed and power the nine channel receiver. The connection of the receiver interface is shown below:

Channel 1: One of the blade attack angle control servo motor.

Channel 2: One of the tilt control servo motor.

Channel 3: Another blade attack angle control servo motor.

Channel 4: Another tilt control servo motor.

Channel 5: One of the fold control servo motor.

Channel 6: Electronic Speed Control (ESC).

Channel 7: Empty.

Channel 8: Another fold control servo motor.

Channel 9: The ESC cooling fan.

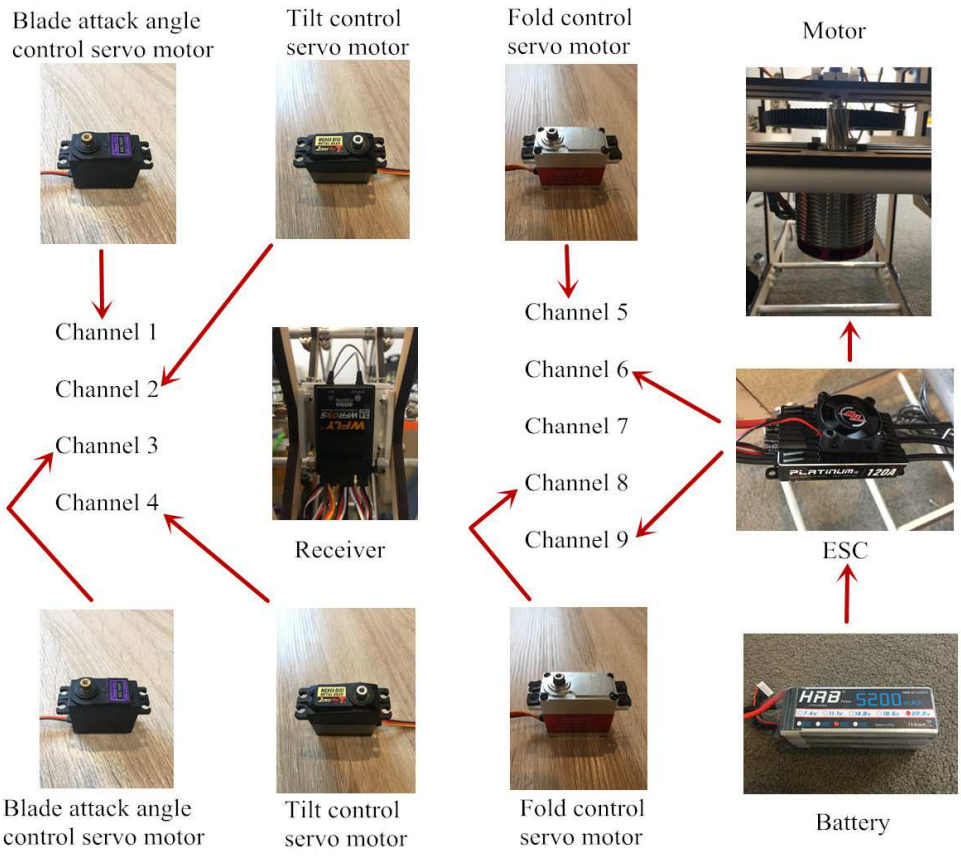

Figure 6.4: A schematic diagram of the circuit connection

By using the mixed control programming program in the transmitter, these channels are mixed controlled by the following methods:

1. Channel 1 is mixed-controlled by Channel 3 with the same rate but the opposite direction.

2. Channel 4 is mixed-controlled by Channel 2 with the same rate but the opposite direction.

3. Channel 3 is mixed-controlled by Channel 1 with the same rate and direction.

4. Channel 2 is mixed-controlled by Channel 4 with the same rate and direction.

5. Channel 5 is mixed-controlled by Channel 8 with the same rate but the opposite direction.

6. Channel 2 is mixed-controlled by Channel 7 with the same rate but the opposite direction.

7. Channel 2 is mixed-controlled by Channel 7 with the same rate and direction.

Since the transmitter has only seven customized mixed-control programming, there is no more mixed control programming for the main motor. So the main motor speed is controlled by Channel 6 individually. By using this mixed-control method, the flight vehicle model can be controlled as a normal helicopter. The control way shows in figure 6.5.

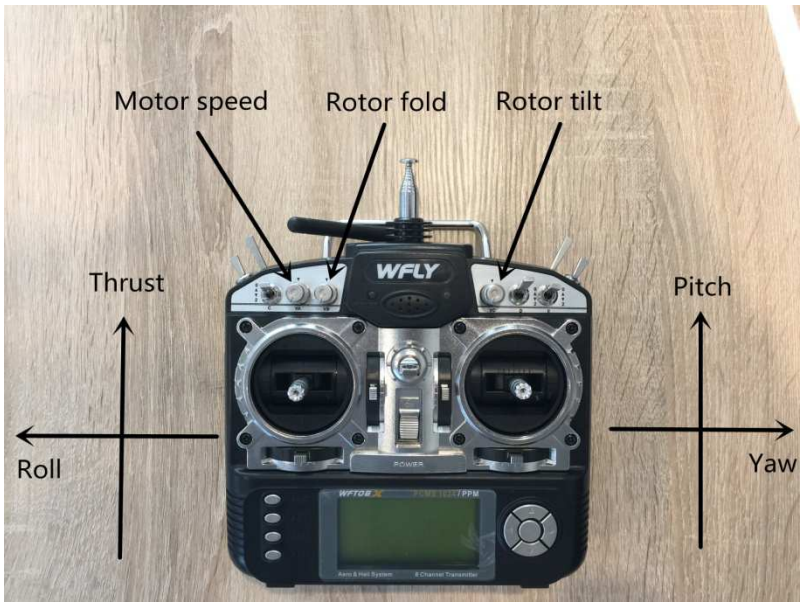

Figure 6.5: Transmitter control mode

6.3 Model test.

This section will show the results of actual control. However, due to using

off-the-shelf tail rotor heads, there is no information to explain its material and strength. With the consideration of the great centrifugal force which generated by the high-speed rotate blades may damage the rotor head and shoot the blades to cause personal damage (If the rotor head is damaged the rotor will shoot like a bullet), the test flight of the model was cancelled, but a running test was carried out.

6.3.1 The fold and open of the rotors.

The fold of the rotors is controlled by the fold knob, and the tilt of the rotors is controlled by the tilt knob. The angle of the rotor arm is based upon the angle of the knobs twist. The open process of the rotors shows in the figure 6.6. And the fold process is the reverse process of the open process.

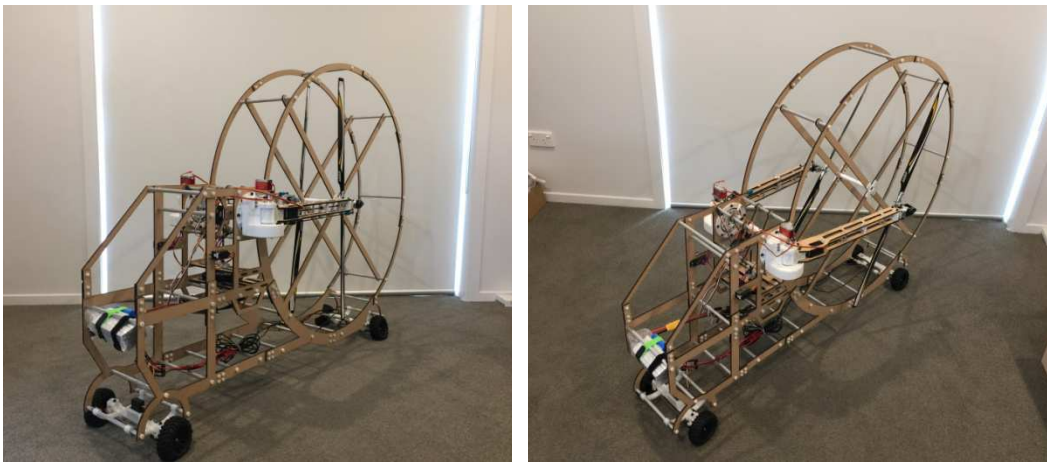

(a) (b)

Figure 6.6: The rotors open process (Continue on next page).

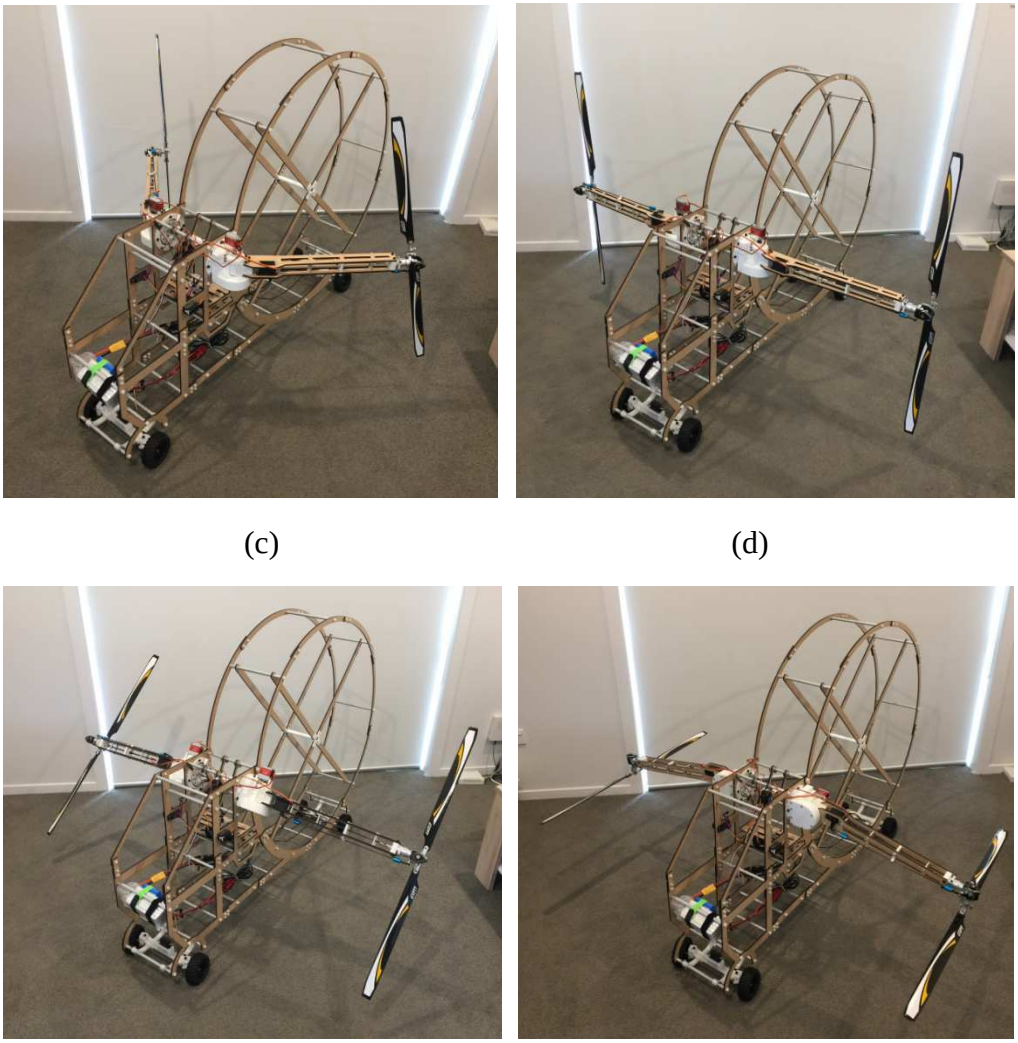

(c) (d)

(e) (f)

Figure 6.6: The rotors open process

6.3.2 The pitch control of the model.

The pitch of the model is controlled by the right control stick. Push forward the control stick, the rotors tilt backward. Push the control stick backward, the rotors tilt forwards. The control process shows below.

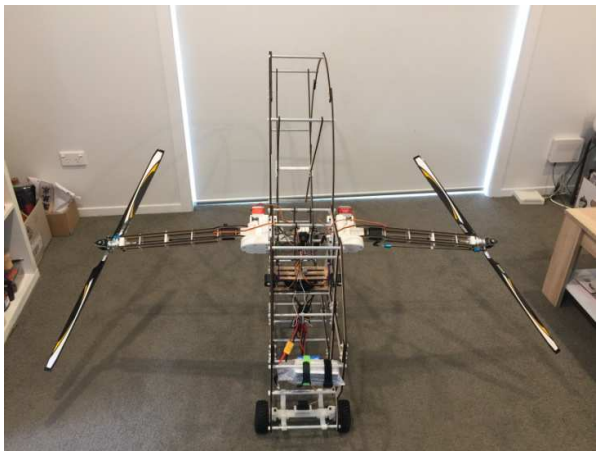


Figure 6.7: Fly forward control

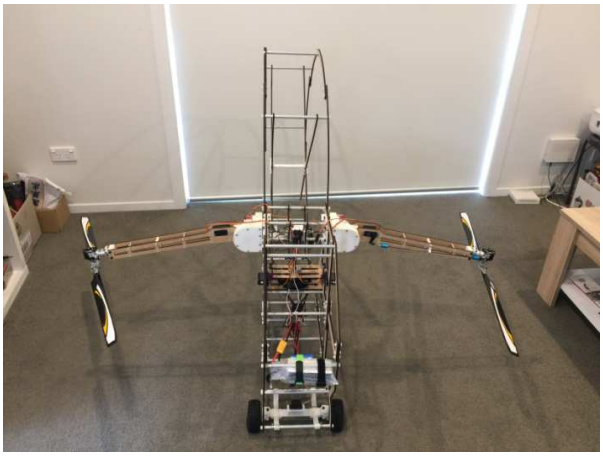


Figure 6.8: Hover control

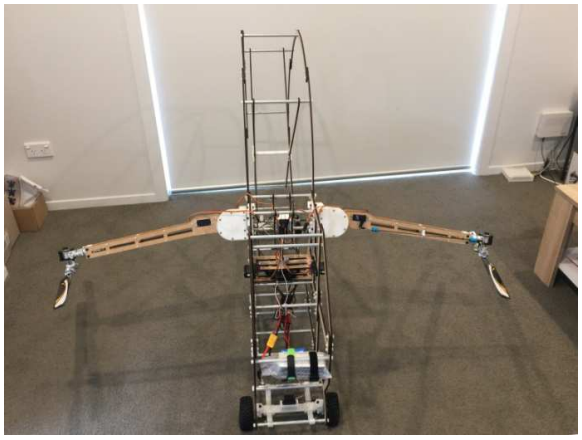


Figure 6.9: Fly backward control

6.3.3 The roll control of the model.

The roll of the model is controlled by the left control stick. Push the control stick to the left, the right rotor tilts backward and the left rotor tilts forward. Push the control stick to the right, the right rotor tilts forward and the left rotor tilts backward. The control process shows below.

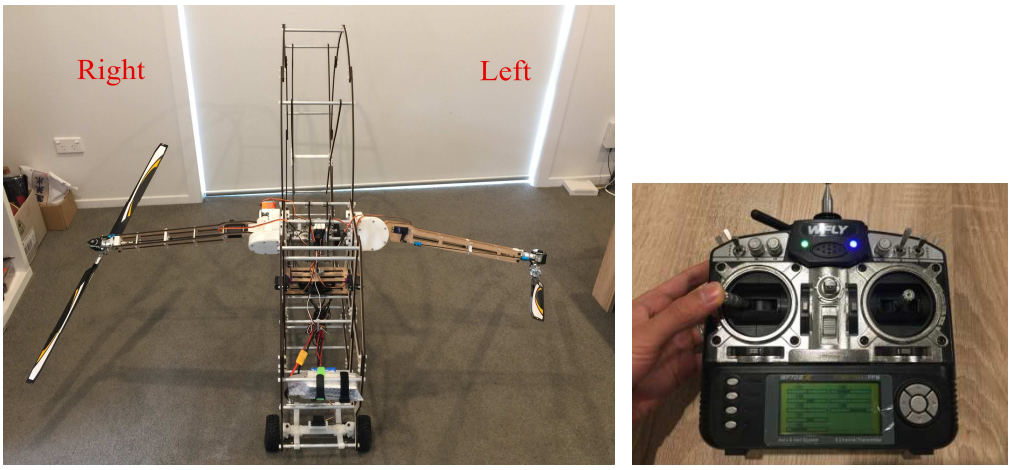

Figure 6.10: Left roll control

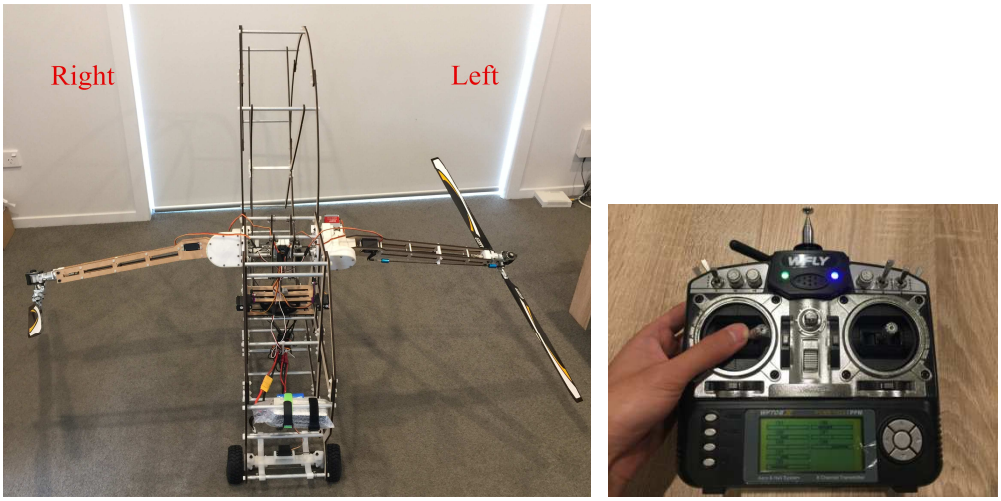

Figure 6.11: Right roll control

6.3.4 The Thrust and yaw control of the model.

The thrust of the model is controlled by the left control stick. Push the control stick forward, the attack angle of the blades increases. On the contrary, the attack angle of the blades reduces. The yaw of the model is controlled by the right control stick. Push the stick left and right to make the attack angle of the two rotors different so that the yaw of the model can be achieved. The attack angle changes show in figure 6.12.

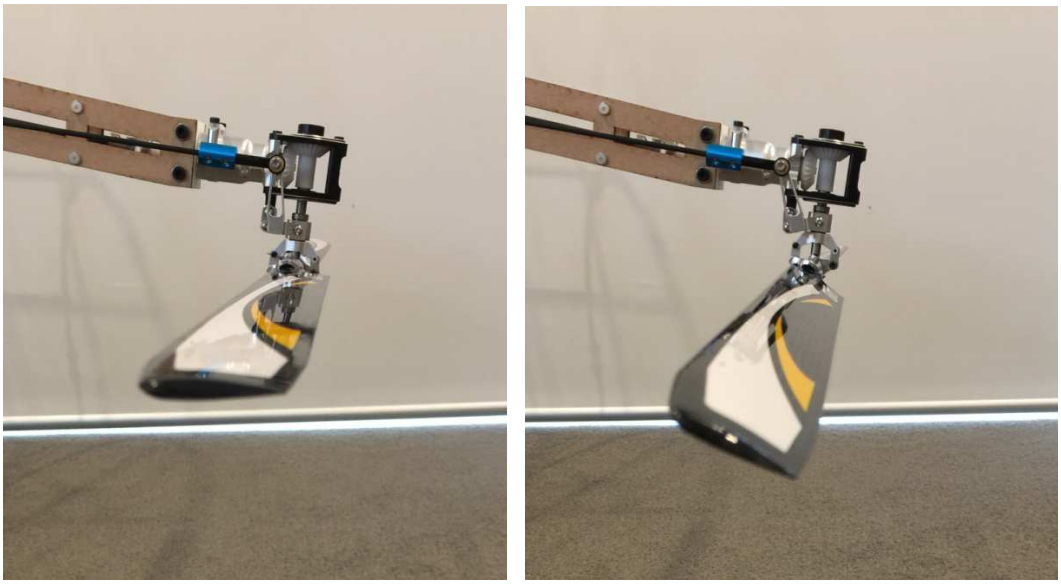

Figure 6.12: The change of the attack angle

6.3.5 Flight system running test.

For the safety reason that mentioned before, only a running test was carried out to verify the feasibility of the system. The screenshots of running videos are as the following figure.

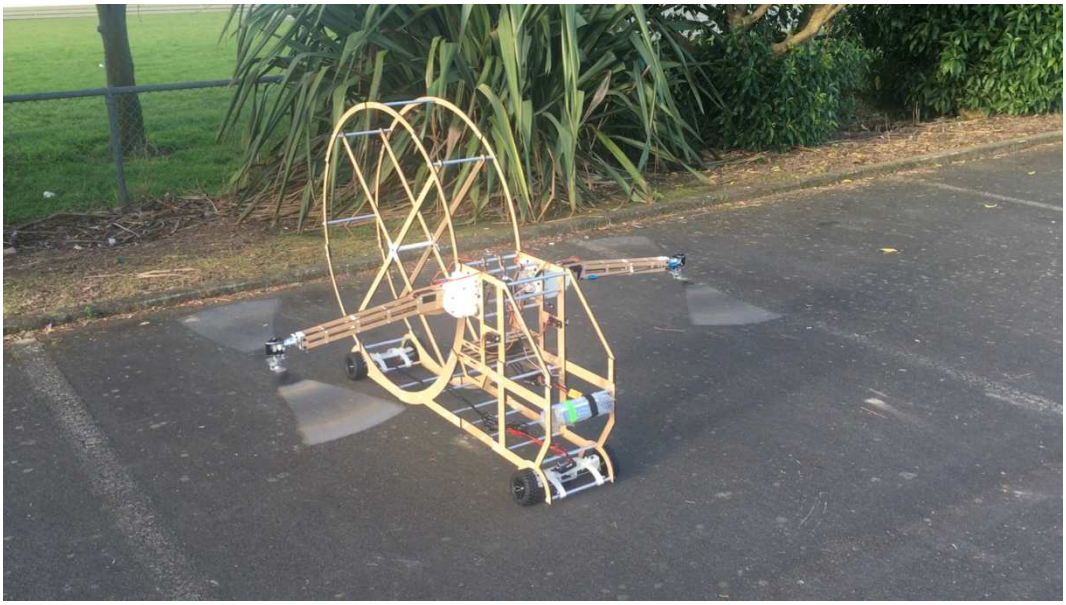

Figure 6.13: The running test of the model

Chapter Seven: Discussion

From the concept, a two foldable and tiltable rotors flight vehicle model was designed and made. After calculation, design and model implementation, a running test shows that the concept is feasible. A viable control method was also presented. Because the research of the concept is in the initial stage, the model still has a lot of room for improvement. This chapter will discuss some main parts and some problems of the model. Due to the time and budget constraints, some problems were solved but some of them are still left behind.

7.1 The folding structures.

The main gearbox and the auxiliary gearbox are the cores in this model. In order to simulate a real flight vehicle, the model uses only one motor to drive two rotors. The gearboxes allow the model to fold its rotors to reduce space occupancy and at the mean time, transmit power from motor to rotors. The foldable gearboxes are not only can be used in this kind of flight vehicle but also can be used in other areas. For instance, it can be used in the field of robotic and manufacturing as a transmission articulation. The fully enclosed gearbox design facilitates the protection and the lubrication of the gears, so that it improves the efficiency of transmission and allows the gearbox to be used for extended periods of time. Moreover, the folding of the rotor arms is controlled by servo motor due to the receiver can only provide 6V voltage. In the future, telescopic rods can replace the

folding servo motors to improve the stability of the model.

7.2 The fuselage.

The fuselage of the model is just a simple frame design and it was cut into pieces due to the size of the laser cutting machine. This not only increased the weight of the structure, but also reduced the strength of the fuselage. About the rotor container, because of the size of the model, there is no locking structure to lock the rotors when they are folded. Just simply hold the rotors on the bracket with the suction of magnets. The advantage of using magnets is that it is simple in structure and light in weight. But its shortcoming is also very obvious: because the magnetic force cannot be eliminated, it is necessary to use strong power to open the rotors. As a result, it will cause the rotors to produce a violent shaking at the moment they are opening. How to improve the way of storage the rotors is also a key problem in the further research. Furthermore, the damping system also can be optimized with a spring.

7.3 The control.

In this thesis, it presented a method for controlling the model on the basis of an eight-channel transmitter. By this method, the automatic folding, opening and tilting of the rotors have been achieved. What is more, it also can be controlled as ordinary as a helicopter model. However, due to the limitations of remote control, there are many functions are not perfect. The first one is that the opening and

folding of the rotors is not a coherent automatic process. It is achieved by manual twist knobs, and the angle of the opening and folding is determined by the angle of the knob. At the meantime, the motor speed control is not a mixed controlled by the thrust stick but with a separate knob control, because there is no more mixed control program can be used in this controller. The best way to solve these problems is to make a dedicated programmable controller for this kind of structure.

7.4 Gears and transmission.

Since the transmission system is operating in strong power and high-speed conditions, high precision gear meshing is required. The tightening strength of the shaft with other parts is also needed to be very high. In the initial test, gears of the auxiliary gear boxes with no high precision meshing were broken under high speed and high-intensity rotation. The gears of the auxiliary gearboxes are damaged as shown in the figure below and there is a new gear in the middle of the figure for reference.

Figure 7.1: Gears damage (The middle one is a new gear for reference)

Although the model can run properly by finding the exact mashing position after adjustment and testing, the gears were damaged for several starts and stops and also the material of gears in the auxiliary gearboxes is copper. It is necessary to increase the modulus of the auxiliary gearbox gears and replace its material. However, increase the gears modulus means to increase the size of the auxiliary gearboxes which need to be printed by SLS 3D print. The price is very dear. The budget for this project can support to print only once. So the problem left for the future research to solve.

The same damage problem also occurs on the shafts. Since the part is not fastened to the shaft, there is a sliding between parts and shafts. In the high-speed rotation, the carbon fiber shafts will be fractured after they were worn. Another reason of wear is the parts were dismantled from shafts for several times. Figure 6.2 shows some broken shafts.

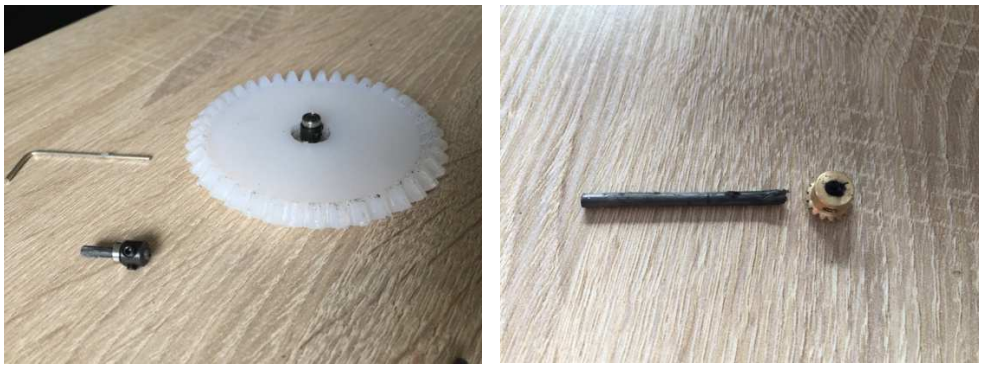

Figure 7.2: Broken shafts

In order to solve this problem, tighten each of the connection and replace shafts

while change the parts are necessary. Meanwhile, increasing the diameter of the shafts is also a solution.

7.5 Rotor head

The rotor head of the flight vehicle model are the tail rotor head of 700 series helicopter model. The reason of using this tail rotor head is that most of the main blades of helicopter uses 3mm hole to connect with rotor head, and only 700 series helicopter model tail rotor head uses 3mm hole to connect tail blade. Other series helicopter model tail rotor head uses 2mm hole to connect tail blade. So the size of the flight vehicle model depends on the 700 series helicopter model tail rotor head. But the tail rotor head is designed for tail blades, not for the main blades and there is no data to show its strength and material. Considering the safety, a dedicated rotor head for the flight vehicle is necessary to be designed in the future research.

Chapter Eight: Conclusion

In order to solve the problem of traffic jam and to facilitate private flight, this thesis presented a concept of the flight vehicle which using one motor to power two foldable and tiltable rotors. A model has been designed and implemented to investigate the feasibility of the concept. According to the model tests, the three main objectives have been achieved (1. Design a mechanism which not only can fold and tilt the rotor but also can transmit power to the rotor. 2. Design a transmission system which can transmit motor power to two rotors. 3. Design a control method to control the flight vehicle). The project was in accordance with the study of a variety of national flying cars, a variety of helicopters and multi-rotor aircrafts. At present, the flying car is a hotspot of research. Unlike other types of flying cars, this two rotors flight vehicle is based on the twin rotors vertical aircraft and truck structure. The advantages of the foldable and tiltable rotors flight vehicle: it can take off and land vertically and its rotors powered by only one motor. Moreover, the twin rotors tilt structure simplified the rotor head (compare with the main rotor head of helicopter) so that it can be fold to the fuselage of the flight vehicle to reduce the overall size of the vehicle. For these reasons, the model has potential to be developed into a real flight vehicle.

References

AeroMobile. (2017). *Evolution*. Retrieved from https://www.aeromobil.com/evolution/#

Aerotime. (2013). *The Largest Helicopter Ever Made: Mil V-12*. Retrieved from https://www.aerotime.aero/en/did-you-know/161-the-largest-helicopter-ever-made-mil-v-12

Airfoil Tools. (2017). *NACA63012A AIRFOIL (n63012a-il).* Retrieved from http://airfoiltools.com/airfoil/details?airfoil=n63012a-il#polars

Align. (2014). *T-REW 700X RC Helicopter.* Retrieved from http://www.align.com.tw/helicopter-en/trex700/

Anonymous. (2006). Dude, where's my flying car? *Aftermarket Business, 116*(2), 62.

Banggood. (2017). *ALZRC 380 FAST RC Helicopter Parts 380mm Carbon Fiber Blades For Ailgn 470L Helicopter.* Retrieved from https://www.banggood.com/ALZRC-380-FAST-RC-Helicopter-Parts-Carbon-Fiber-Blades-p-1027088.html

Bell. (2011). Army concept team in Vietnam. In S. C. Tucker (Ed.), *Encyclopedia of the Vietnam war: a political, social, and military history* (2nd ed.). Santa Barbara, CA: ABC-CLIO.

Burkhard Domke. (2009). *Sikorsky CH-53GS.* Retrieved from http://www.b-domke.de/AviationImages/Stallion/20042.html

Cable, J. (2012). This Flying Car is No Flight of Fancy. *Industry Week, 261*(5), 36

Case, K. (2002). Coming soon: The future. *Quality Progress,35*(11), 25-29.

Century of Filght. (n.d.). Igor Sikorsky VS-300. Retrieved from http://www.century-of-flight.net/Aviation%20history/helicopter%20history/Igor%20Sikorsky.htm

Ciment, J. (2015). Social Issues in America: An Encyclopedia (pp.1762). New York, USA: Taylor and Francis.

Cornu, Paul, 1881-1944. (2008). A Biographical Dictionary of People in Engineering: From Earliest Records to 2000.

Dong, J. (2001). *Helicopter Yaw Control Methods*. Retrieved from

http://www.aerospaceweb.org/question/helicopters/q0034.shtml

Ebay. (2017). *GARTT SAB Goblin 380 RC Helicopter Part 380mm Carbon Fiber RC Align 380 Blade.* Retrieved from http://www.ebay.com/itm/GARTT-SAB-Goblin-380-RC-Helicopter-Part-380mm-Carbon-Fiber-RC-Align-380-Blade-/112162705669

Egozi, A. (2004). X-Hawk developers to build policing model.*Flight International*, *166*(4952), 28.

Egozi, A. (2006). Bell backs X-Hawk. *Flight International,169*(5040), 30.

EHang. (2017). *EHang 184*. Retrieved from http://www.ehang.com/ehang184/

Encyclopedia Britannica Online. (2016). Helicopt*er*. Retrieved from http://waikato.summon.serialssolutions.com/#!/search?bookMark=ePnHCXMw42JgAfZbUzkZuDJSc4CeKSgBle7Sbq4hzh66SaAObx5o10N8alI8qOthAronCJ8sAKhtF38

Flying Car Makes Successful Maiden Flight. (2012, April 02). *PR Newswire*, p. PR Newswire, Apr 2, 2012. Retrieved from

https://search-proquest-com.ezproxy.waikato.ac.nz/docview/963468776?rfr_id=info%3Axri%2Fsid%3Aprimo

FLYING CARS. (2017). Plane and Pilot, 53(5), 10. Retrieved from http://ezproxy.waikato.ac.nz/login?url=https://search-proquest-com.ezproxy.waikato.ac.nz/docview/1900107094?accountid=17287

Fulton, R. (2002, February). Robert E. Fulton Jr.'s airphibian. *Flight Journal, 7*(1), 56.

Gordon Leishman J. (2001). The Breguet-Richet Quad-Rotor Helicopter of 1907. *AHS International Directory*, 1-4.

Heli Freak. (2016). *Align unit centering.* Retrieved from https://www.helifreak.com/showthread.php?t=760504

Helicopter Magazine. (2007). *Paul Cornu's 1907 Helicopter.* Retrieved from https://www.helicoptersmagazine.com/procedures/paul-cornus-1907-helicopter-552

Hemmerdinger, J. (2017). AEROMOBIL STEPS ON THE GAS WITH FLYING CAR. *Flight Daily News,* (4), 22.

Historic Wings. (2013). *The Traian Vuia 1*. Retrieved from http://fly.historicwings.com/2013/02/the-traan-vuia-1/

HobbyKing. (2017). *325mm RotorStar Premium 3K Carbon Fiber Flybarless Helicopter Main Blades.* Retrieved from https://hobbyking.com/en_us/325mm-rotorstar-premium-3k-carbon-fiber-flybarless-helicopter-main-blades.html

Huntington, S. (2001, June 05). A few historical flights of fancy Not every experimental aircraft succeeds, but failures may point the way to getting a good idea off the ground. The Christian Science Monitor, p. 22.

Jeffrey, J. (2013). *Transition to the skies: Terrafugia's flying car could change general aviation forever*. Retrieved from http://www.nydailynews.com/autos/transition-skies-terrafugia-flying-car-change-general-aviation-article-1.1411630

Jelaska, D. (2012). *Gears and Gear Drives*. West Sussex, United Kindom: John Wiley & Sons Ltd.

Kenneth G. Munson. (1969). Helicopters and Other Rotorcraft Since 1907. New York, U.S.A.: MacMillan Publishing Company.

Komarjohari. (2013). *ISUZU LEADS MALAYSIA'S LIGHT-DUTY TRUCKS MARKET.* Retrieved from https://komarjohari.wordpress.com/2013/02/20/isuzu-leads-malaysias-light-duty-trucks-market/

Martin D. Maisel, Demo J. Giulianetti and Daniel C. Dugan. (2000). *The History of the XV-15 Tilt Rotor Research Aircraft: From Concept to Flight.* Washington, D.C., United States: NASA History Division

Martin D. Maisel, Demo J. Giulianetti, & Daniel C. Dugan. (2000). *The History of the XV-15 Tilt Rotor Research Aircraft: From Concept to Flight*. Washington, D.C., U.S.A.: National Aeronautics and Space Administration Office of Policy and Plans.

Matt, P. (2015). *The Long, Weird History of the Flying Car*. Retrieved from http://www.popularmechanics.com/technology/infrastructure/g2021/history-of-flying-car/

NASA. (2015). *The Lift Equation*. Retrieved from http://www.grc.nasa.gov/WWW/k-12/airplane/lifteq.html

PAL-V. (2017). *Benefits*. Retrieved from https://www.pal-v.com/en/

Radek Baranek & Frantisek Solc. (2012). *Modelling and Control of a Hexa-copter* (13th ed.). High Tatras, Slovakia: IEEE International Carpathian Control Conference (ICCC).

Saeed, B., & Gratton, G. (2010). An evaluation of the historical issues associated with achieving non-helicopter V/STOL capability and the search for the flying car. *Aeronautical Journal, 114*(1152), 91-102.

Simonsen, D. (2012). The Sky My Kingdom: Memoirs of the Famous German World War II Test Pilot. *Air Power History,59*(4), 51-52.

SKY Berry. (2014). *KAMOV KA-50*. Retrieved from https://www.skybrary.aero/index.php/KA50

Terrafugia. (2017). *A New Dimension of Freedom*. Retrieved from https://www.terrafugia.com/tf-x/

Terrafugia. (2017). *A World-Class Team*. Retrieved from http://www.terrafugia.com/about-terrafugia/

The Aviation History Online Museum. (2013). *Bell UH-1 Iroquois.* Retrieved from

http://www.aviation-history.com/bell/uh1.htm

The Boeing Company. (2017). *CH-47 CHINOOK*. Retrieved from http://www.boeing.com/defense/ch-47-chinook/

The Boeing Company. (2017). *V-22 Osprey*. Retrieved from http://www.boeing.com/defense/v-22-osprey/

The Economist. (2016). Pocket World in Figures 2017 (pp. 96). London, British: Profile Books.

The Engineering ToolBox. (n.d.). *Electrical Motor Efficiency.* Retrieved from http://www.engineeringtoolbox.com/electrical-motor-efficiency-d_655.html

Warwick, G. (2013). Transforming Ideas. *Aviation Week & Space Technology, 175*(16), 48.

Watkinson, J. (2003). Art of the Helicopter. Burlington, United State: Elsevier Science.

Wikipedia. (2017). *Truck.* Retrieved from https://en.wikipedia.org/wiki/Truck

"Flying Car Company" Takes Off. (2007). *PR Newswire*, N/a. Retrieved from https://search-proquest-com.ezproxy.waikato.ac.nz/docview/453824804/fulltext/10E7C24E69E548E6PQ/1?accountid=17287

13 November 1907. (2016). The Hutchinson Chronology of World History.

Appendix 1

Purchased components list

(1). ALIGN HML73M01 730MX motor

Figure A.1: ALIGN HML73M01 730MX motor

Specifications:

KV value: 850KV

Max electricity: 115A/195A (5S)

Max power: 2550W/4330W (5S)

Input Voltage: 6S (22.2V)

Weight: approximately 380g

(2). HRB 5200mAh 6S Li-ion battery

Figure A.2: HRB 5200mAh 6S Li-ion battery

Specifications:

Discharge rate: 35C

Voltage: 22.2V

Weight: 800g

(3). HobbyWing - Pentium 120A V4 Electronic speed control

Figure A.3: HobbyWing - Pentium 120A V4 Electronic speed control

Specifications:

Sustained current/peak current: 120A/150A

Battery: 11.1V – 22.2V Li-ion battery

BEC (Battery Elimination Circuit) output: 5-8V, 10A

(4). WFLY WFT08X 2.4GHz 8 channel transmitter and receiver.

Figure A 4: WFLY WFT08X 2.4GHz 8 channel transmitter and receiver

(5). Tower Pro MG996R servo motor

Figure A 5: Tower Pro MG996R servo motor

Specifications:

Weight: 55g

Stall torque: 9.4kg.cm (4.8V) 11kg.cm (6V)

Operating voltage: 4.8V-6.6V

(6). Tower pro MG958 servo motor

Figure A 6: Tower pro MG958 servo motor

Specifications:

Weight 65g

Stall torque: 18kg.cm (4.8V) 20kg.cm (6.6v)

Operating voltage: 4.8V-6.6V

(7). 0.6 module bevel gear, bore size (3mm)

Figure A 7: 0.6 module bevel gear bore size (3mm)

Specifications:

Module: 0.6

Number of teeth: 16

Bore size: Φ3mm

(8). 0.6 module bevel gear, bore size (5mm)

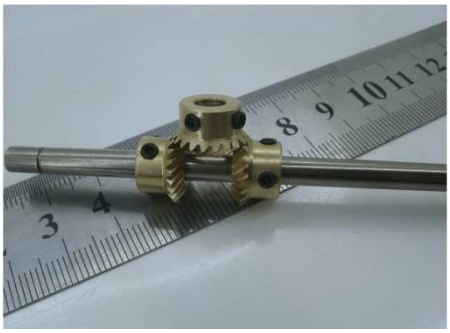

Figure A 8: 0.8 module bevel gear bore size (5mm)

Specifications:

Module: 0.8

Number of teeth: 20

Bore size: Φ5mm

(9). ALIGN 11T motor gear H55G002XXW

Figure A 9: ALIGN 11T motor gear H55G002XXW

Specifications:

Module: 1

Number of teeth: 11

(10). ALIGN 112T main gear H60G001XXW

Figure A 10: ALIGN 112T main gear H60G001XXW

Specifications:

Module: 1

Number of teeth: 112

(11). GARTT 700 metal tail holder

Figure A 11: GARTT 700 metal tail holder

(12). SAB Goblin FK 380 carbon fiber main blade

Figure A 12: SAB Goblin FK 380 carbon fiber main blade

Specifications:

Length: 389.94mm

Width: 33.82mm

(13). Universal joint

Figure A 13: Universal joint

Size:

Φ4mm to Φ6mm

Φ3mm to Φ4mm

Φ4mm to Φ5mm

(14). 2" 6STARBrand CNC Alu. Alloy Half Servo Arm

Figure A 14: 2" 6STARBrand CNC Alu. Alloy Half Servo Arm

Specifications:

2" futaba 25T

(15). KST X20 - 8.4 - 50 Servo motor.

Figure A 15: KST X20 - 8.4 - 50 Servo motor

Specifications:

Weight 78g

Stall torque: 38kg.cm (6V) 42kg.cm (7.4v) 45kg.cm (8.4V)

Operating voltage: 6V-8.4V

(16). Flange

Figure A 16: Flanges

Specifications:

Bore size: Φ5mm

(17). Aluminum tube

Figure A 17: Aluminum tube

Specifications:

M3* Φ6mm*30mm

(18). Bearing seat

Figure A 18: Bearing seat

Specifications:

Bearing bore size: Φ5mm

(19). Motor bracket

Figure A 19: Motor bracket

Specifications:

370 motor bracket

(20). ASLONG JGA25-370 gear motor

Figure A 20: ASLONG JGA25-370 gear motor

Specifications:

Operating voltage: 6V

Rotate speed: 35rpm

(21). Electronic Speed Control (ESC) and receiver integrated receiver

Figure A 21: Electronic Speed Control (ESC) and receiver integrated receiver

(22). 7.4V 1500mAH battery

Figure A 22: 7.4V 1500mAH battery

(23). Five-line servo motor

Figure A 23: five-line servo motor

(24). 2-channel radio transmitter.

Figure A 24: 2-channel radio transmitter

(25). Ball head

Figure A 25: Ball head

Specifications:

M3* Φ3mm

(26). Tire coupling

Figure A 26: Tire coupling

Specifications:

Bore size: Φ4mm

(27) Tire

Figure A 27: Tire

Specifications:

Size: Φ96mm

(28). Coupling

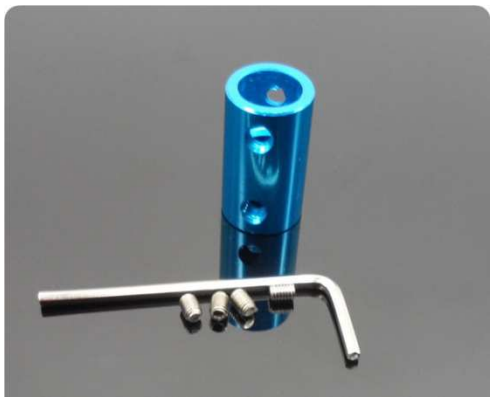

Figure A 28: Coupling

Specifications:

Φ3mm to Φ3mm

(29). Magnet

Size:

Φ6mm*3mm

Φ12mm*3mm

(30). Aluminum tube

Specifications:

M6* Φ10mm*190mm

M6* Φ10mm*200mm

(31). MR63ZZ-2 bearing

Size:

Φ3mm* Φ6mm* 2mm

(32). 684ZZ bearing

Size:

Φ4mm* Φ9mm*4mm

(33). MR85ZZ bearing

Size:

Φ5mm* Φ8mm*2.5mm

(34) MR126ZZ bearing

Size:

Φ6mm* Φ12mm*4mm

(35). 6814-2RS bearing

Size:

Φ30mm* Φ42mm*7mm

(36).6806-2RS bearing

Size:

Φ70mm* Φ90mm*10mm

(37). Stop collar

Size:

Bore size Φ3mm

Bore size Φ4mm

Bore size Φ5mm

(38). Screws

M2.5*50mm screws

M3*8mm self-tapping screws

M3*10mm nylon screws

M3*15mm nylon screws

M3*16mm self-tapping screws

M3*22mm screws

M3*45mm screws

M4*10mm screws

M4*10mm nylon screws

M4*15mm screws

M4*20mm nylon screws

M4*30mm screws

M4*45mm screws

M5*15mm nylon screws

M6*8mm nylon screws

(39).Nuts

M2.5 nuts

M3 nuts

M3 nylon nuts

M4 nuts

M4 nylon nuts

M5 nylon nuts

Appendix 2

The drawing of the main gearbox gear set